7-25-2019 1:00 PM

Brain-specific and systemic inflammatory response following repetitive concussive impact in a mouse model

So Young Eo
The University of Western Ontario

Supervisor
Dekaban, Gregory A
The University of Western Ontario

Graduate Program in Microbiology and Immunology
A thesis submitted in partial fulfillment of the requirements for the degree in Master of Science

Abstract

Concussion is the most common form of mild traumatic brain injury (mTBI). TBI resolution is modulated by neuroinflammation, which is augmented by the infiltration of innate immune cells from the circulation. Peripheral, myeloid immune cells not only invade neural tissues but other organs as well causing local inflammation and tissue damage, known as systemic inflammatory response syndrome. Here, I assessed the temporal and anatomical nature of the neural and systemic cellular inflammatory response to repetitive, mTBI in a 3-hit mouse model of concussion. The results showed significant microglial activity, accumulation of peripheral myeloid cells and prominent axonal damage post-injury. The peripheral immune cells emerged through the brain microvasculature and resided in the parenchyma, along the pia mater and within the ventricles. There was also evidence of systemic inflammation in the lungs as well as in the cervical spinal cords of the mTBI mice.

Keywords

Concussion, mTBI, inflammation, myeloid cells, microglia

Summary for Lay Audience

Traumatic brain injury (TBI) has emerged as a silent epidemic of increasing importance and frequency as it has gained global recognition as a high-profile public health issue. Concussion falls under the milder end of the TBI severity spectrum, accounting for 70-90% of all brain injury cases. However, since most individuals survive the initial trauma and do not seek medical treatment, the total number of concussion is greatly underreported. As there are many causes of TBI, injuries pertaining to the brain are often known as "the most complicated disease of the most complex organ in the human body." Despite this increasing awareness of concussion and the possibility of long-term impairments, effective means of diagnosis, prognosis and treatment options fail to exist and remains as a major unmet clinical need. Furthermore, not only single but repeated occurrences of head injuries constitute mounting concerns, and emerging literature supports both pathological and behavioral differences between a single injury and multiple injuries. This is particularly a major concern in the context of sports or military activities where these individuals are subjected to multiple insults. There is evidence to suggest that immediately following a head trauma, a period of vulnerability window exists and if a second concussion was sustained within that period, a significant and even fatal damage can occur, known as second impact syndrome. Prognosis and effective management guidelines are difficult especially when social pressures exist for individuals to return to play or combat duties. Moreover, there is a high level of uncertainty regarding the threshold for diagnosis, the recovery trajectory and the predicted outcome. Here, I assessed the temporal and anatomical nature of the brain and systemic cellular inflammatory response to repetitive TBI in a 3-hit mouse model of concussion. The results showed significant activity of certain immune cells in the brain called microglia and an accumulation of other types of immune cells in the brain as well as in other organs. Overall, this study characterizes the inflammatory responses following repeated concussive injuries in a mouse model to establish its suitability for testing future therapeutics for clinical translation.

Acknowledgements

Firstly, I would like to acknowledge my supervisor, Dr. Gregory Dekaban, for your consistent guidance and support throughout my graduate degree. You have fostered my curiosity for research, challenged and encouraged me to think and discover. To my advisory committee members, Drs. Arthur Brown, and Steven Kerfoot, I thank you for the ongoing advice and direction with my work and for sharing their knowledge and offering invaluable advice throughout this thesis. Furthermore, I would like to extend my gratitude to Drs. Kathy Xu, Nicole Hryciw, Todd Hryciw, Natalie Kozyrev and Kristen Chadwick for their assistance in the techniques and procedures used for my project. Special thanks to the 4th year students; Ami Patel and Sharon Law for all the hours you spent on the cryostat. Lastly, a big thanks to all past and current laboratory colleagues and everyone else on the concussion research team, who have helped me in the completion of my experiments, troubleshooting issues, and providing overall support throughout the years of my work in the Dekaban laboratory.

Contributions

Dr. Kathy Xu aided me in learning how to perform the closed head injury surgical procedure along with other forms of staining.

Dr. Natalie Kozyrev took representative images of the double stained slides on the confocal microscope and helped optimize many immunohistochemical staining procedures.

Christy Barreira and Kevin Blackney both assisted in the perfusion process and staining blood cells and splenocytes for flow cytometry.

Dr. Kristen Chadwick trained me on the LSRII and guided me through troubleshooting and using FlowJo.

Table of Contents

List of Tables

List of Figures

List of Appendices

List of Abbreviations

α	Alpha
β	Beta
γ	Gamma
μg	Microgram
μL	Microliter
°C	Degrees Celsius
ARDS	Acute Respiratory Distress Syndrome
AIF-1	Allograft Inflammatory Factor 1
BBB	Blood Brain Barrier
BSA	Bovine Serum Albumin
CCI	Controlled Cortical Impact
CHIMERA	Closed Head Impact Model of Engineered Rotational Acceleration
CTE	Chronic Traumatic Encephalopathy
CNS	Central Nervous System
DAB	3,3′-Diaminobenzidine
DAI	Diffuse Axonal Injury
DAMP	Damage Associated Molecular Pattern
DD	Double Distilled
EGFP	Enhanced Green Fluorescent Protein
FACS	Fluorescence Activated Cell Sorting
FPI	Fluid Percussion Injury
GCS	Glasgow Coma Scale
GM-CSF	Granulocyte Macrophage Colony Stimulating Factor
Iba-1	Ionized Calcium-Binding Adapter Molecule 1
IL	Interleukin
Lys-EGFP-*ki*	Lysozyme M-EGFP- knock in
mTBI	mild Traumatic Brain Injury
MMP	Matrix Metallopeptidase
N/A	Not Applicable
NK	Natural Killer

NMDA	N – methyl – D Aspartate
OCT	Optical Cutting Temperature
RBC	Red Blood Cell
PBS	Phosphate Buffer Solution
PFA	Paraformaldehyde
PRR	Pattern Recognition Receptor
SCI	Spinal Cord Injury
SIRS	Systemic Inflammatory Response Syndrome
TNF	Tumour Necrosis Factor
TGF	Transforming Growth Factor
TBI	Traumatic Brain Injury
WD	Weight Drop

CHAPTER 1 – INTRODUCTION

1.1 Overview

Traumatic brain injury (TBI) has emerged as a silent epidemic of increasing importance and frequency as it has gained global recognition as a high-profile, public health issue. Concussion falls under the mild end of the TBI severity spectrum, accounting for 70-90% of all brain injury cases (1, 2) out of 2.5–3.8 million TBI cases per year in the United States (3). However, since most individuals survive the initial trauma and do not seek medical treatment, the total incidence of concussion is greatly underreported (4). As a disease of multiple etiologies, injuries pertaining to the brain are often known as "the most complicated disease of the most complex organ in the human body" (5). Despite the increasing awareness of concussion and the possibility of long-term impairments, effective means of diagnosis, prognosis and treatment options fail to exist and remain as a major unmet clinical need (6, 7). Furthermore, not only single but repeated occurrences of head injuries constitute mounting concerns, and emerging literature supports both pathological and behavioral differences between a single injury and multiple injuries (8, 9). This is particularly a major concern in the context of sports or military activities where patients are subjected to multiple insults. There is evidence to suggest that immediately following a head trauma, a window of increased neural vulnerability exists during which a second concussion could result in a significant and even fatal brain injury. This is known as second impact syndrome (10-12). Prognosis and effective management guidelines are difficult especially when social and workplace pressures exist for individuals to return to play, work or combat duties (13). Moreover, there is a high level of uncertainty regarding the threshold for diagnosis, the recovery trajectory, and the predicted outcome.

Overall, the clinical impact of TBI is not only highlighted by the incident rate but also by the long-term health consequences reported by individuals who have survived their injuries. Imprecise classification, methodological inconsistencies and some uncertainty about underlying pathophysiology hinder definitive methods of diagnosis and therapy for concussions (14). Thus, this study aims to further characterize the pathogenesis of repeated concussive injuries in an animal model in order to establish its suitability for testing future therapeutics for clinical translation.

1.2 Concussion

The majority of TBI cases (70-90%) are categorized as a mild injury within the TBI severity spectrum (1). The term concussion has been popularized in the context of sports medicine which is an injury known to exist under the umbrella of mild TBI (15). Commonly found in literature, the word concussion and mTBI have been used synonymously. The Quality Standards Subcommittee of the American Academy of Neurology defines concussion as a transient neurological dysfunction induced by a biomechanical force without gross lesions and structural abnormalities (16). An external force to the head and neck region or a blow anywhere else in the body can produce a whiplash effect that is transmitted to the brain. The acceleration/deceleration and rotational forces induce a change in pressure and tissue strain that drives the pathological alterations associated with concussion (17). It typically results in a rapid onset of acute neurological dysfunction and the clinical symptoms of concussion reflect a functional disturbance induced by a neurometabolic cascade of events (18). When a brain injury is suspected, it is classified normally by the Glasgow Coma Scale (GCS) (19) ranging from mild, moderate to severe in one spectrum (20). Dizziness, nausea, headaches, and amnesia are common symptoms of mild to moderate TBI and usually resolves within days to weeks following the injury. Occasionally, these symptoms can progress into long term consequences leaving the patient with cognitive or behavioral deficits. It has been found that moderate to severe TBI and even multiple mTBI are associated with an elevated risk of certain neurodegenerative diseases including Alzheimer's disease (21), chronic traumatic encephalopathy (CTE) (22) and Parkinson's disease (23). Specifically, NFL football players, long-term career boxers as well as military personnel have been described to have some cognitive impairments (24), neuroimaging abnormalities (25) and altered brain metabolism (26), disproportionate to their age. This highlights the importance of understanding not only the impact of a single concussion but also repeated injuries as well. It is now understood that at some undefined point, concussion stops being a recoverable injury and accelerates to a chronic neurodegenerative disorder.

1.3 Concussion pathophysiology theories

Despite all the recent research in concussion, there is still a lack of consensus on the pathophysiology which has led to an inconclusive pathological definition of concussion and thereby no effective clinical treatment (15). Many concussion researchers state that the literature is vast and that it may not be possible to simplify concussion into one neuropathological explanation (27). As there are many etiologies of concussion, there exist a plethora of theories for concussion pathophysiology (27). Concussions, like all other forms of TBI, have a dynamic and biphasic injury progression that evolves over time. The primary phase is the mechanical damage to the central nervous system (CNS) caused by the application of acceleration/deceleration and rotational forces. More importantly, regarding clinical aspects, secondary injuries arise from the complex network of vascular, cellular and biochemical cascades that lead to further damage and exacerbation of long-term neurological symptoms (28-30).

Older theories of concussion pathophysiology describe that immediately following a biomechanical injury, there is an abrupt disturbance in the electrochemical gradient and an indiscriminate release of glutamate (31, 32), a prominent excitatory neurotransmitter. The injury increases the permeability of the membrane to various ions that lead to a large influx of sodium ions (Na^+) and calcium ions (Ca^{2+}) and the efflux of potassium ions (K^+) (31, 32). The rapid shift in ionic balances depolarizes the neuronal membrane and the result is a massive release of glutamate (18). The excessive extracellular glutamate leads to glutamate excitotoxicity via activation of neuronal glutamate receptors such as N-methyl-D-aspartate (NMDA) receptor. Sudden excitation of the brain is followed by a wave of neuronal suppression called “spreading depression” (33). It is thought that loss of consciousness, amnesia and other cognitive dysfunction following a concussive impact is a manifestation of the post-traumatic spreading depression-like state. To restore the axonal membrane potential, the sodium-potassium pump is overworked, causing hyper-glycolysis and quick depletion of intracellular energy reserves (18). This state of hyper-metabolism leads to a disparity between glucose supply and demand which can result in an “energy crisis” (18). The effects of accelerated glucose consumption can be seen by the accumulation of lactate production and decreased cerebral blood flow, worsening the energy crisis (18). Elevated lactate levels, reduction in oxygen and glucose supply to hypermetabolic neurons further drives neuronal dysfunction and axonal damage. The latter

is referred to as diffuse axonal injury (DAI) (18). Shown by experimental animal studies using various TBI models, there is no question that TBI induces a multitude of cellular and molecular changes within the brain. However, it is problematic when these alterations do not necessarily manifest into clinical symptoms. Studies have seen depressed cerebral glucose metabolism after the initial period of hyperglycolysis in patients who presented with no clinical symptoms (34). Clearly, significant neurometabolic abnormalities can occur without any clear symptomatic indications. It is suggested that it takes 30 to 45 days for the physiological parameters to resolve, which is well beyond when symptoms usually settle (35). Much of the pathobiology of concussion has been elucidated through animal models of TBI, but, further validation of these mechanisms need to be established in humans.

As concussions are a common occurrence in sports, more recent studies in the literature have described 5 predominant theories of pathophysiology specifically for sports-related concussions: 1) tauopathy 2) white matter tract changes 3) changes in neuronal activity 4) reduced cerebral perfusion and 5) gray matter atrophy (27). 1) The tauopathy theory is described as the abnormal elevation of phosphorylated tau protein in the cortical sulci of the brain (36). Tau proteins are normally found in the brain, function to stabilize microtubules in axons and are essential for neuronal communication. Hyperphosphorylated tau leads to the accumulation of neurofibrillary tangles that affect neuronal network connectivity that can result in cell dysfunction and cell death (37). 2) The theory that involves the white matter tract changes is based on the degeneration of myelin, a lipid-rich insulator surrounding axons that is responsible for efficient transmission of electrical signals along neurons (38). Some examples of white matter tract changes include widening of frontal and occipital sulci, the release of neuronal protein into the damaged brain and DAI (39). 3) The neuronal connectivity theory indicates a reduction in global neuronal networks occur that lead to less efficient coordinated communication between different brain regions (40). 4) The cerebral perfusion theory is centered on the change in blood flow arising following trauma that potentially leads to ischemia (41). 5) Lastly, a less common theory proposes that concussion symptoms arise from trauma due to an overall shrinking of cortical and subcortical structures including the thalamus and hippocampus (42). Although many theories of concussion have been shared amongst TBI researchers, there is

still ongoing debate and new theories are constantly being generated. It is no surprise that concussion is caused by both structural and functional damage (43) that are heterogeneous and multifactorial.

1.4 Repetitive concussion

While patients typically recover from a single incidence of concussion, cumulative effects of multiple head injuries pose a more serious problem. Particularly in athletes and military personnel, repetitive concussions are a common occurrence. Studies have shown that repetitive concussions that occur during a period of increased neural vulnerability can result in severe outcomes (12, 44). Clinical evidence of these severe outcomes is seen in athletes who have sustained multiple traumas as evidenced by poor performance in neurocognitive tests and demonstrating slower processing speed (45). Additionally, the extent to which these athletes show neurocognitive dysfunction is attributed to the length of time between sustained injuries. Clinical and experimental data have shown that repetitive injuries with shorter durations between consecutive insults result in a markedly greater cognitive, histological and behavioral impairments compared to injuries separated by a longer period (46, 47). As mentioned previously, research has shown the potential for multiple mTBI producing cumulative effects leading to long-lasting neurological impairment including age and non-age related neurodegenerative disorders (CTE, Alzheimer's disease, Parkinson's disease). Due to the high prevalence of concussions, it is becoming increasingly important to uncover the underlying secondary injury mechanisms that can explain brain sensitization to subsequent neurotraumas.

1.5 Neuroinflammation

The term neuroinflammation is used to describe the robust and complex inflammatory response generated by the interaction between the cellular and soluble components of the CNS and the periphery (48). Inflammation is a biological response to tissue injury that is both necessary and beneficial because it promotes the clearance of dead cells and debris and starts the process of tissue repair. However, too much inflammation for an extended period of time is detrimental to the surrounding tissues and can progress to chronic neurodegeneration (49-51). Immune targeting interventions for post-traumatic

inflammation aims to limit acute inflammation just enough to promote regeneration and prevent the development of chronic neuroinflammation. The mechanical damage of the primary injury during a TBI induces the release of self-derived warning signals called damage-associated molecular patterns (DAMPs) (52). DAMPs are endogenous molecules that are released from stressed or dying cells which can include host proteins, nucleic acids and metabolites (53) and they are sensed by pattern recognition receptors (PRRs). Upon binding of DAMPs to PRRs, an inflammatory response is generated and amplified such that pro-inflammatory mediators are released from all brain cell types and neural leukocytes (perivascular and meningeal macrophages). Although neurons, astrocytes, microglia, oligodendroglia, and endothelial cells are all capable of producing pro-inflammatory cytokines such as interleukin (IL)-1β, IL-6, tumor necrosis factor (TNF)-α, the microglia are the most critical immune cell in the first line of defense (54). Microglia are normally quiescent, anti-inflammatory and charged with maintaining neuro-homeostasis (55). However, activation of microglia lead to excessive amounts of pro-inflammatory cytokines being released that can exacerbate the initial trauma, and hinder both brain repair and functional recovery (54) while decreasing the levels of anti-inflammatory cytokines (IL-4, IL-10 transforming growth factor (TGF)-β). Anti-inflammatory cytokines are important for counteracting and downregulating the inflammatory and cytotoxic reactions (56). TBI also compromises the blood brain barrier (BBB)- a physical barrier separating the brain parenchyma from cellular and soluble blood components (57). Breaching of this barrier allows infiltration of peripheral immune cells into the parenchyma to exacerbate the inflammatory response (58). A compromised BBB allows extravasation of not only cells, but also plasma proteins into the brain. An example of such plasma protein is fibrinogen, a plasma adhesion protein. Accumulation of fibrinogen induces neuroinflammation and astrocyte scar formation by initiating TGF-β signalling pathway (59). Although primary injury occurs in a matter of seconds with a neuroinflammatory cascade commencing thereafter, a prolonged state of inflammation after the injury can linger for many years and predispose the patient to other neurodegenerative diseases (60). Chronic microglial activation, alterations in neuronal activity, reduced dendritic spine density in post-TBI patients all occur in parallel with long-lasting inflammatory responses (61). It is becoming increasingly clear that persistent neuroinflammation is associated with an elevated risk of

developing progressive life-long impairments in a patient's physical, cognitive, behavioral and social performance (49, 50). However, the initial inflammation also sets the stage for neural regeneration and recovery (62). Inflammation is referred to as a "double-edged sword" with both ameliorating and deleterious effects. This could explain why immune-suppressing drugs administered immediately post-TBI in human clinical trials have failed (63). Targeted therapeutic interventions are required to balance the benefits of the initial inflammatory response to promote neuro-regeneration and restoration of normal brain function while preventing detrimental, chronic inflammation that further undermines neurocognitive function.

1.6 Microglia

Microglial activation is a key hallmark of TBI. As the brain's resident, parenchymal macrophages, it's important to understand their normal functions during homeostasis, diseases and traumas inflicted on the CNS. It has been over a century since the discovery of microglia as the "third element" of the CNS (64). After much debate on the origin of microglia, it has only been recently shown that microglia arise from embryonic yolk sac (YS) precursors, which also gives rise to some tissue macrophages (65-67). This means that microglia and tissue resident macrophages are developmentally and functionally different from blood derived myeloid lineage cells (68). The previous notion that microglia are a static bystander in the healthy CNS that have minimal functions besides scavenging and immune surveillance has also been proved to be a misconception (68). In fact, microglia interact with all components of the CNS, constantly monitoring the brain microenvironment by extending their processes and maintaining tissue integrity (69, 70). Early in development during embryogenesis, the YS myeloid precursors travel to the brain before developing into immature microglia. Thus, microglia participate and interact with the development of other CNS cells including neurons, astrocytes and oligodendrocytes (71). It is not surprising that microglia activation is a key hallmark of almost all diseases and injuries related to the CNS (72, 73). While quiescent microglia have a ramified morphology, activated microglia are characterized by a hypertrophied, "bushy" and "amoeboid" phenotype (74). In a repetitive concussion rat model, microglial morphological change was clearly noticeable in the sub-cortical white matter, the cortex and the

hippocampus (75). Within hours after a TBI, the microglia adopted a pro-inflammatory, "classically activated" M-1 phenotype (75) exemplified by a significant upregulation of many M-1 markers including CD86, iNOS, MHC II, Nos2, IL-1β, CCL2, CXCL1(76). Only a few M-2 "alternatively activated" markers such as Arg-1, TGF-β, CCL22 and Lif (76) were upregulated, indicating that pro-inflammatory M-1 phenotype dominated in the early hours after concussive injury (75). However, other transcriptome analyses of microglia revealed that these states are transitory and during the chronic stage of microglial activation includes a mixed expression of both M-1 and M-2 phenotypic markers (55). The acute function of activated microglia following TBI is to migrate to the site of lesion, phagocytose cellular debris, re-establish a neuroprotective environment by orchestrating neurorestorative processes (54). However, microglia are also capable of producing inflammatory mediators such as reactive oxygen and nitrogen species, neurotransmitter glutamate and inflammatory cytokines (77). Depending on the amount released, glutamate can directly cause neurotoxic effects in neurons, synapses and astrocytic functions by hindering the glutamate buffering ability of astrocytes and blocking their glutamate transporters (78).

Microglial cells are commonly identified by their ionized calcium-binding adaptor molecule 1 (Iba-1), also referred to as allograft inflammatory factor 1 (AIF-1). This molecule is an actin binding protein involved in membrane ruffling and phagocytosis (79). This marker has been widely accepted to identify microglia, as well as tissue-resident macrophages and monocyte-derived macrophages but is not expressed by circulating or infiltrating monocytes (80).

1.7 Neutrophils

As the most abundant leukocyte in peripheral circulation and the earliest to arrive at the site of injury, neutrophils come armed with an array of antimicrobial effector molecules (81). Many human and animal studies have shown that following TBI, profound neutrophilia is found in the bloodstream both in absolute number (82-84) as well as in frequency (82, 84). Neutrophils are polymorphonuclear cells, generated and matured in the bone marrow from a myeloid precursor (85). They are located in the bone marrow, spleen, lungs, liver and in circulation, but rarely found in the brain parenchyma due to the BBB

(86). They become activated and/or differentiate into more mature effector cells depending on the environmental stimuli. Endogenous factors such as granulocyte-colony stimulating factor (G-CSF) and granulocyte-macrophage-colony stimulating factor (GM-CSF) (87) as well as external stimuli induced by stress or trauma (88) lead to the upregulation of different membrane receptors and expression of various granule proteins essential for degranulation and become phagocytic (89). Additionally, the list of neutrophil-derived cytokines is extensive (90, 91). Tumor necrosis factor (TNF) family; pro-inflammatory cytokines; CXC- chemokines; CC- chemokines as well as other anti-inflammatory, immunoregulatory, angiogenic and neurotrophic factors were all associated with TBI-induced cytokine release from neutrophils (92-97). Recruitment of neutrophils into the brain parenchyma and hence, their activation is associated with different characteristics of TBI. Hypoperfusion, seen in moderate to severe TBI cases enhances the interactions of neutrophils with blood vessels (98) increasing neutrophil adherence to endothelial cells (99). Neutrophil-derived neutrophil elastase (NE) (100, 101) and matrix metalloproteinase (MMP) also play a role in BBB dysfunction (102, 103). Free radicals generated by neutrophils also cause direct oxidative damage interfering with the BBB integrity (104).

1.8 Monocytes/Macrophages

Monocytes are crucial immune cells responsible for initiating innate immune responses (105). These myeloid-derived cells originate from the bone marrow and reside in peripheral blood and spleen until they are trafficked to the site of tissue injury. Monocytes are a heterogeneous population of inflammatory cells, making up 5-10% of leukocytes in the circulation. There are 3 subclasses of monocytes in humans, differentiated by their surface expression of CD14 and CD16: classical ($CD14^{++}16^{-}$), non-classical ($CD14^{lo/+}16^{++}$), and intermediate ($CD14^{++}16^{lo/+}$) (106). The role of each cell type has been studied extensively in infectious diseases, however, the importance of these cells in sterile injury is only just being elucidated. In a trauma-induced inflammatory cascade, classical monocytes are recruited out from the bone marrow and into the blood stream (105). Human studies have reported a significant elevation in the absolute number of circulating monocytes (83, 84) while murine models have shown a reduction in monocyte numbers in the early hours and days post-TBI (107). In mice, monocyte subtypes are classified into

classical ($Ly6C^+$) and non-classical ($Ly6C^-$), each with a unique phenotype and function. The classical monocytes have been described as inflammatory migrating cells that are recruited from the bone marrow to the inflamed tissues to produce TNFα and IL-1β. The chemokine, monocyte chemoattractant protein-1 (CCL2) is largely responsible for this monocyte chemotaxis along with its receptor, CCR2 (108). CCL2 is not only important for monocyte mobilization but it also promotes adhesion onto the endothelial vessel wall (109). Shown in a rat model of TBI, the epithelial cells of choroid plexus secreted CCL2 which encouraged monocyte migration across the blood-cerebrospinal fluid barrier (110). Once in the tissues, the classical monocytes differentiated into macrophages or dendritic cells (111). The non-classical monocytes arise from the classical monocytes with downregulated expression of Ly6C and are situated along blood vessel walls with the role of "patrolling" the vasculature (111). Thus, under conditions of injury and inflammation, non-classical monocytes rapidly extravasate into the tissues and participate as one of the first responders (112). Within the tissues, the non-classical monocytes convert into more specialized phagocytic cells such as $CD11c^+$ MHC II^+ dendritic cells and MHC II^+ macrophages (111). In a closed-head mouse model of TBI, while classical monocyte frequency is downregulated, the non-classical monocytes increase in circulation 60 days post-injury, suggesting that TBI shifts into an anti-inflammatory state (107). In parallel, when monocytes were isolated from TBI patients at that time post-TBI, IL-10 expression was upregulated, indicating an anti-inflammatory response in circulating monocytes (113).

While monocytes are in circulation, macrophages reside in tissues and have more of an M-2 phenotype to maintain tissue homeostasis. In disease pathology, the influx of pro-inflammatory monocytes at the site of injury outnumber the tissue-resident macrophages and differentiate into classically activated macrophages. Particularly in chronic inflammatory conditions and tissue degradation, macrophages stay activated, suppress their tissue-repair functions and delay wound-healing processes (114). Both monocytes and macrophages are not only implicated in TBI, but they also play a role in spinal cord injury, ischemic stroke injury, cardiovascular diseases as well as hepatic injury (114).

1.9 Systemic inflammatory response syndrome

It has been established in the literature that trauma evokes a systemic immune reaction that can often be more fatal than the initial primary injury itself (115). This acute, nonspecific immune response results in damage to organs by the cascade of inflammatory events that subsequently lead to sepsis which the individual is susceptible to (115). Collectively, this is called systemic inflammatory response syndrome (SIRS). Particularly following a severe injury such as severe TBI or spinal cord injury, the initial inflammatory cascade elicits the release of endogenous factors, DAMPs and alarmins that bind and activate innate immune cells via PRRs (116). Alarmins are defined as self-molecules that are released during non-programed cell death, by some immune cells and have the ability to initiate homeostasis and repair mechanism (53). DAMPs also activate the complement system, generating C3a and C5a (117, 118) further contributing to the pro-inflammatory milieu. Subsequently, pro-inflammatory mediators are rapidly generated and released into the damaged area and further contribute to an inflammatory state. Additionally, the increased pro-inflammatory cytokines also reduce the integrity of the blood brain barrier, allowing increased permeability. This not only permits the entry of peripheral cells and molecules to enter the CNS but the lesion-generated inflammatory mediators, DAMPs, cytokines and acute phase reactant mediators can now pass into the systemic circulation. Particularly, neutrophils have been shown to actively participate in migration to, sequestering in and damaging "by-stander" organs (119). Acute respiratory distress syndrome (ARDS) is a well-recognized complication in TBI patients and is a primary example of organ damage caused by a brain injury-driven systemic inflammatory responses. Neutrophils are known to migrate into the alveoli (120) and release toxic mediators including proteases and reactive oxygen species that normally function to kill pathogens but in the case of ARDS, also cause damage to healthy tissue. Alveolar edema and arterial hypoxaemia (121) occur as a result of increased lung epithelial and endothelial permeability (122). Importantly, although neutrophils are implicated in the acute development of SIRS, their functions are markedly decreased the following days after TBI (123).

Understanding of the mechanisms that mediate central regulation of immune functions through the autonomic nervous system has been a major development in the field of neuroimmunology (124). The discovery of the vagal nerve stimulation causing

attenuation of the systemic inflammatory response is an important concept related to TBI. Under inflammatory conditions, the brain sends signals via the vagus nerve to attenuate inflammatory cytokine production as a brain protective mechanism (125). The vagus nerve is the 10^{th} cranial nerve of the CNS, as a part of the parasympathetic nervous system, regulating critical organ functions necessary for survival. While 80% of the vagal nerve are sensory fibres, gathering information from the heart, liver, spleen and gastrointestinal tract, it also has the ability to sense and respond to peripheral inflammatory process through efferent fibres (125). Collectively, the efferent and afferent sensory fibers participate in a this mechanism known as the inflammatory reflex (126). The "Cholinergic anti-inflammatory pathway" has been termed to describe the regulatory activity of the vagus nerve carrying signals to resident macrophages via their primary neurotransmitter, acetylcholine (ACh) to modulate local and systemic inflammation (125, 127). Upon ligation of ACh to α7 nicotinic acetylcholine receptor on macrophages and dendritic cells, the major pro-inflammatory cytokine TNF's release was attenuated (127, 128). Thus, in TBI, this inflammatory reflex can become disrupted contributing to cytokine dysregulation and exacerbating the overall inflammatory response (125). Given the implication of inflammation in numerous diseases processes, the cholinergic anti-inflammatory mechanisms are being investigated for translational studies in animal models to humans.

1.10 Mouse models of TBI

Human TBI is challenging to study due to a large amount of heterogeneity in patient and injury characteristics with a wide variety of patient outcomes. To characterize such complex pathogenesis, no one pre-clinical animal model can capture the full breadth of TBI, thus many animal models have been developed and modified to enable systemic exploration of the concussion pathophysiology. Out of the various existing models of TBI that can be applied, the following four models have been shown to be well-suited for replicating concussive injuries; 1) fluid percussion injury (FPI), 2) Marmarou weight drop (WD) model, 3) the closed-head impact model of engineered rotational acceleration model (CHIMERA), and 4) the controlled cortical impact (CCI) (129).

FPI uses a hydraulic pressure pulse onto the exposed dura of the brain following a craniotomy. The pulse is generated when a pendulum strikes a fluid-filled piston. Mild,

moderate or severe injury can be achieved by adjusting the intensity of the pressure and this model has been used on a number of animals including mice, rats, cats and pigs to generate a diffuse brain injury that has corresponding pathological and neurobehavioral changes (130-132). Brain contusions are clearly visible in this model, along with pronounced microglial activation and astrocytosis (133, 134) while cerebral hypoxia, death and apnea are common complications from FPI due to brainstem trauma (135, 136). The weight drop model involves a mass that is dropped from a certain height onto a metal plate that is attached to the skull of an animal. The metal plate prevents the skull from fracturing while allowing the head to accelerate during the impact causing DAI, axonopathy, neuromotor and cognitive deficits (137-139). CHIMERA is a newer variation of closed head injury model that enables traumatic flexion of the cervical spine and additional rotational acceleration of the head causing a whiplash effect. The neuropathological consequences seen in this model are DAI, reactive microgliosis, the release of inflammatory cytokines, and hyperphosphorylated tauopathy (140). CCI also delivers a direct impact to the intact dura through a craniotomy by using a pneumatic piston. The depth, speed and duration of the impact can be adjusted according to each experiment. CCI causes cortical tissue loss, disturbance of the BBB, neuroinflammation, axonopathy and brain contusions (141-144). While this model enables a continuum of injury severity, it also induces tissue necrosis in and around the impact depression area. Thus, an alternative configuration of this model has been developed where the impact is made onto the skull (extracranial CCI) to reflect more of a human concussion. Each animal model has its unique strengths and limitations. One of the biggest weaknesses in all of these models is the requirement of anesthesia during experimental neurotrauma (145). This is important to consider because time-dependent changes in reflex responses latencies are commonly employed for initial neurological assessment following concussions in humans. These include corneal, papillary and pinna reflexes, which are metrics used to capture the constellation of neurological signs and symptoms of concussion which are not translatable in animal models (129). The impact of the anesthesia is compounded when these models are used to create a repetitive TBI model requiring anesthesia to be applied each time the animal is subjected to an experimental TBI. A common strength in these models is the robust secondary injury that is elicited in all TBI models. Currently, it is evident that no

one model encompasses all aspects of human concussion perfectly (146), and thus the development of new animal models and extrapolation of findings from different models need to be adopted. This study used the extracranial CCI, or a closed-head injury (CHI) model as this model reliably delivers controlled impact to the skull of each animal that allows for a consistently reproducible head injury that is reflective of a human concussion.

1.11 Lys-EGFP-*ki* transgenic mouse model

The *Lys*-EGFP-*ki* mice is a transgenic mouse model that expresses the enhanced green fluorescent protein (EGFP) gene into the murine lysozyme (lys) M locus. Lysozyme is highly expressed in myelomonocytic cells, thus, only mature, granulomyelomonocytic cells will exclusively be EGFP positive ($EGFP^+$) (147). This includes hematogenous macrophages, monocytes and neutrophils. The advantage of using this mouse strain is that it allows for the distinction between the hematogenous monocyte derived macrophages and the microglia which do not express EGFP.

1.12 Purpose, goals and objectives

In this study, I assessed the temporal and anatomical nature of the neural and systemic cellular inflammatory response to mTBI following repetitive concussive impacts using the extracranial CCI model. As there remains a clear medical need to treat brain injuries, there is a strong rationale supporting the need to understand and characterize TBI-associated inflammation within the CNS as well as in the periphery to identify targets for pharmacological interventions. To accomplish this, it is essential to select a suitable animal model for testing anti-inflammatory therapies post- TBI. This study can lay the foundation for the early pre-clinical testing in a mouse model of TBI of anti-inflammatory immunotherapies to limit secondary injury and promote regeneration. Advances in understanding the central and peripheral inflammatory responses to TBI can open a new frontier in ways we can manage and prevent the ramifications of concussion and other forms of TBI.

Thus, I hypothesize that the repetitive, closed-head injury of mTBI using a mouse model will initiate cellular inflammatory events in the brain and in the periphery manifested

via infiltration of hematogenous leukocytes. This will result in greater mature myeloid cell accumulation in the brain and in various organs, following the injury.

1.13 Specific aims

1) Qualitatively and quantitatively assess the spatial and temporal appearance of the microglial and the hematogenous myeloid inflammatory cell response in the brain after repetitive concussive impacts.
2) Quantitatively assess the systemic hematogenous myeloid cell response to repetitive concussive impacts.

CHAPTER 2 – MATERIALS AND METHODS

2.1 Animal ethics

In accordance with the *Canadian Guide to Care and Use of Experimental Animals*, all animal procedures were approved by Animal Care Committee at Western University (London, ON) and were performed according to the principles of the Guide for the Care and Use of Laboratory Animals (AUP# 2016-019, Expiry date: 10/01/2020, Appendix 1).

2.2 Lys-EGFP-*ki* mice

C57BL/6, *lysozyme*-EGFP-*knock in* (*lys*-EGFP-*ki*) transgenic mice were originally provided by Thomas Graf, from Albert Einstein College of Medicine (Bronx, NY). Homozygous *lys*-EGFP-*ki* mice were bred in the barrier facility at the West Valley Building, Western University. Animals were housed single-caged with a 12 h light/dark cycle and free access to food and water at all times. This study involved a total of approximately 80 animals (males and females combined) which were between 11-17 weeks of age and between 17g-32g in weight.

2.3 Pre-operative treatment

Prior to experimental use, the animals were acclimated for 1 week in the pre- and post-operative animal room. The experimental *lys*-EGFP-*ki* mice were anaesthetized using 4% isoflurane (Baxter Corporation, Mississauga, ON) in 2% oxygen, this was reduced and maintained at 3.5% isoflurane once the surgery began. The toe pinch reflex was performed to ensure the animals were anesthetized before the procedure commenced. The hair on the back of the head and neck was sterilized with 75% ethanol followed by a midline incision to peel back the skin and expose the skull.

2.4 Closed-head injury model

TBI was experimentally induced by a computer controlled Precision Systems Instruments TBI device (Lintech, Monrovia, CA). The piston settings to achieve the mild brain injury were the following: speed of 3.5m/s, depth of 1.5mm and dwell time of 500ms. The actual recorded impact speed can be found in Table 1. The 4mm silicone tip was set to

Table 1. The recorded velocity of the impactor shown in m/s

		mTBI Cohorts					
		8hr	24hr	48hr	72hr	1w	2w
mouse 1	day 1	3.62	3.59	3.67	3.82	3.62	3.61
	day 2	3.72	3.83	3.47	3.80	3.64	3.70
	day 3	3.58	3.72	3.62	3.79	3.59	3.58
mouse 2	day 1	3.44	3.57	3.76	3.86	3.86	3.78
	day 2	3.77	3.54	3.78	3.57	3.66	3.70
	day 3	3.55	3.56	3.64	3.73	3.79	3.74
mouse 3	day 1	3.61	3.65	3.79	3.56	3.69	3.67
	day 2	3.59	3.85	3.68	3.59	3.72	3.73
	day 3	3.42	3.73	3.56	3.54	3.60	3.72
mouse 4	day 1	3.75	3.70	3.74	3.72	3.68	3.59
	day 2	3.71	3.73	3.52	3.62	3.78	3.52
	day 3	3.61	3.58	3.85	3.62	3.86	3.66
mouse 5	day 1	3.74	3.74	3.54	3.74	3.59	3.61
	day 2	3.60	3.64	3.83	3.69	3.64	3.70
	day 3	3.72	3.66	3.49	3.59	3.84	3.51

impact the brain in the middle of the skull, on the bregma suture. Immediately following the impact, the mice were injected with an analgesic, Buprenorphine (RB Pharmaceuticals Ltd, Berkshire, UK; 0.05 mg/kg) after the injury. The incision was closed and sutured with 4-0 vicryl (Ethicon, USA) and the animals were placed under a heat lamp, in the dark for recovery. A total of three impacts were made, 24h apart. A group of sham-injured mice were also included in this study. Sham cohort received the same treatment as the injured group without the delivery of the impacts.

2.5 Perfusion

The mice were euthanized at 8h, 24h, 48h, 72h, 1- and 2-weeks post-surgery to evaluate the inflammatory response of circulating blood leukocytes to mTBI. Each time point included 6-10 mice of equal male/female ratio. For euthanasia, each mouse received a total of 50μL of ketamine (68 mg/mL) and xylazine (6.8 mg/mL) through intraperitoneal injection). The cardiac puncture method was used to withdraw peripheral blood from the right atrium of the heart after administration of 1μL of heparin (0.01 USP/mL). Subsequently, the spleens were harvested and placed on ice until processing.

Immediately following the removal of the spleen, a 23G perfusion needle was inserted into the left ventricle of the heart and the mice were perfused into the apex of the heart with 100mL of RPMI 1640 medium (Gibco by Life Technologies, Dulbecco's Modified Eagle Medium), followed by 100mL of freshly prepared 4% paraformaldehyde (PFA, polyoxymethylene, Bioshop Canada Inc., Burlington, ON) in phosphate-buffered saline (PBS). On completion of the perfusion, the following organs were removed: brain, cervical spinal cord, lungs, liver, kidneys, and heart. All organs were cryopreserved in 10%, 20% and 30% sucrose solutions for 24h each at 4 °C.

2.6 Cryosectioning

All organs were frozen and embedded in optimum cutting temperature compound (OCT) (Sakura Finetek, USA, Torrance, CA) and cryosectioned using the Leica Cryostat (Leica CM 1950). One lung and one lobe of the liver from each mouse were transversely sectioned in 16μm thickness. The cervical spinal cords were also cut in cross sections, in 16μm thickness. The peripheral organ sections were mounted onto a series of 6 Superfrost

plus-charged slides (Fisher Scientific, Pittsburgh, PA), with a distance of at least 96μm between each section on a single slide.

The brains were coronally sectioned to generate 20μm slices from the end of the olfactory bulb all the way to the beginning of the cerebellum. The brain sections were mounted in the same manner as described above for the organs, with a 120μm distance between each consecutive section on the same slide. Once the section of the brain directly underneath the bregma suture was identified and marked as 0mm, two consecutive sections 0.5mm and 1mm rostral to the bregma and two consecutive sections 0.5mm and 1mm caudal to the bregma were identified (5 sections in total), see Fig. 1. These sections were later co-stained for immunohistochemical analyses. All slides were stored at -20°C.

2.7 Blood processing and staining for flow cytometry

The blood collected from each mouse was processed and stained with appropriate antibodies to characterize the myeloid and lymphoid cell populations. 100μL of blood from each mouse was aliquoted to individual fluorescence activated cell sorting (FACS) tubes (Falcon, BD). All samples were incubated with LIVE/DEAD Fixable Aqua Dead Cell Stain (Thermo Fisher Scientific) in the dark for 20min. Then, fluorescently-labelled antibodies were added to the appropriate samples on ice for 20min. A comprehensive list of the antibodies used for the myeloid panel can be found in Table 2 and the antibodies used for the lymphoid panel can be found in Table 3. Anti-mouse CD19, NKp46, CD3ε and CD45 (BioLegend Inc., San Diego, CA) antibodies were used for the lymphoid panel. Anti-mouse CD11c, CD11b, CD45, Ly6G, Ly6C (BioLegend Inc.), CD115 (eBioscience Inc., San Diego, CA) and F4/80 (BIO-RAD, Hercules, CA) antibodies were used for the myeloid panel. All antibodies were incubated in a total cell suspension of 100 μL. Red blood cells (RBC) were lysed with BD Pharm Lyse Lysing buffer (BD) for 12 min before being washed with Hank's Balanced Salt Solution (HBSS) (Thermo Fisher Scientific) +0.1% bovine serum albumin (BSA) (EMD Millipore, Billerica, MA). Samples were then centrifuged at 4°C for 5min at 500xg, the supernatant was poured off and the cells were washed again with HBSS+0.1%BSA. All samples were resuspended in 200μL of HBSS+0.1%BSA and 100μL of 4% PFA. Finally, 50μL of CountBright Absolute Counting Beads (Thermo

Figure 1. The five alternate brain sections selected for analysis. The number above each brain image indicates the distance away from the bregma suture. 0mm section is the area directly underneath the bregma. +1mm section is 1mm distance rostral to the bregma and -1mm section is 1mm distance caudal to the bregma. The images were obtained from ©1999 RW Williams, designed by AG Williams, Atlas by T Capra.


+1mm
+0.5mm
0mm
-0.5mm
-1mm

Table 2. Antibodies used for the myeloid panel

Cell/Protein target	Antibody	Antibody dilution	Flurophore	RRID	Source
Macrophage	F4/80	1:200	PE	322048	BIO RAD
Dendritic cell	CD11c	1:80	PE/Dazzle 594	2563655	Bio Legend
Monocyte	CD115	1:160	PE-Cyanine7	2566460	Bio Legend
Myeloid Lineage	CD11b	1:400	Alexa 647	493546	Bio Legend
Leukocyte	CD45	1:500	Alexa 700	493715	Bio Legend
Neutrophil	Ly6G	1:40	Brilliant Violet 421	2562567	Bio Legend
Monocyte	Ly6C	1:200	Brilliant Violet 711	2562630	Bio Legend
Dead cells	Live/Dead Aqua Vital Dye	1:200	N/A	N/A	Thermo Fischer Scientifc

Table 3. Antibodies used for the lymphoid panel

Cell/Protein target	Antibody	Antibody dilution	Flurophore	RRID	Source
T cell	CD3ε	1:40	Brilliant Violet	11203705	Bio Legend
B cell	CD19	1:1500	PE	313643	Bio Legend
NK cell	Nkp46	1:50	APC	10612758	Bio Legend
Leukocyte	CD45	1:500	Alexa 700	493715	Bio Legend
Dead cells	Live/Dead Aqua Vital Dye	1:200	N/A	N/A	Thermo Fischer Scientific

Fischer Scientific) were added and the samples were stored in the dark at 4°C. UltraComp antibodies capture beads (eBioscience Inc.) were used for electronic compensation.

2.8 Spleen processing and staining for flow cytometry

The spleens collected from each mouse were minced and pushed through a 70μm filter (Falcon, BD) into a 50mL falcon tube. Splenocytes were washed with 1x PBS and spun at 4°C for 5min at 500xg, the supernatant was poured off and the cells were resuspended in 4mL of RPMI media. Cells were filtered again with a 40μm filter, washed with 1x PBS and spun at 4°C for 5min at 500xg, the supernatant was poured off and the cells were resuspended in 5mL of ammonium chloride lysis buffer (Stemcell Technologies, Vancouver, BC) for 7min to lyse RBC. Additional PBS was added to each sample before the spin and discarding of the supernatants and resuspension in 1x PBS. The cell suspensions were stained using the same protocol as for blood.

2.9 Flow cytometry

Blood cells and splenocytes were analyzed by an LSRII analytical flow cytometer (BD). All samples were run for maximum event collection and the data was analyzed using FlowJo Software version 10 (Tree Star Inc., Ashland, OR).

2.10 Iba-1 and EGFP co-staining for immunohistochemistry

To phenotype the EGFP cells and distinguish them from the microglial cells, the sectioned brains were co-stained with anti-Iba-1 and anti-GFP specific antibodies. Iba-1 is a calcium ion binding protein expressed on macrophages and microglia (79). On day 1, the slides were extensively washed with PBS and blocked for 3h with 5% normal goat serum (Jackson ImmunoResearch Laboratories, Inc., West Grove, PA) and 0.3% Triton X-100 (Bioshop, Burlington ON) for non-specific binding. The slides were then incubated with a rabbit monoclonal anti-Iba-1 antibody (1:300) (Abcam, Cambridge, United Kingdom) at 4° C overnight in the dark. On Day 2, the slides were briefly washed with PBS before being incubated with a secondary goat anti-rabbit IgG directly conjugated to Alexa 546 (1:500) (Life technologies, Eugene, OR) at room temperature for 1h. Finally, the slides were stained with Alexa 488 conjugated anti-GFP rabbit polyclonal antibody (1:1000) (Invitrogen,

Carlsbad, CA) overnight at 4°C in the dark. On Day 3, the slides were washed and rinsed in double distilled (DD) water before being air-dried and cover-slipped with hard set mounting media containing DAPI (4,6-diamidino-2-phenylindole, Vector Laboratories, Burlingame, CA). A comprehensive list of all antibodies used for immunohistochemistry can be found in Table 4. The specificity of the Iba-1 antibody was confirmed by staining one section with the Iba-1 primary antibody and one section without the primary antibody. A representative image showing this specificity can be found in Appendix 2.

2.11 Ly-6G DAB staining for immunohistochemistry

DAB (3,3′-Diaminobenzidine) is a derivative of benzene and when oxidized by hydrogen peroxide, a brown precipitate forms. To distinguish between the neutrophils and the monocytes in the brain, DAB staining with Ly-6G antibody from the DAB peroxidase substrate kit (Vector Laboratories, Inc., Burlingame, CA) was used. Neutrophils are $Ly6G^{+}EGPF^{+}$ and monocytes are $Ly6G^{-}EGPF^{+}$. The slides were extensively washed with PBS followed by quenching of endogenous peroxidases using 3% H_2O_2 solution (RW Packaging Ltd., Winnipeg, MB) in PBS for 10 min at room temperature. Then, slides were washed with PBS and the sections were blocked with 5% normal goat serum for 2h at room temperature. Next, sections were blocked with fragment goat anti-mouse IgG (0.13mg/mL; Sigma Life Science) in PBS for 2h at room temperature to reduce non-specific binding of mouse IgG (Fc fragment specific). Then, the slides were incubated with biotin conjugated anti-mouse Ly-6G (1:300; eBiocience Inc.) overnight at 4°C. The next day, slides were washed with PBS, and incubated with secondary antibody horse radish peroxidase (HRP) conjugated to streptavidin (1:500; Invitrogen) for 1h. Following 4 washes with DD water, DAB solutions from the DAB peroxidase substrate kit were added for 7-10 min. The slides were then rinsed with DD water and air-dried before being dehydrated and cover-slipped with Cytoseal mounting media (Thermo Fisher Scientific).

Spleen and excitotoxin brain sections were provided by a previous Master student in the Dekaban Lab, Oleksandr Prokopchuk, who used an excitotoxin-induced model of TBI to study immune responses in the CNS.

Table 4. Antibody used for immunohistochemistry

Cell/Protein target	Antibody	Antibody Dilution	Flurophore	RRID	Source
Microglia & Macrophage	Primary Rabbit monoclonal anti-Iba-1	1:300	N/A	2636859	Abcam
Microglia & Macrophage	Secondary goat anti-rabbit	1:500	Alexa 546	2534077	Life technologies
Monocyte/Macrophage Neutrophils	Rabbit anti-GFP	1:1000	Alexa 488	221477	Invitrogen
Endothelial cells	rabbit polyclonal anti-CD31	1:300	N/A	726362	Abcam
Endothelial cells	Secondary goat anti-rabbit IgG	1:300	Alexa 546	2534077	Invitrogen
Neutrophils	fragmented goat anti-mouse IgG	0.13mg/mL	N/A	N/A	Sigma Life Science
Neutrophils	biotin conjugated monoclonal Anti-mouse Ly-6G	1:300	N/A	469757	eBioscience
Neutrophils	secondary antibody HRP conjugated to streptavidin	1:500	N/A	N/A	Invitrogen

2.12 CD31 and EGFP co-staining for immunohistochemistry

In order to evaluate whether $EGFP^+$ cells enter the brain from the blood stream, the brain sections were stained for CD31, a platelet endothelial cell adhesion molecule. On day 1, all slides were washed extensively with PBS and blocked with 5% normal goat serum and 0.3% Triton X-100 for non-specific binding for 3h. The slides were then incubated with the rabbit polyclonal anti-CD31 antibody (1:300; Abcam) at 4° C overnight in the dark. On Day 2, the slides were briefly washed with PBS before being incubated with secondary goat anti-rabbit IgG directly conjugated to Alexa 546 (1:300) at room temperature for 1h. Finally, the slides were incubated with Alexa 488 conjugated anti-GFP rabbit polyclonal antibody (1:1000) overnight at 4° C in the dark. On Day 3, the slides were washed with PBS and rinsed in DD water before being air-dried and cover-slipped with hard set mounting media containing DAPI.

2.13 Silver staining

To detect axonal damage in the concussed brains, 50μm sections were cut on the cryostat and preserved as floating sections in 4% PFA for 1 week. Using FD NeuroSilver™ Kit II (FD NeuroTechnologies, Inc.), the exact protocol provided in the user manual was followed. Upon completion, the floating sections were mounted on a superfrost plus-charged slides, washed in xylene before being coverslipped with cytoseal. The sections were viewed with a light microscope (Olympus BX50) and Q-Imaging Retiga 1300 camera was used to image the silver stained sections.

2.14 Fluorescent microscopy

The Iba-1/EGFP stained brain sections along with the chosen peripheral organ slides were cover-slipped using hard set mounting media containing DAPI. All brain sections were viewed on the epifluorescent microscope (Olympus IX50) and imaged at 10X magnification using a digital camera Q-Imaging Retiga 1300. Only certain areas of the brain region were imaged due to the large area of the whole brain. In total, eleven areas were individually acquired from one section of the brain. See Fig. 2 below for the areas that were imaged. These areas capture the most prominent parts of the brain; superior and lateral cerebral cortex, corpus callosum, hippocampus, third and lateral ventricles, cerebral

Figure 2. Areas of the brain that were acquired on the epifluorescent microscope. Each area labeled A to K were individually imaged at 10x magnification. These areas capture the most prominent parts of the brain; superior (A&B) and lateral cerebral cortex (D&G), the third ventricle (C), corpus callosum, hippocampus and lateral ventricles (E&F), cerebral peduncles and cerebral nuclei (H&I), optic tract and hypothalamus (J&K). The image of this brain was obtained from Melbourne Brain Center by Dr. Kay L Richards.

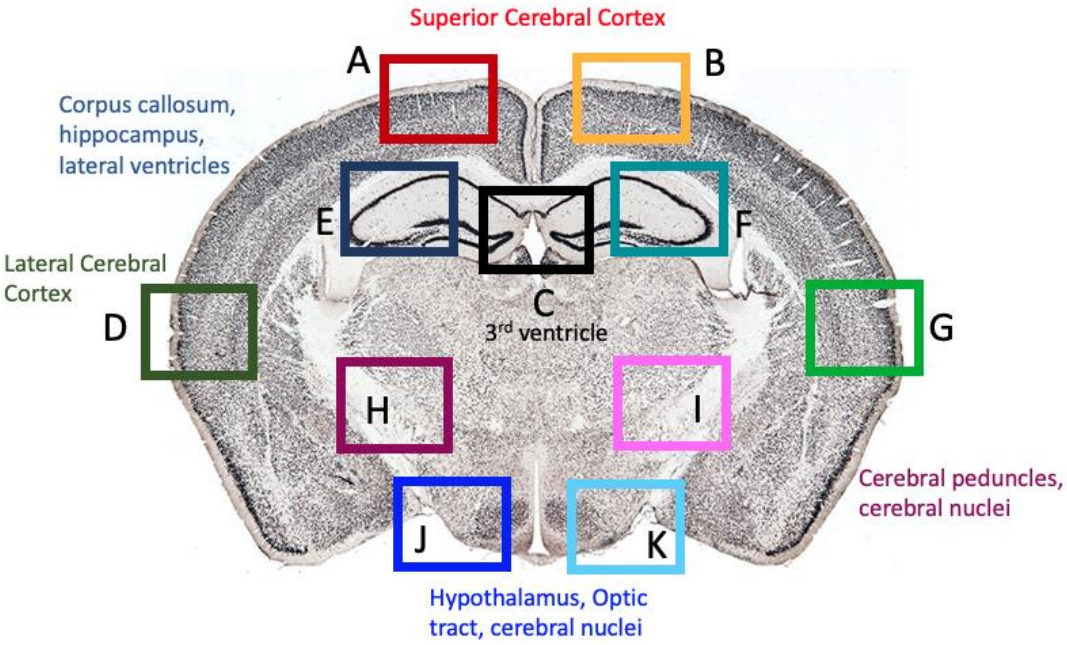
Superior Cerebral Cortex
A
B
Corpus callosum, hippocampus, lateral ventricles
E
F
Lateral Cerebral Cortex
D
C
3rd ventricle
G
H
I
Cerebral peduncles, cerebral nuclei
J
K
Hypothalamus, Optic tract, cerebral nuclei

peduncles, optic tract, hypothalamus and cerebral nuclei. The Olympus GFP and RFP filter cubes were used appropriately to capture EGFP and Iba-1 fluorescent signal, respectively.

All other organs slides including the lungs, livers and spinal cord sections were viewed and imaged on the EVOS FL Auto 2.0 microscope (Thermo Fisher Scientific). For each organ, five alternating sections were chosen to be acquired at 10x magnification to generate images of the entire organ. The 10x tiles were automatically tiled using the EVOS software. The GFP excitation wavelength of 470 nm and emission wavelength of 510 nm were used for GFP channel imaging, and 357 nm excitation and 447 nm emission wavelengths were used for DAPI channel imaging.

2.15 Digital morphometry

All images taken on the Olympus and EVOS fluorescent microscopes were viewed and the fluorescent signal was quantified using Image Pro Plus 7.0. Tissue sections were traced to outline the area of interest (AOI), excluding any spaces that are not part of the tissues, and any morphological abnormalities that were attributed to cryosectioning. Using manual colour selection, a mask was created to capture Iba-1 or EGFP fluorescent signals. The same mask was used for the five alternating sections of one organ (lung, liver, spinal cord). This allows consistency from one section to the next, picking up pixels above the threshold defined by the mask. Then, the program calculated the "area of EGFP fluorescence per AOI" and the average of all the five sections from one organ was generated.

For each brain, five alternate sections 500μm apart were selected, stained, and analyzed. The final Iba-1/EGFP fluorescence was determined by the taking the mean of individual "area of Iba-1/EGFP fluorescence per AOI" number from the five alternate sections. For example, the "area of Iba-1/EGFP fluorescence per AOI" number of "area A" was determined from each of the five alternate sections and those numbers were then averaged. The same thing was done for all areas A-K. This method of averaging the immunofluorescence from five alternate sections was used to produce graphs in the following figures, with the exception of graphs from Fig. 4. Thus, each point on the graph with the exception from Fig. 4 will represent the average of "A's, B's, C's" etcetera... from one brain. See Fig. 3 below.

2.16 Confocal microscopy

Images of microglial, EGFP and CD31 cells at a higher power were acquired on a Leica-TSC SP8 confocal microscope (Leica Microsystems, Concord, ON) at 63x magnification. This part of the project was done in conjunction with Dr. Natalie Kozyrev.

2.17 Statistical analysis

Kruskal-Wallis one-way analysis of variance (ANOVA) followed by post-hoc Dunnett's tests were performed for the statistical analyses using GraphPad Prism software version 7.0 (GraphPad Software Inc, La Jolla, CA). Sample size for each group of animals was between 4 to 10 except for the group of animals used for silver staining, where n=3-4. Data is presented as a group mean ± standard mean of error (SEM). Differences were considered significant when $p \leq 0.05$.

Figure 3. Method of analysis for quantifying brain immunofluorescence. For each brain, five alternate sections were analyzed. Each “area of fluorescence per AOI” of “area A” from the five sections were determined individually, then the average immunofluorescence was calculated. This method was applied to all areas from A to K.

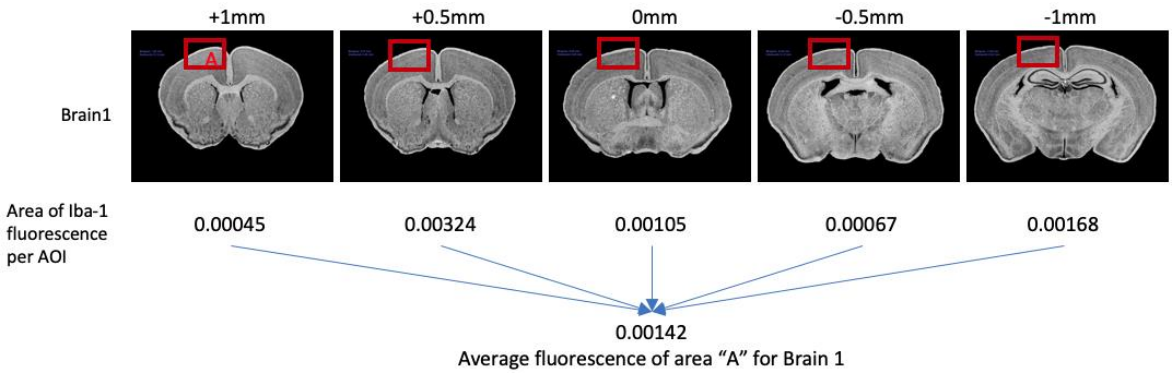
+1mm
+0.5mm
0mm
-0.5mm
-1mm
A
Brain1
Area of Iba-1 fluorescence per AOI
0.00045
0.00324
0.00105
0.00067
0.00168
0.00142
Average fluorescence of area “A” for Brain 1

CHAPTER 3 – RESULTS

3.1 Closed-head injury model of repetitive concussion is a diffuse brain injury

Examining different areas within the same section of the brain and looking at five different sections within the same brain showed that this model of closed-head, repetitive concussion is a diffuse brain injury. Five alternate sections from each brain are shown in Fig. 4A with 0mm being the area directly underneath the bregma. I observed that while there were differences in the Iba-1 and EGFP immunoreactivity between the time points (8h, 24h, 48h, 72h, 1w, 2w) compared to controls, there were no spatial differences (+1mm, +0.5mm, 0mm, -0.5mm, -1mm) in the immunoreactivity within each time point. Thus, the increase in Iba-1 immunoreactivity at 8h compared to control is relatively constant regardless of which section is chosen within the same brain. The spatial progression of Iba-1 immunoreactivity at each time point in areas A&B and E&F showed no significant differences between the five sections within each brain (Fig. 4B). The spatial progression of EGFP immunoreactivity within the same time points in areas A&B and E&F also showed no significant differences (Fig. 4C). Similarly, areas; C, D&G, H&I, J&K showed no significant differences between the five alternate sections at any given time point (graphs not shown). Taken together, the inflammatory response as seen by the increase in Iba-1 and EGFP immunoreactivity following repetitive mTBI at the indicated time points are consistent throughout the analyzed brain structure (from +1mm to -1mm). Since the tip of the impactor is 4mm in diameter, the five sections I have chosen were directly underneath the area of impact. However, other sections of the brain away from the site of injury should also be looked at to conclude whether no spatial difference in immunoreactivity exists in all sections of the brain.

3.2 Increased microglial activation and Iba-1 immunoreactivity in repetitive mTBI brains

To characterize the local CNS-specific inflammatory response following repetitive concussion in a closed-head injury model, the brains of the mice were removed at 8h, 24h, 48h, 72h, 1w and 2w post-injury, sectioned and doubled stained with Iba-1 and GFP antibodies. This allows for the distinction of Iba-1^{+}/$EGFP^{-}$ microglia and Iba-1^{+}/$EGFP^{+}$ hematogenous macrophages and Iba-1^{-}/$EGFP^{+}$ monocytes and neutrophils. Each area of

Figure 4. Closed-head, 3 hit model of concussion produces a diffuse brain injury. The five alternating sections from each brain are shown (A) with 0mm being the area directly underneath the bregma. The spatial progression of Iba-1 immunoreactivity at each time point (CNTR, 8h, 24h, 48h, 72h, 1w, 2w) in areas A&B and E&F area shown (B). Similarly, other areas of the brain including C, D&G, H&I, J&K showed no significant differences between the five alternate sections (graphs not shown). The spatial progression of EGFP immunoreactivity at the same points in areas A&B and E&F also showed no significant differences (C). No significant differences were found between +1mm, +0.5mm, 0mm, -0.5mm and -1mm in all the examined time points. One way ANOVA followed by Dunnett's test was performed, significance was determined when *= $p \leq 0.05$. Data is presented as the group mean ± SEM with 4-5 mice per group.

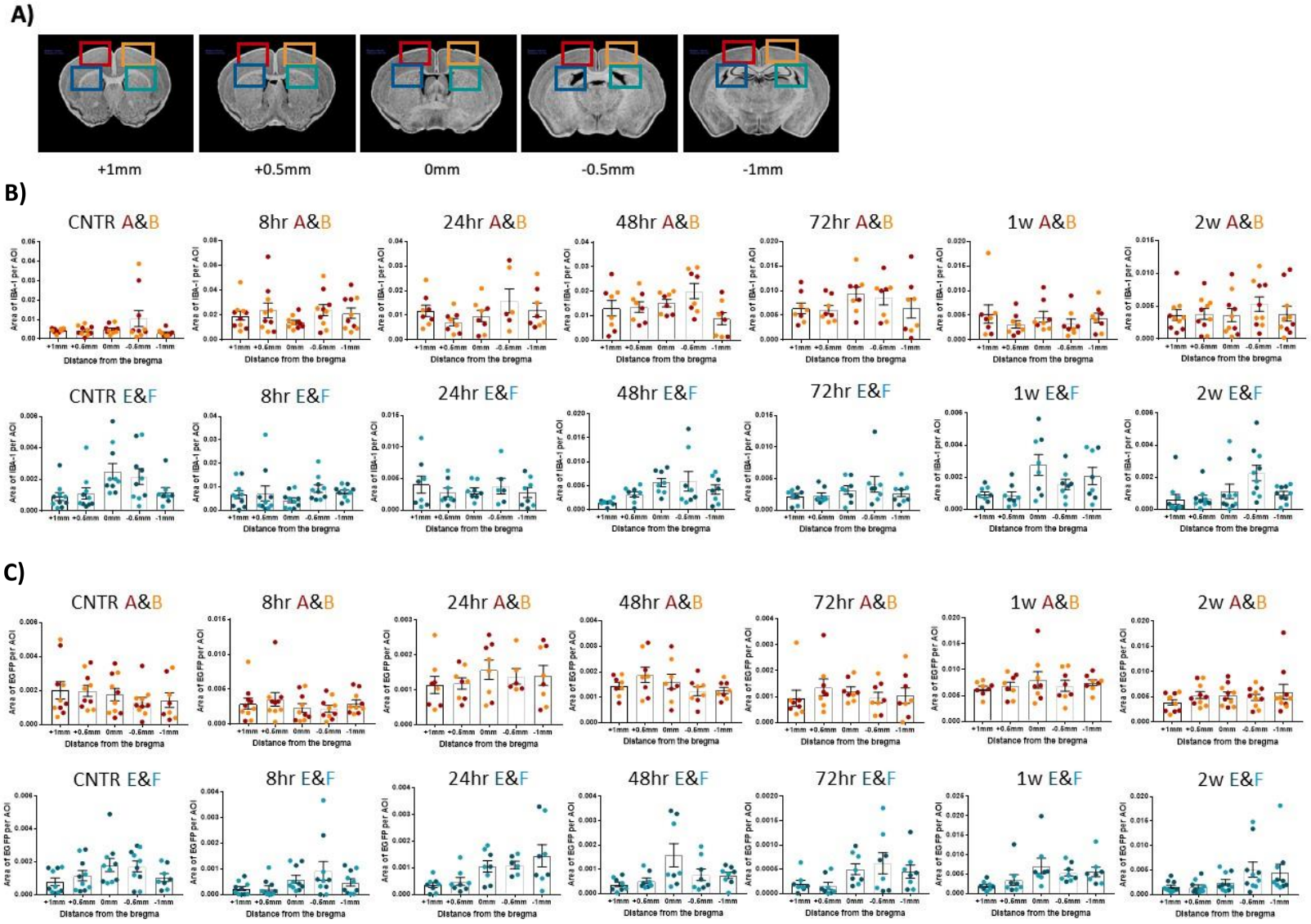
A)
+1mm
+0.5mm
0mm
-0.5mm
-1mm
B)
CNTR A&B
8hr A&B
24hr A&B
48hr A&B
72hr A&B
1w A&B
2w A&B
CNTR E&F
8hr E&F
24hr E&F
48hr E&F
72hr E&F
1w E&F
2w E&F
Area of IBA-1 per AOI
Distance from the bregma
C)
Area of EGFP per AOI

Figure 5. Summary of the temporal assessment of Iba-1 immunoreactivity in the control and repetitive mTBI brains. Quantified Iba-1^{+} area within the AOI, as determined by digital morphometry are shown in various areas of the brain at the indicated time points. Significant increase in Iba-1 immunoreactivity were found at 8h $p<0.0001$ and 48h $p=0.0015$ post-injury in areas containing the superior cerebral cortex (A) as well as the 3^{rd} ventricle $p=0.0064$ (B) lateral cortex $p<0.0001$, $p<0.0001$ (C), hippocampus and corpus callosum $p<0.0001$, $p=0.0113$ (D), cerebral peduncles nuclei $p=0.0015$, $p=0.0275$ (E) and hypothalamus, optic tract and cerebral nuclei $p=0.0052$, $p<0.0001$ (F) all showed the same pattern of increase in immunoreactivity at 8h and 48h. One way ANOVA followed by Dunnett's test was performed, significance was determined when $*=p\leq0.05$. Data is presented as the group mean ± SEM with 4-5 mice per group.

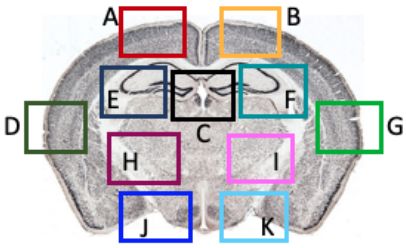
A
B
C
D
E
F
G
H
I
J
K

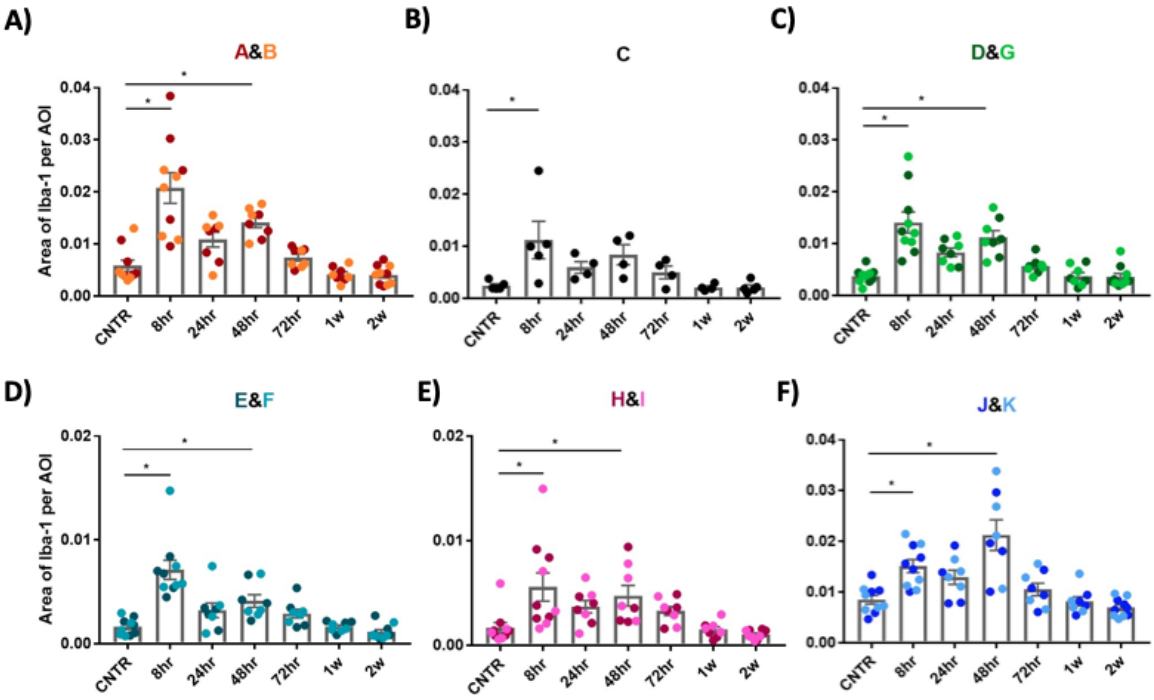
A)
A&B
B)
C
C)
D&G
D)
E&F
E)
H&I
F)
J&K
Area of Iba-1 per AOI
CNTR
8hr
24hr
48hr
72hr
1w
2w

the brain labeled A to K (Fig. 5) were individually imaged and quantified by digital morphometric analyses. Compared to the controls, animals that sustained three concussive impacts had significantly higher Iba-1 immunoreactivity, reflective of microglial activation at 8h and 48h post-concussion for areas A and B which contain regions of the superior cerebral cortex (Fig. 5A). Examining other areas of the brain, the lateral cortex (Fig. 5C), hippocampus and corpus callosum (Fig. 5D), cerebral peduncles nuclei (Fig. 5E) and hypothalamus, optic tract and cerebral nuclei (Fig. 5F) all showed the same pattern of increase in immunoreactivity at 8h and 48h. The area of Iba-1 immunoreactivity encompassing the third ventricle and corpus callosum (Fig. 5B) was only significant at 8h. In all areas, the Iba-1 immunoreactivity returned to baseline levels by 1 week. Although the data showed no statistical significant increase in Iba-1 immunoreactivity at 24h, there was still a noticeable increase compared to controls. This may represent a biological significance, albeit statistically not significant.

Digital brain images representative of the quantitative findings are presented in Fig. 6. Compared to the controls (Fig. 6A, D), the mTBI brains had increased Iba-1 immunoreactivity at 8h (Fig. 6B, D), which returned to control levels by 1 week (Fig. 6C, F) in both the cerebral cortex and in the corpus callosum. Fluorescent images of Iba-1 at 48h were reflective of that shown at 8h (data not shown). Changes in microglial morphology were also clearly noticeable. While "resting" and quiescent microglia have a ramified morphology, activated microglia take on a hypertrophied and bushy appearance. In the control brains, ramified microglia were observed (Fig. 7A, D) while activated phenotype was evident at 8h post-injury in both the cortex and corpus callosum in the 3-hit brains (Fig. 7B, E). Iba-1 immunoreactivity decreased back to control levels at 1 week following repetitive concussion, although some microglia appeared to remain activated (Fig. 7C, F).

3.3 Recruitment of EGFP$^+$ myeloid peripheral immune cells into the brain following repetitive concussion

Using the same double stained sections imaged for Iba-1, temporal assessment of EGFP immunoreactivity was determined. A significant increase in EGFP immunoreactivity was not observed until 1 and 2 weeks post-injury in all imaged areas of the brain (areas A-

Figure 6. Representative images of Iba-1 immunoreactivity in the superior cortex and corpus callosum. Fluorescent microscopic images of control and mTBI brains at 8h and 1 week post-injury are shown. Panel A shows the superior cortex and panel D shows the corpus callosum of control brains. Panel B shows the superior cortex and panel E shows the corpus callosum of mTBI brains at 8h. Panel C shows the superior cortex and panel F shows the corpus callosum of mTBI brains at 1 week. All images were acquired on the Olympus IX50 microscope at 10x magnification.

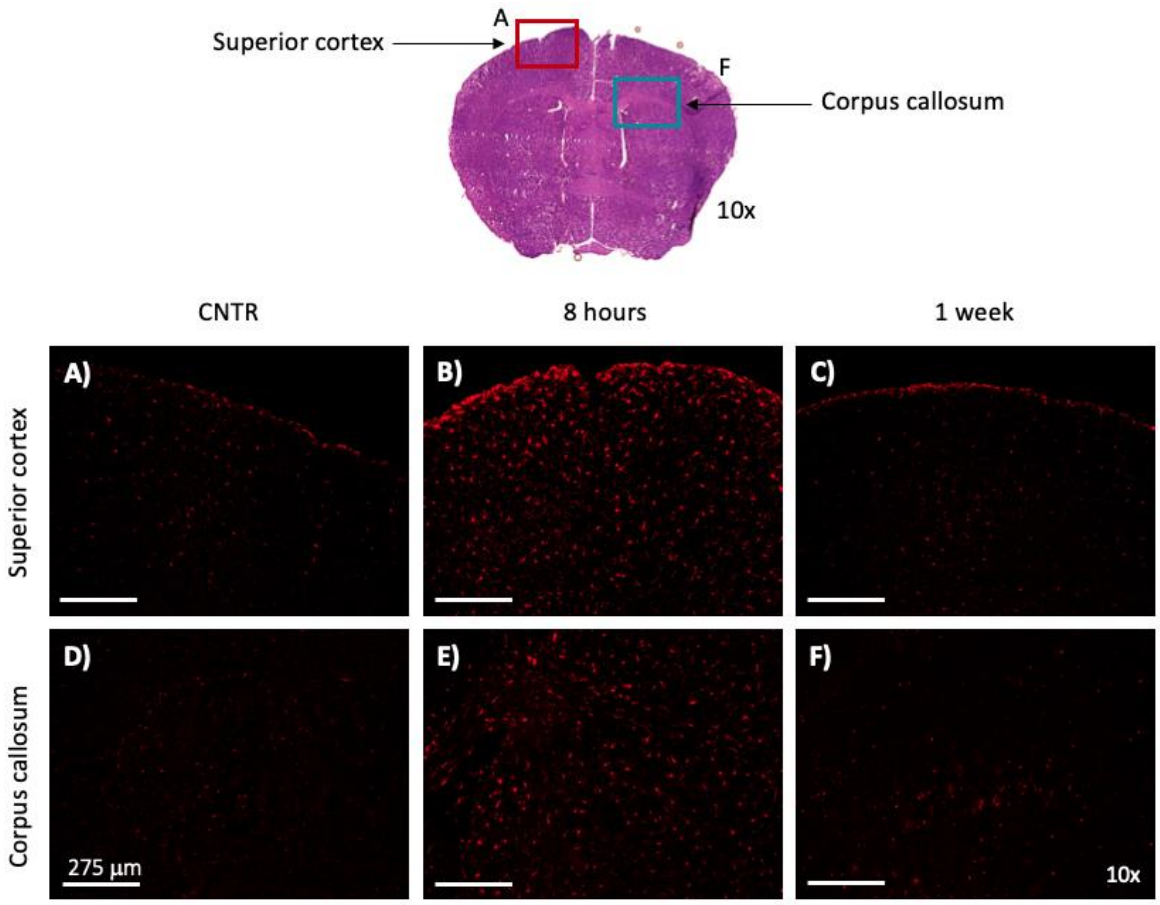
A
Superior cortex
F
Corpus callosum
10x
CNTR
8 hours
1 week
A)
B)
C)
Superior cortex
D)
E)
F)
Corpus callosum
275 µm
10x

Figure 7. Representative images of the change in microglial morphology following repetitive concussive injury. Images of small and ramified microglial morphology from the control brains in the superior cortex (A) and corpus callosum (D) are shown. Hypertrophied and busy microglial cells in the superior cortex and corpus callosum in mTBI brains at 8h (B, E) and 1 week (C, F) are shown. All images were acquired on the confocal microscope at 63x magnification.

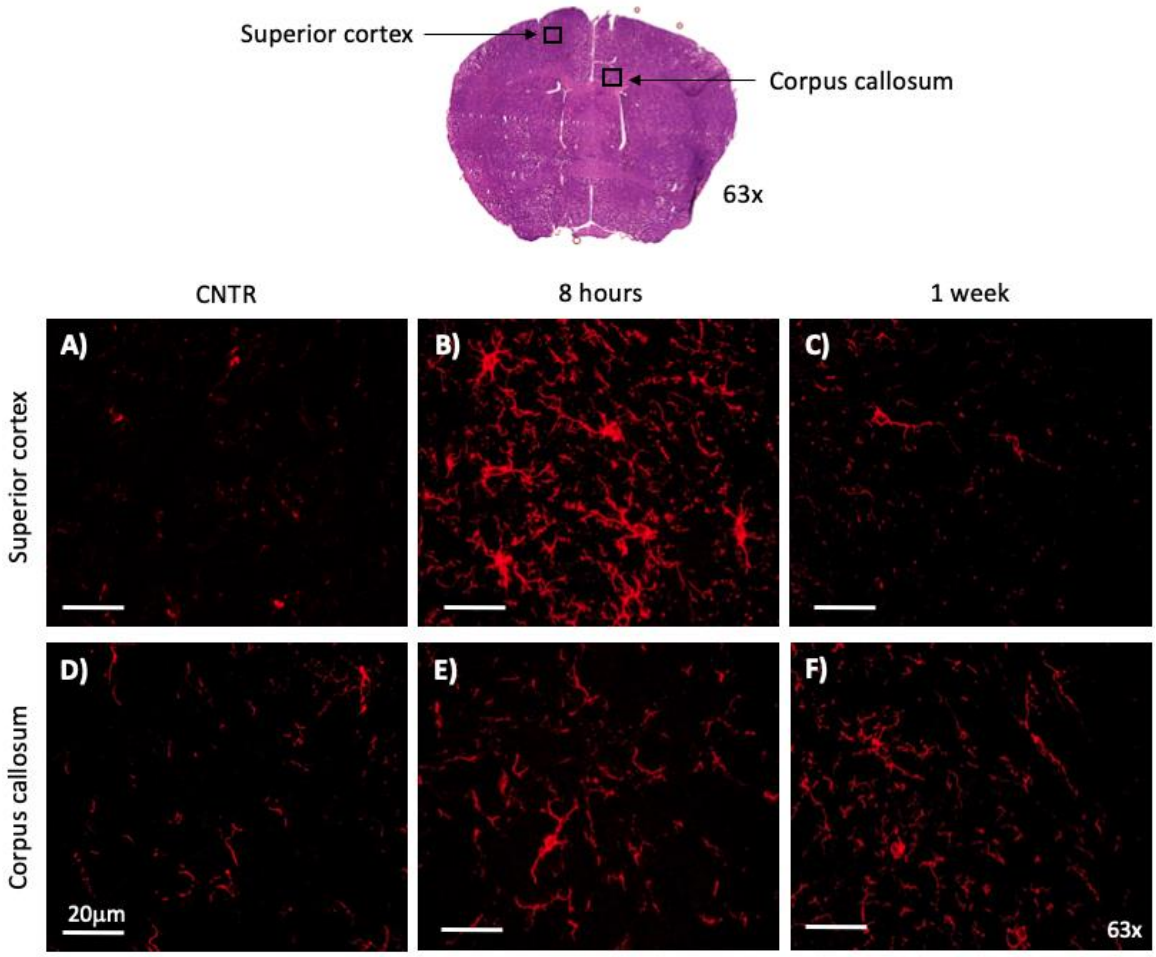
Superior cortex
Corpus callosum
63x
CNTR
8 hours
1 week
A)
B)
C)
D)
E)
F)
Superior cortex
Corpus callosum
20µm
63x

Figure 8. Summary of the temporal assessment of EGFP immunoreactivity in the control and mTBI brains. Quantified $EGFP^+$ area within the AOI, as determined by digital morphometry are shown in various areas of the brain at the indicated time points. Significant increases in EGFP immunoreactivity were found at 1 week $p<0.0001$ and 2 weeks $p<0.0001$ post-injury in areas containing the superior cerebral cortex (A) as well as the 3^{rd} ventricle $p=0.0033$, $p=0.0108$ (B) lateral cortex $p<0.0001$, $p<0.0001$(C), hippocampus and corpus callosum $p<0.0001$, $p=0.0042$ (D), cerebral peduncles nuclei $p<0.0001$, $p<0.0001$ (E) and hypothalamus, optic tract and cerebral nuclei $p<0.0001$, $p<0.0001$ (F) all showed the same pattern of increase in immunoreactivity at 1 and 2 weeks. One way ANOVA followed by Dunnett's test was performed, significance was determined when *= $p\leq0.05$. Data is presented as the group mean ± SEM with 4-5 mice per group.

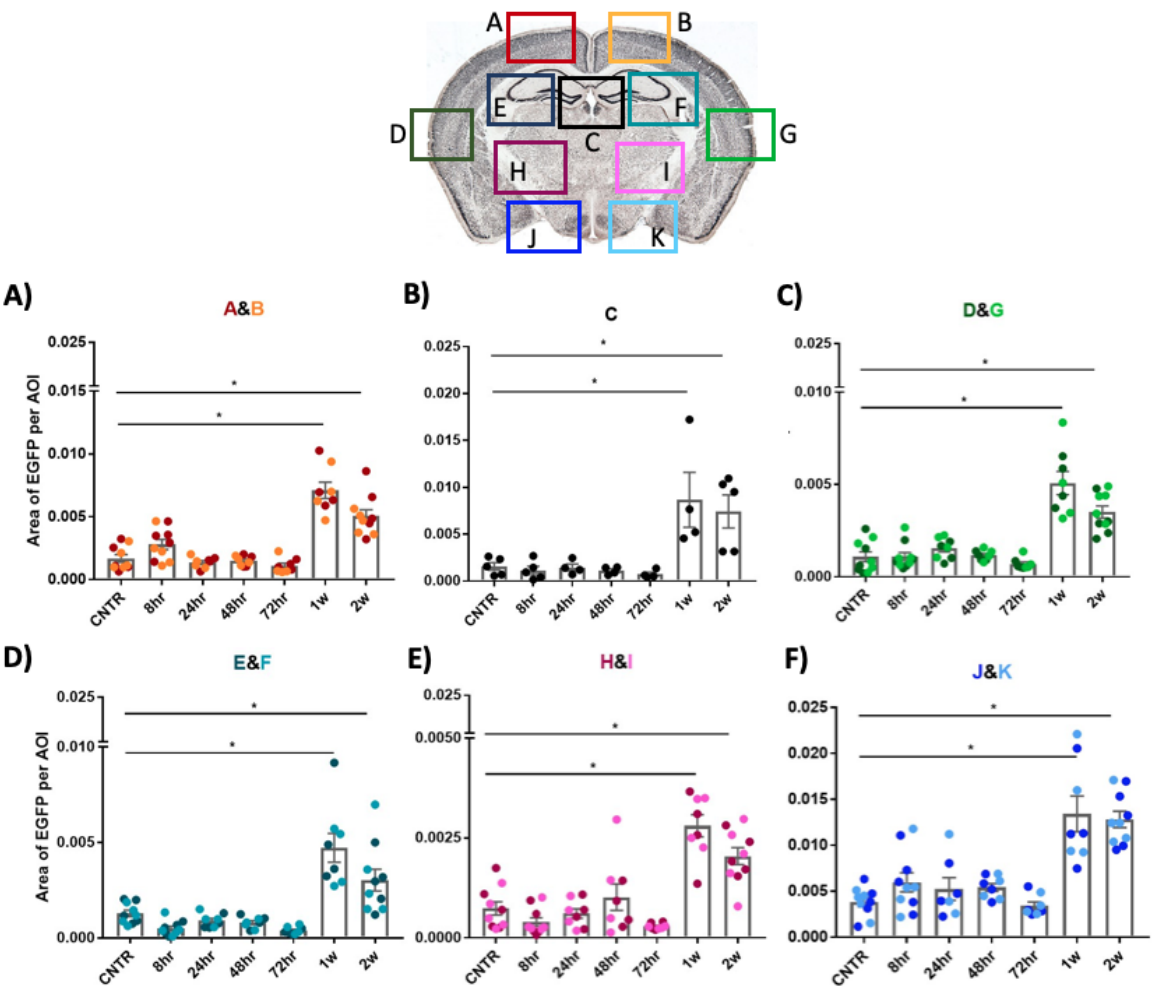
A
B
C
D
E
F
G
H
I
J
K
A)
A&B
B)
C
C)
D&G
D)
E&F
E)
H&I
F)
J&K
Area of EGFP per AOI
CNTR
8hr
24hr
48hr
72hr
1w
2w

Figure 9. Representative images of EGFP immunoreactivity in the superior cortex and corpus callosum. Fluorescent microscopic images of control and mTBI brains at 8h and 1 week post-injury are shown. Panel A shows the superior cortex and panel D shows the corpus callosum of control brains. Panel B shows the superior cortex and panel E shows the corpus callosum of mTBI brains at 8h. Panel C shows the superior cortex and panel F shows the corpus callosum of mTBI brains at 1 week. All images were acquired on the Olympus IX50 microscope at 10x magnification.

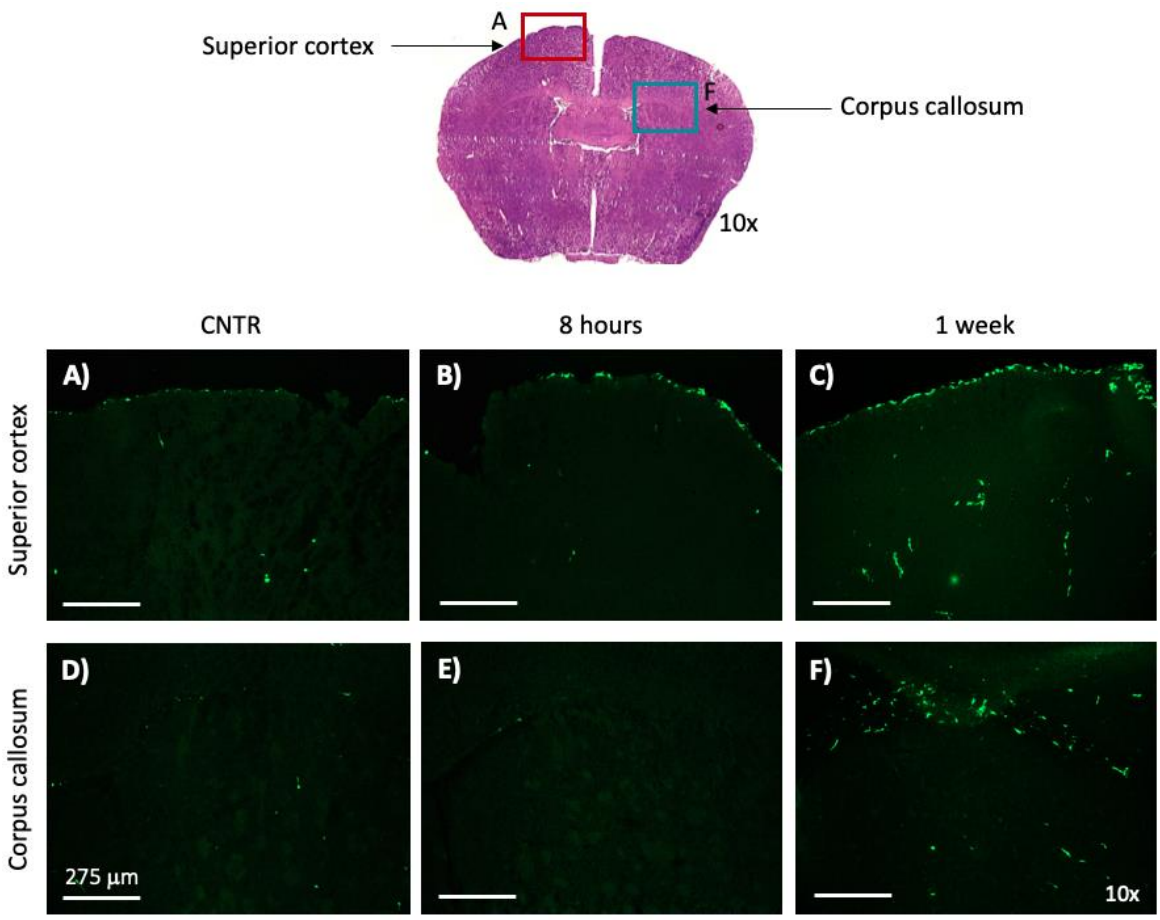
A
Superior cortex
F
Corpus callosum
10x
CNTR
8 hours
1 week
A)
B)
C)
Superior cortex
D)
E)
F)
Corpus callosum
275 µm
10x

K; Fig. 8). Representative immunohistological images showed no difference in EGFP immunoreactivity at 8h after repetitive concussion (Fig. 9B, E) compared to controls (Fig. 9A, D) but a significant increase was distinctly visible at 1 week post-injury (Fig. 9C, F) in both the cortex and corpus callosum. Similarly, 2 weeks following repetitive mTBI showed significant EGFP immunoreactivity compared to controls (data not shown). Additionally, comparing between the different regions within one brain section, areas A&B, C and J&K had the highest levels of EGFP immunoreactivity.

3.4 No neutrophils were found in the mTBI brains

There are three predominant types of $EGFP^+$ cells in the *lys*-EGFP-*ki* transgenic mice; neutrophils, monocytes and macrophages. To phenotype these cells and distinguish them from the brain resident microglial cells, the sections that were double-immunostained with Iba-1 and EGFP antibodies were observed more closely to see which cells co-expressed or independently expressed Iba-1 and EGFP. As microglia are $EGFP^-Iba\text{-}1^+$ and hematogenous macrophages are $EGFP^+Iba\text{-}1^+$ and hematogenous monocytes and neutrophils are $EGFP^+Iba\text{-}1^-$, a merged image of EGFP and Iba-1 showed these phenotypes (Fig. 10C, F).

To determine if any of the $EGFP^+$ myeloid cells were neutrophils, the brain sections were stained with a neutrophil marker Ly6G. As the most abundant leukocyte in the circulation and the first responder to injury and inflammation, neutrophils are known to extravasate into the brain parenchyma following TBI (148). However, Ly6G staining showed that very few cells were $Ly6G^+$ (Fig. 11). A stained section of a spleen served as a positive control (Fig. 11A) to confirm the staining procedure, and another section was stained without the addition of the primary antibody to show Ly6G specificity (Fig. 11B). A separate section of a brain from an excitotoxin TBI injury showed $Ly6G^+$ neutrophils (Fig. 11C), however, in the closed-head repetitive mTBI model, almost no neutrophils were found in any of the brain regions. Fig. 11D shows the absence of neutrophils in the mTBI brain at 24h, and this is a representative image for all the time points examined.

3.5 $EGFP^+$ myeloid cells are found in the parenchyma, pia mater, along the choroid plexus and in the brain microvasculature

Figure 10. Representative images of EGFP and Iba-1 double immunofluorescence staining in the cortex of mTBI brains. Superior and lateral cortex areas of mTBI brains at 1 week showing EGFP immunoreactivity (A, D) Iba-1 immunoreactivity (B, E) and merged images of EGFP and Iba-1 immunoreactivity (C, F) are shown. Arrow heads indicate whether they are monocytes or neutrophils, microglia or macrophages. All images were taken on the confocal microscope at 63x magnification.

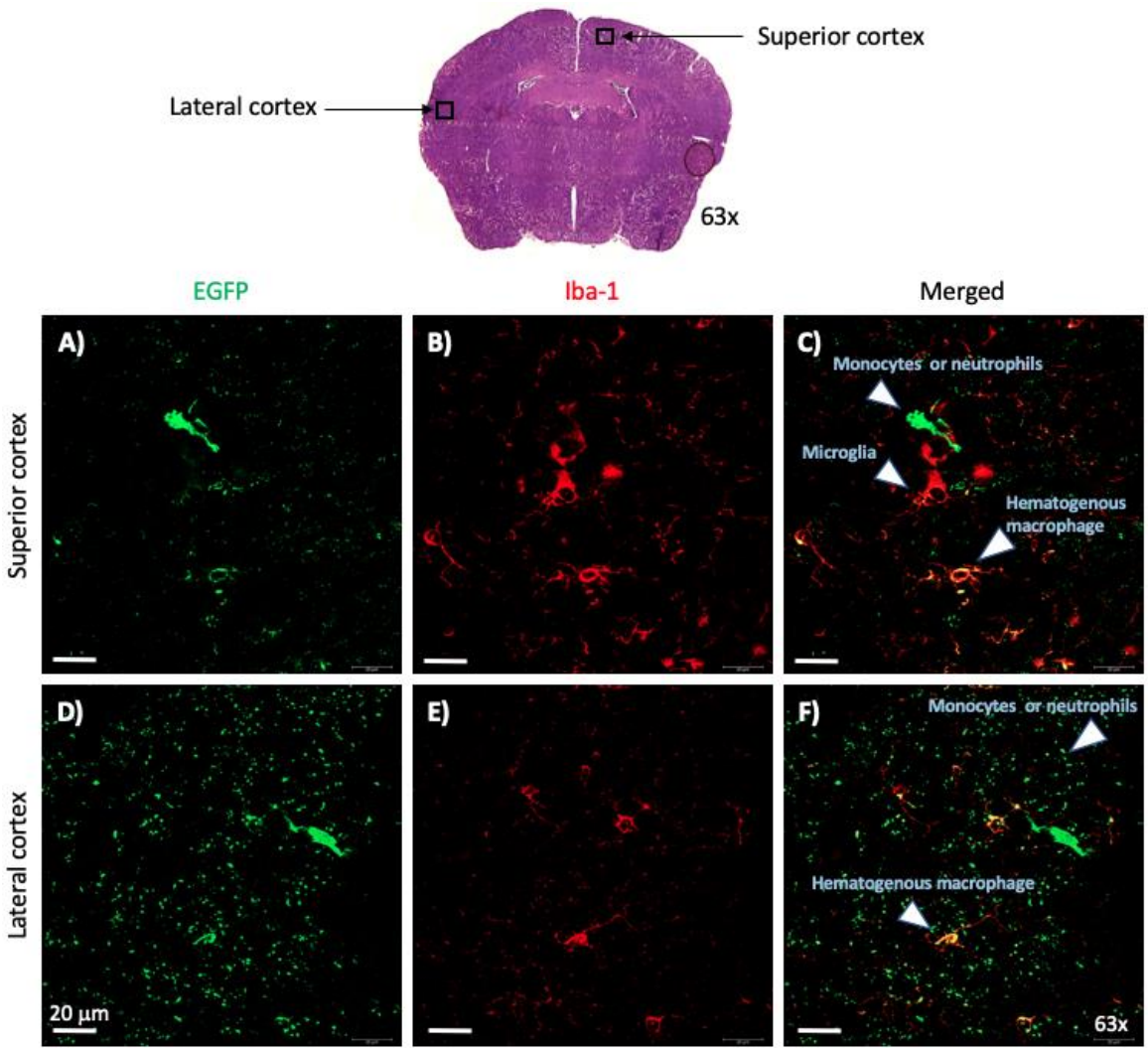
Superior cortex
Lateral cortex
63x
EGFP
Iba-1
Merged
A)
B)
C)
Monocytes or neutrophils
Microglia
Hematogenous macrophage
Superior cortex
D)
E)
F)
Monocytes or neutrophils
Hematogenous macrophage
Lateral cortex
20 µm
63x

Figure 11. Almost no neutrophils get recruited to the brain following repetitive mTBI. Spleen was used as a positive control for the staining procedure (A), and the absence of a primary antibody served as a negative control (B). A separate section of a brain from an excitotoxin TBI injury showed $Ly6G^{+}$ neutrophils at 24h (C) while no neutrophils were found in the closed-head repetitive mTBI brains at 24h (D). All images were acquired on the EVOS fluorescent microscope at 20x magnification.

Spleen – 1˚ antibody

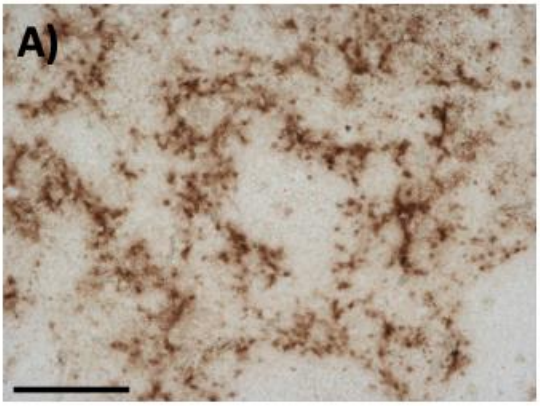

Spleen – no 1˚ antibody

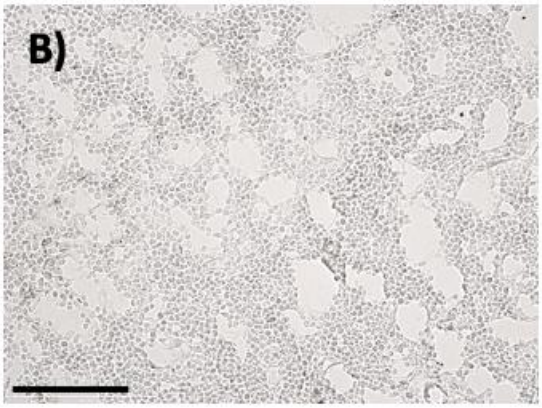

Excitotoxin Brain

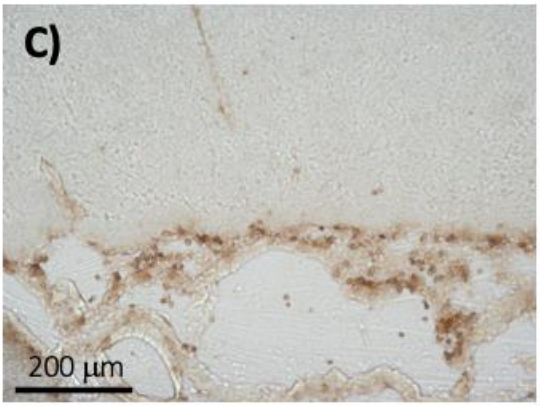

mTBI Brain

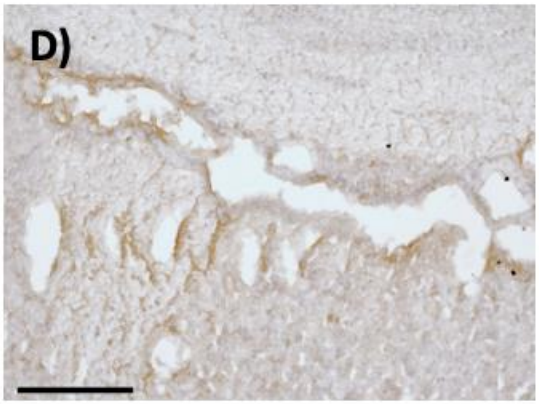

A separate set of brain sections were double-immunostained with antibodies recognizing EGFP and blood-vessel endothelial marker CD31. This was to determine the location of the $EGFP^+$ myeloid cells and if these cells emerge from the brain microvasculature or through the choroid plexus of the lateral ventricles. Fluorescent images revealed that many larger, phagocytic looking $EGFP^+$ cells were in the brain parenchyma in the cortex and in the corpus callosum (Fig. 12C, F). However, in the surrounding area, some smaller $EGFP^+$ cells were found to be co-localized with $CD31^+$ microvessels indicating the presence of these cells inside the microvasculature (Fig. 12C). Many $EGFP^+$ cells were also found along the edge of the cortex, likely in the pia mater (Fig. 13C, F), but they did not co-localize with CD31. Lastly, $EGFP^+$ myeloid cells were located along the choroid plexus within the lateral (Fig. 14C) and 3rd ventricle (Fig. 14F), but again, did not co-localize with CD31. Altogether, this suggests that the blood-derived myeloid cells entered the brain through the microvasculature and located in the parenchyma, pia mater and the ventricles.

3.6 White matter abnormalities found after repetitive concussion

Silver staining is used to observe white matter tract abnormalities based on the idea that degenerating neurons become argyrophilic, meaning that they have an affinity for silver. Silver staining was also performed on a separate group of mice (uninjured controls and those that received 3 closed-head hits; n=3-4 per time point) and sacrificed 72h, 1 and 2 weeks post-injury. The corpus callosum was mainly examined to detect axonal pathology as this structure is the main white matter tract in the brain. The silver staining data showed no visual axonal damage in the controls (Fig. 15A) or in the 72h mTBI brains (Fig. 15C). Additionally, a very small number of $EGFP^+$ cells were found in the corpus callosum (Fig. 15B, D). However, a noticeable increase in axonal injury was evident at 1 and 2 weeks following repetitive concussion as indicated by strings of small black staining beads (Fig. 15E, G). The presence of $EGFP^+$ myeloid cells was also clearly visible in the corpus callosum at 1 and 2 weeks after repetitive concussion (Fig. 15F, H).

3.7 Repetitive concussion alters circulating monocyte and neutrophil frequencies in blood and spleen

Figure 12. Representative images of $EGFP^+$ cells that are found in the brain parenchyma. $EGFP^+$ cells are shown in green (A, D) and endothelial cells of blood vessels are shown in red (B, E). Merged images of EGFP and CD31 showed $EGFP^+$ cells located in the microvessels as well as in the parenchyma, indicated by arrow heads (C, F). All images were taken on the confocal microscope at 63x magnification.

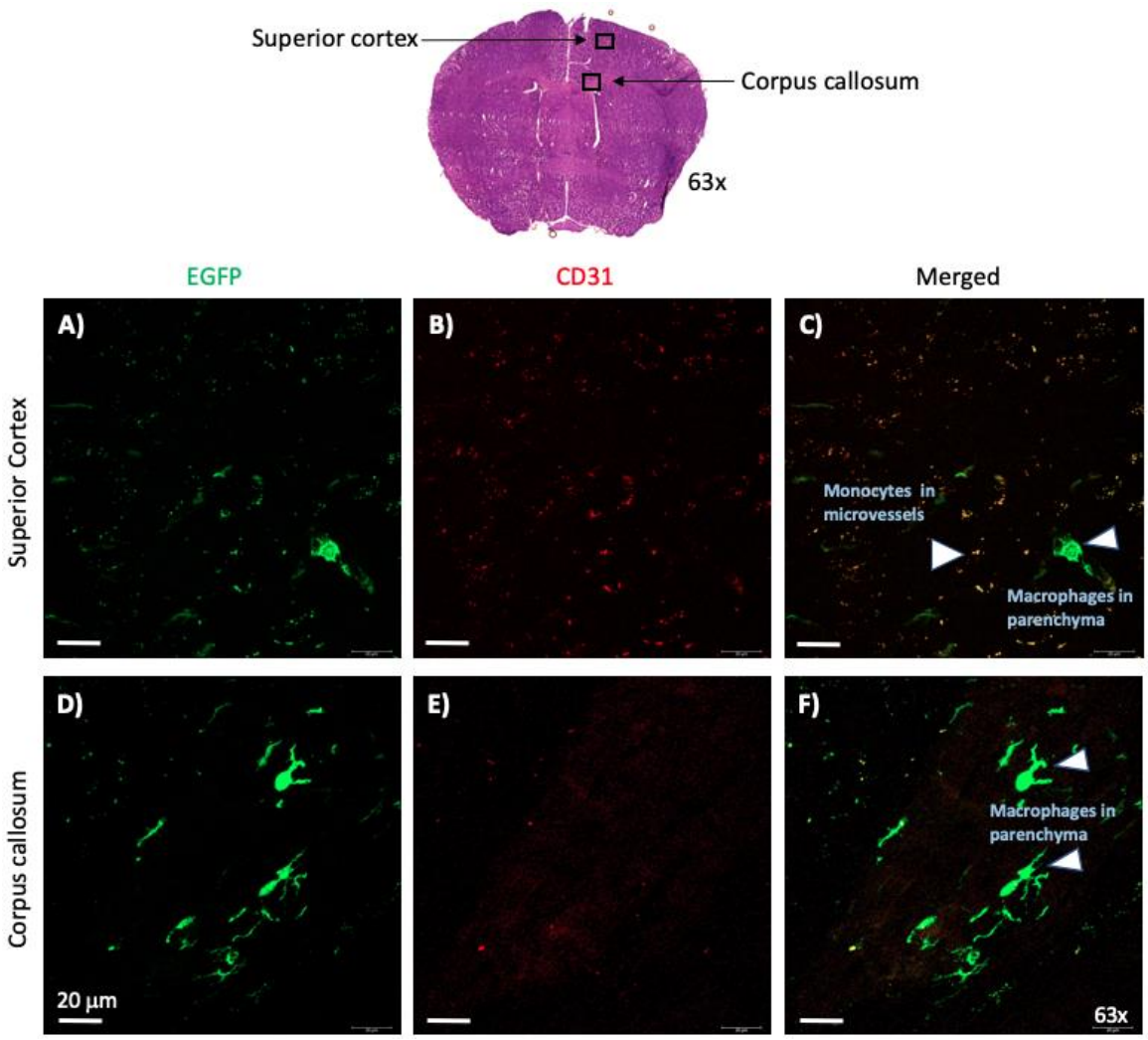
Superior cortex
Corpus callosum
63x
EGFP
CD31
Merged
A)
B)
C)
Superior Cortex
Monocytes in microvessels
Macrophages in parenchyma
D)
E)
F)
Corpus callosum
Macrophages in parenchyma
20 µm
63x

Figure 13. Representative images of $EGFP^+$ cells that are distributed along in the edge of the cortex, in the pia mater. $EGFP^+$ cells in the pia mater of superior and lateral cortex are shown in green (A, D) and endothelial cells of blood vessels are shown in red (B, E) and merged images of EGFP and CD31 are also shown (C, F). All images were taken on the confocal microscope at 63x magnification.

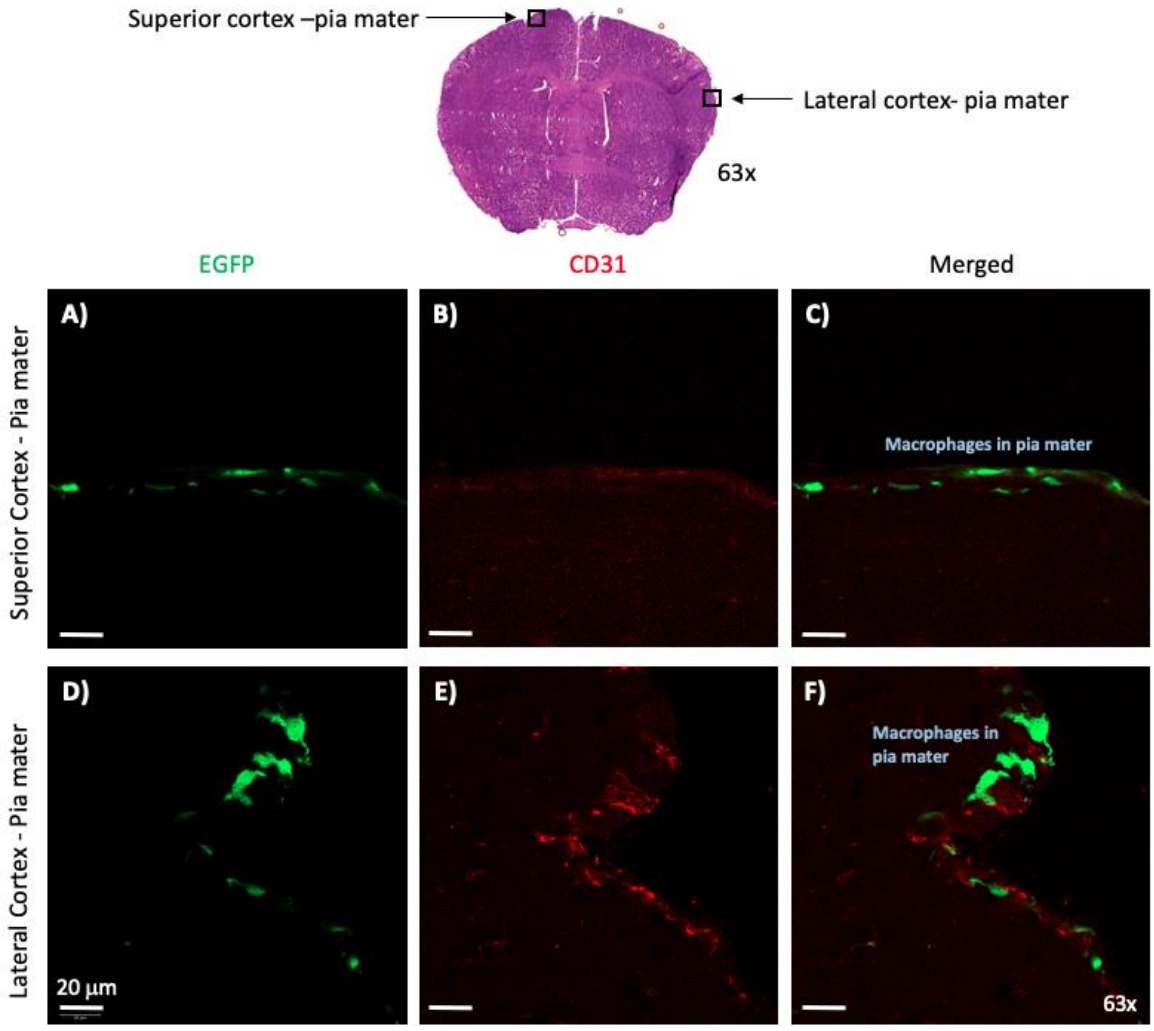
Superior cortex –pia mater
Lateral cortex- pia mater
63x
EGFP
CD31
Merged
A)
B)
C)
Macrophages in pia mater
Superior Cortex - Pia mater
D)
E)
F)
Macrophages in pia mater
Lateral Cortex - Pia mater
20 µm
63x

Figure 14. Representative images of $EGFP^+$ cells that are found along the choroid plexus in the lateral and 3^{rd} ventricles. $EGFP^+$ cells are shown in green (A, D) and endothelial cells of blood vessels are shown in red (B, E) and merged images of EGFP and CD31 are also shown (C, F). All images were taken on the confocal microscope at 63x magnification.

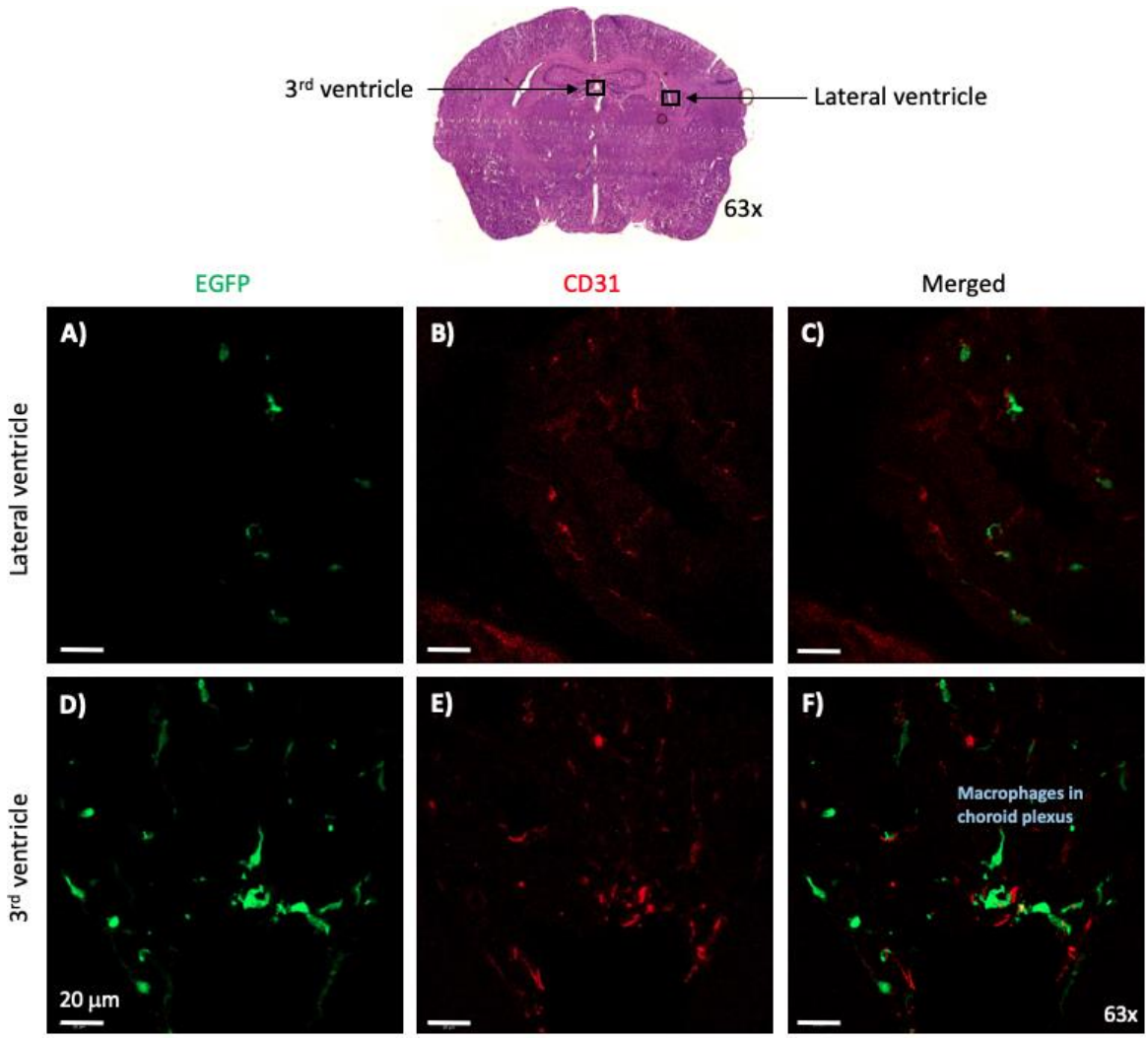
3rd ventricle
Lateral ventricle
63x
EGFP
CD31
Merged
A)
B)
C)
D)
E)
F)
Lateral ventricle
3rd ventricle
20 µm
Macrophages in choroid plexus
63x

Figure 15. Axonal pathology found in mTBI brains, 1 and 2 weeks following repetitive concussion. Silver staining was performed on control (A) and repetitive mTBI brains at 72hr (C), 1 week (E) and 2 weeks (G). Adjacent EGFP fluorescent images of areas surrounding the corpus callosum are shown at the corresponding time points (B, D, F, H). The rounded black spots in panels A and C show the stained nuclei of the axons. The arrows in panels E and G indicate the silver varicosities while the arrow heads in panels B, D, F and H point to the $EGFP^{+}$ cells in the corpus callosum. Images of silver stained sections were acquired at 40x magnification on the Olympus BX50 microscope and the fluorescent images were acquired at 10x magnification by the EVOS microscope.

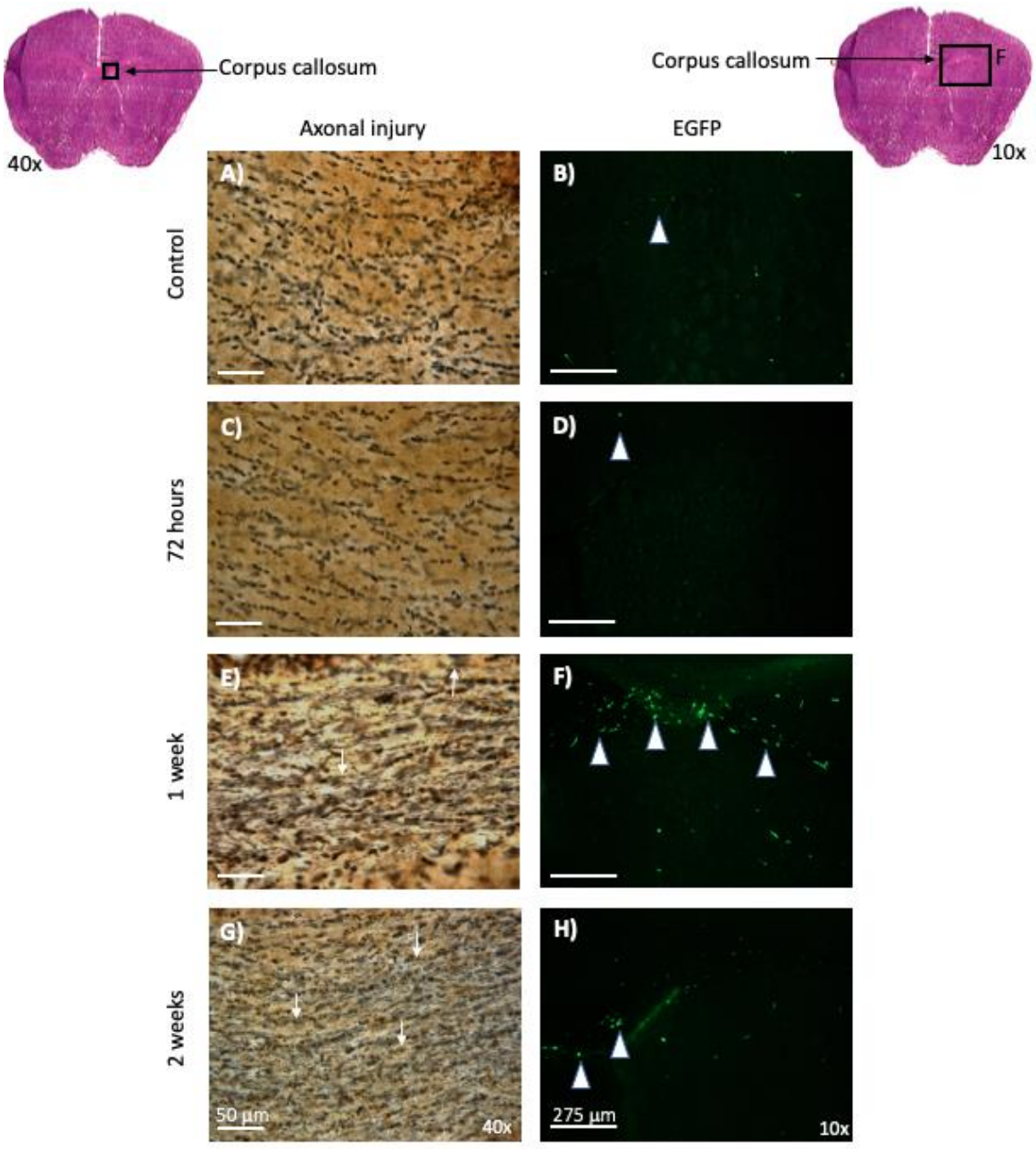
Corpus callosum
40x
Corpus callosum
F
10x
Axonal injury
EGFP
Control
72 hours
1 week
2 weeks
A)
B)
C)
D)
E)
F)
G)
H)
50 µm
40x
275 µm
10x

To investigate the effects of repetitive concussion on circulating neutrophils and monocyte subsets, the leukocyte frequencies in peripheral blood and spleen were assessed. Peripheral whole blood samples and spleens from the control, sham-injured and closed-head 3 hit mice cohorts were stained and analyzed by flow cytometry. Cell populations were determined using gating strategies for flow cytometry to delineate specific populations of myeloid cells (Appendix 3). Initial gating selected for, live, single $CD45^+$ hematopoietic lineage cells and negatively selected for myeloid cells by selecting out $CD19^+$, $CD3^+$, $NKp46^+$ lymphocyte lineage cells. After gating the myeloid cells for $CD11b^+Cd11c^+$ cells, this population was separated based on the expression of F4/80 or Ly6G. The $F4/80^+$ population was then selected for $CD115^+$ surface expression followed by Ly6C surface expression. Pro-inflammatory $CD11b^+F4/80^+CD115^+Ly6C^{+/hi}$ and non-classical monocytes $CD11b^+F4/80^+Ly6C^{lo/+}$, while neutrophils are distinguished by $CD11b^+F4/80^-Ly6G^+$. EGFP expression was detected in all relevant myeloid subsets, while EGFP was not detected in the blood-derived lymphocyte subsets of T, B and NK cells. The graphs show the percentages of each of the cell populations out of the total number of $CD45^+$ leukocytes. The results showed that in peripheral blood, the classical monocyte frequency decreased significantly from 8h-1week post-concussion and increased back to control levels at 2w (Fig. 16A). The non-classical monocytes however, increased slightly up to 1week before significantly increasing at 2 weeks (Fig. 16B). The trend for neutrophil frequency was similar to the trend seen in classical monocytes, the neutrophils in circulation decreased from 8h-1week before significantly increasing at 2 weeks (Fig. 16C). However, in the spleen, while classical monocytes decreased slightly from 8h to 1week post-injury (Fig. 16D), non-classical monocytes (Fig. 16E) and neutrophil (Fig. 16F) frequencies remained at control levels at the same times but also increased after 2 weeks.

3.8 Repetitive concussion causes some changes in the adaptive immune cells in blood and spleen

To determine the effects of repetitive concussion on circulating lymphocytes, B cell, T cell and NK cell frequencies in peripheral blood and spleen were assessed. The gating strategy for the lymphoid panel is shown in Appendix 4. The cells were first gated for the $EGFP^-$ population, followed by single, live $CD45^+$ cells, then $CD19^+$ B cells, and finally

Figure 16. Innate immune cell frequencies in peripheral blood and spleen following repetitive concussion. $Ly6C^+$ Classical monocytes, $Ly6C^-$ non-classical monocytes and $Ly6G^+$ neutrophils were identified using flow cytometry. Circulating classical monocyte frequency were significantly decreased at 8h $p=0.0162$, 24h $p=0.0089$, 48h $p=0.0141$, and 1week $p=0.0052$ post-injury (A), while non-classical monocytes significantly increased at 2 weeks $p=0.0002$ (B) and neutrophils were also significantly increased at 2 weeks $p<0.0001$ (C). In the spleens, the classical and non-classical monocyte frequencies significantly increased at 2 weeks $p=0.0231$, $p<0.0001$ (D, E). One way ANOVA followed by Dunnett's test was performed, significance was determined when *= $p\leq0.05$. Data is presented as the group mean ± SEM with 6-10 mice per group.

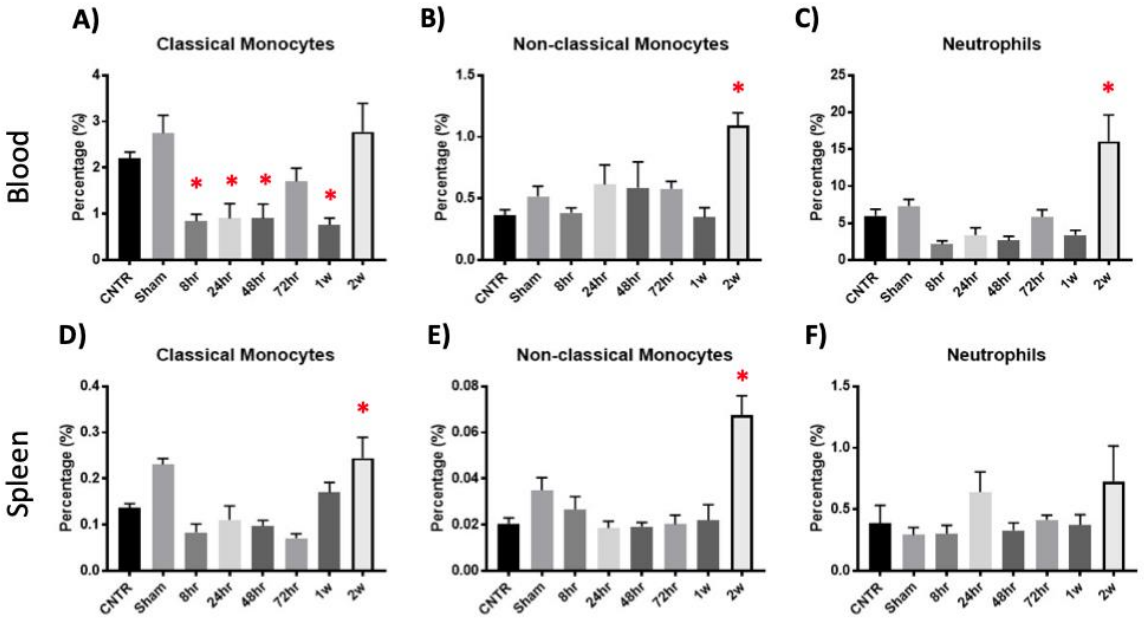
A)
Classical Monocytes
B)
Non-classical Monocytes
C)
Neutrophils
Blood
D)
Classical Monocytes
E)
Non-classical Monocytes
F)
Neutrophils
Spleen
Percentage (%)
CNTR
Sham
8hr
24hr
48hr
72hr
1w
2w

Figure 17. Adaptive immune cell frequencies in peripheral blood and spleen. Using flow cytometry, lymphocyte subsets were identified; B cells as $CD19^+$, T cells as $CD3e^+$ and NK cells as $Nkp46^+$. Circulating B cells were significantly decreased at 24h $p<0.0001$ and 48h $p<0.0001$ (A), while T cells were found to be significantly increased at 1 week $p<0.0001$ (B) and NK cells were significantly decreased at 8h $p=0.0165$ and 72h $p<0.0001$ (C). In the spleens, T cells and NK cells were both significantly increased at 2 weeks $p=0.0073$, $p=0.0043$ (E, F). One way ANOVA followed by Dunnett's test was performed, significance was determined when *= $p\leq0.05$. Data is presented as the group mean ± SEM with 6-10 mice per group.

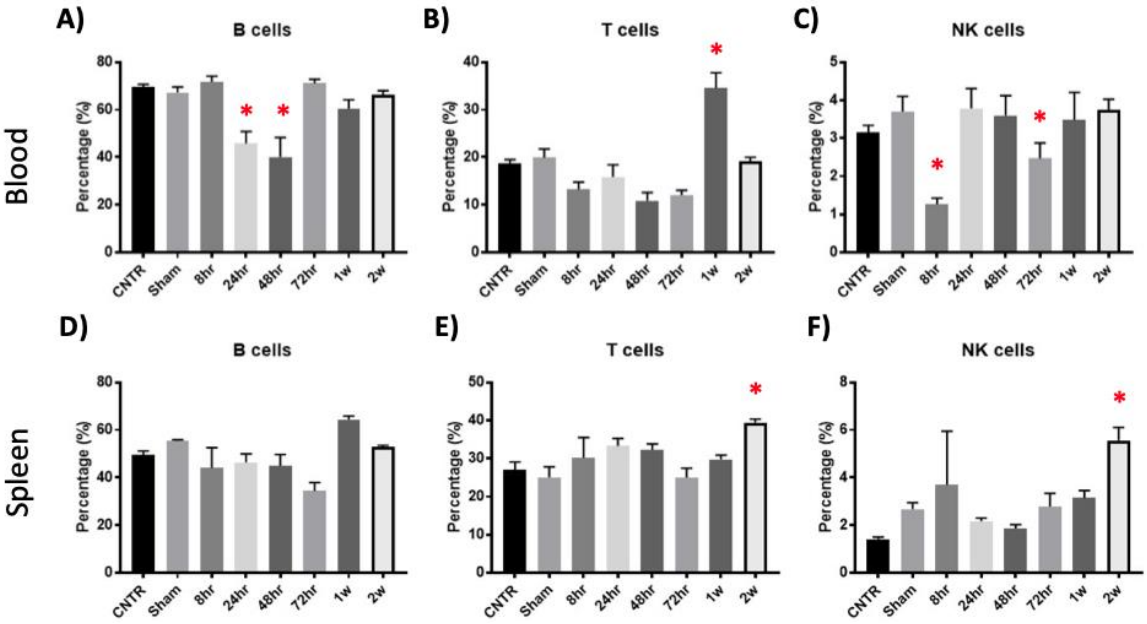
A)
B cells
B)
T cells
C)
NK cells
Blood
D)
B cells
E)
T cells
F)
NK cells
Spleen
Percentage (%)
CNTR
Sham
8hr
24hr
48hr
72hr
1w
2w

NKp46$^+$ NK cells and CD3$^+$ T cells. In peripheral blood, B cell frequency significantly decreased from 24h-48h following TBI (Fig. 17A), while T cells significantly increased at 1 week post-injury (Fig. 17B). In the spleens, T cells and NK cells significantly increased at 2 week following repetitive concussion (Fig. 17E, F).

3.9 Change in EGFP fluorescence in myeloid cells in the peripheral organs following repetitive mTBI

To investigate whether repetitive concussion induced a systemic inflammatory response, livers, lungs and cervical spinal cords were examined for the presence of EGFP$^+$ cells by quantifying the EGFP immunofluorescent signal. These organs were obtained from the same groups of mice from which the brains, blood and spleens were obtained. Alternate sections from these organs were imaged using fluorescent microscopy and analyzed using digital morphometry. The results from livers indicate that while concussion elicited a small increase in EGFP fluorescent signal, no significant difference between healthy controls and injured group were found at the indicated time points (8h-2w) (Fig. 18A). Some clusters of EGFP$^+$ cells were found in both the controls and injured cohorts for all time points (Fig. 18B, C). The results from the lungs revealed that repetitive mTBI lead to a significant increase in EGFP immunofluorescent signal at 24h (Fig. 19A). However, the EGFP fluorescence digital signal returned to baseline levels at subsequent time points (48h-2w). Representative images of lungs from controls and mTBI mice are shown (Fig. 19B, C). Next, the cervical part of the spinal cords of each animal were analyzed. The cervical region is the most superior part of the cord, that is directly attached to the brainstem. This area would likely be the most affected non-brain area from mTBI due to the close, anatomical proximity to the brain. The results indicated that the 3-hit repetitive brain injury caused significant accumulation of EGFP$^+$ cells in and surrounding the spinal cords at 8h post-TBI (Fig. 20A). The EGFP immunofluorescence was greater than a 2-fold increase compared to healthy controls. This increase was also observed at 24h and 48h, however, to a lesser extent. At 72h, the EGFP fluorescence returned to control levels and by 2 weeks, it reached below control levels. Representative images of the spinal cords from controls and injured cohorts at 8h is shown (Fig. 20B, C).

Figure 18. No change in EGFP fluorescence of the myeloid cells in the liver following repetitive mTBI. No significant change in EGFP immunoreactivity was found in the livers between controls and injured mice cohorts (A). Representative images of the livers are shown at 10x magnification (B, C). Confocal images of $EGFP^+$ cells (D) acquired at 63x magnification, along with DAPI (E), and EGFP merged with DAPI (F) are shown. One way ANOVA followed by Dunnett's test was performed, significance was determined when *= $p \leq 0.05$. Data is presented as the group mean ± SEM with 4-5 mice per group. Two livers from the control and 72h cohorts were omitted from the analysis due to loss of integrity of the tissue samples.

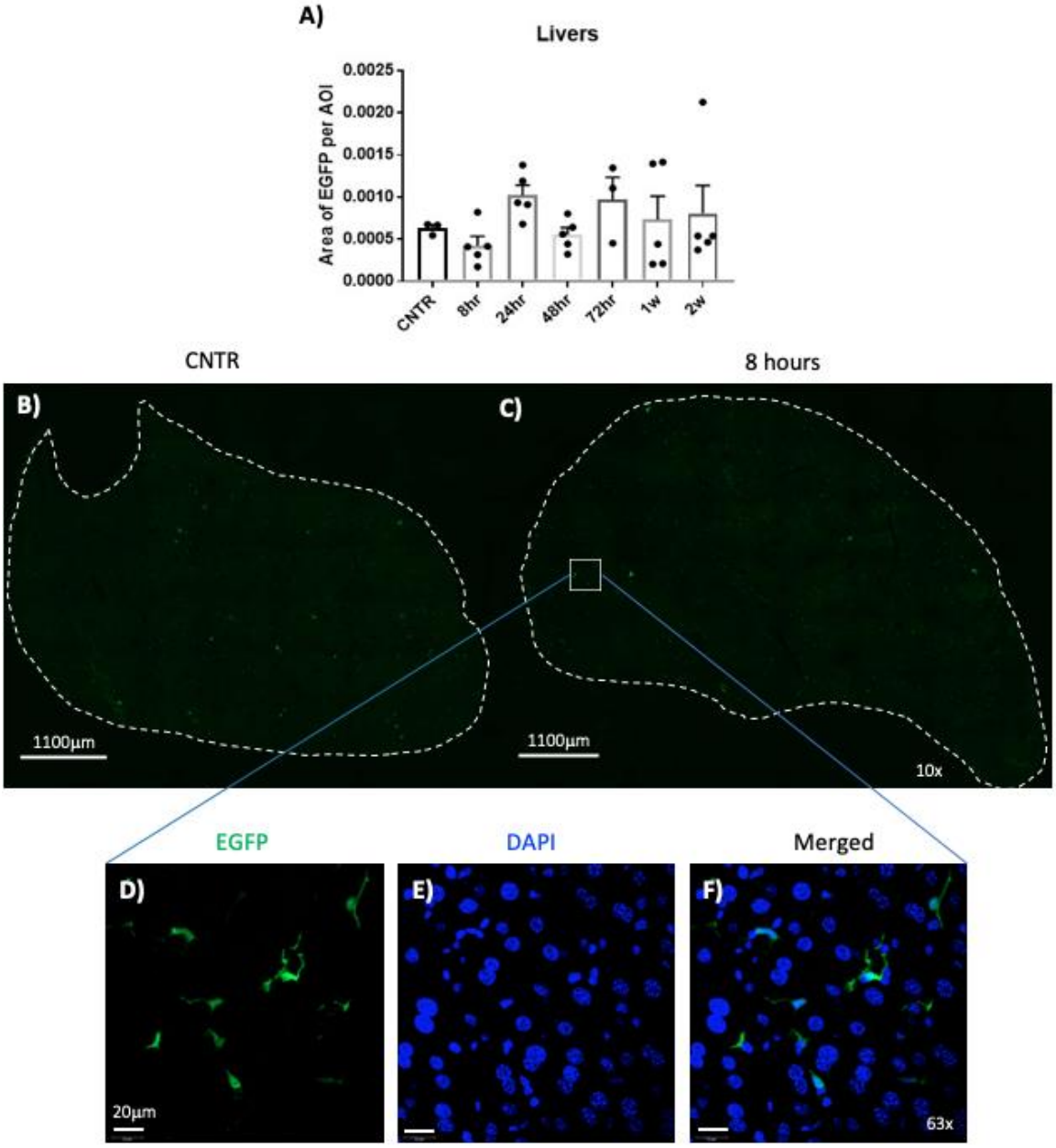
A)
Livers
Area of EGFP per AOI
0.0025
0.0020
0.0015
0.0010
0.0005
0.0000
CNTR
8hr
24hr
48hr
72hr
1w
2w
CNTR
8 hours
B)
C)
1100µm
1100µm
10x
EGFP
DAPI
Merged
D)
E)
F)
20µm
63x

Figure 19. $EGFP^+$ fluorescence of myeloid cells increase in the lungs at 24 hours post-repetitive concussion. A significant change in EGFP fluorescent signal was found in the lungs at 24h in the injured mice cohort p=0.00026 (A). Representative images of the lungs are shown at 10x magnification (B, C). Confocal images acquired at 63x magnification of $EGFP^+$ cells (D), along with DAPI (E), and EGFP merged with DAPI (F) are shown. One way ANOVA followed by Dunnett's test was performed, significance was determined when *= $p \leq 0.05$. Data is presented as the group mean $\pm$ SEM with 4-6 mice per group.

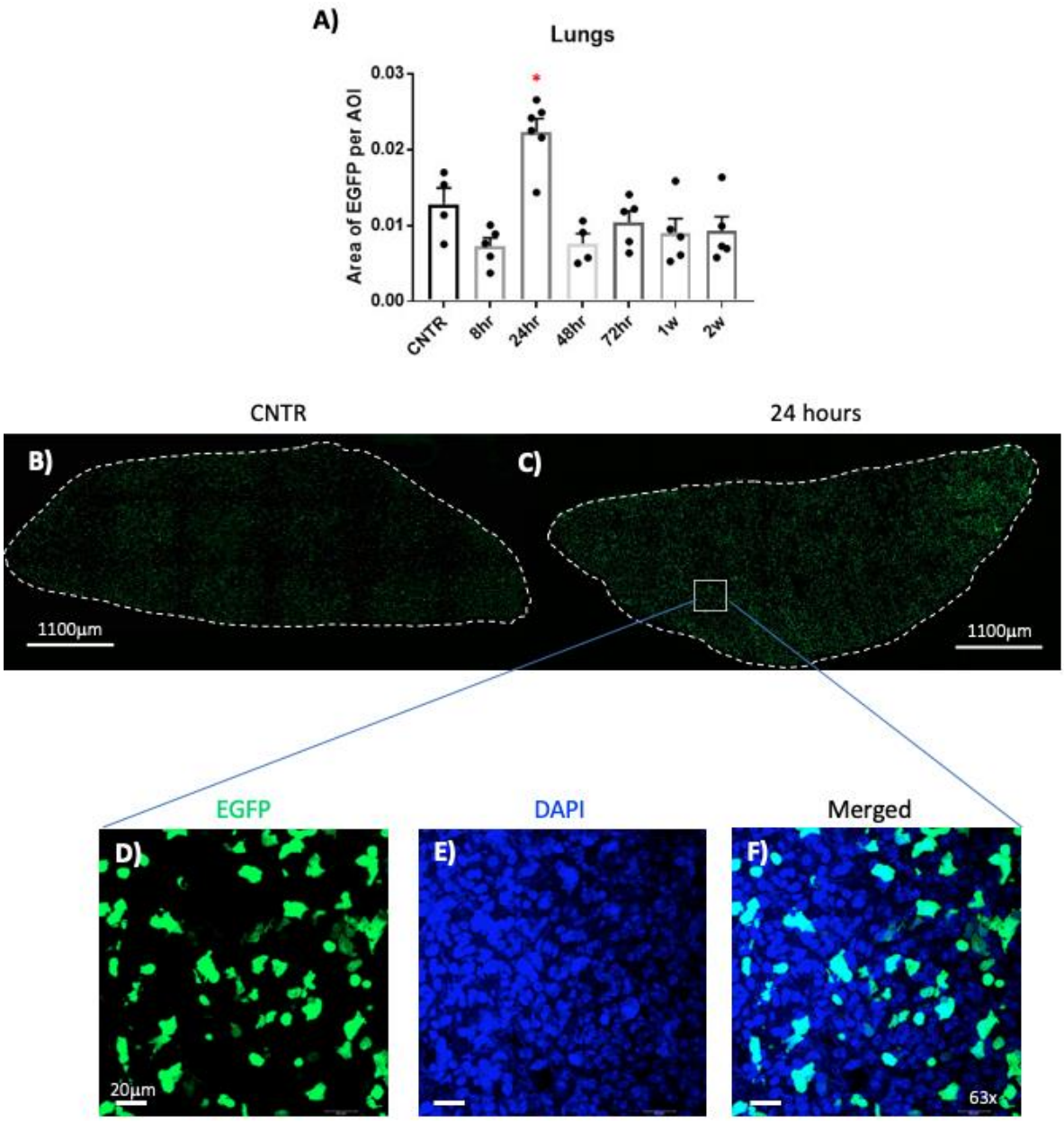
A)
Lungs
Area of EGFP per AOI
0.03
0.02
0.01
0.00
*
CNTR
8hr
24hr
48hr
72hr
1w
2w
CNTR
24 hours
B)
C)
1100µm
1100µm
EGFP
DAPI
Merged
D)
E)
F)
20µm
63x

Figure 20. $EGFP^+$ fluorescence of myeloid cells increase in the cervical spinal cord at 8hours post-injury. Significant increase in EGFP fluorescent signal was found in the cervical region of the spinal cord at 8h $p<0.0001$, 24h $p=0.0009$, 48h $p=0.045$ following repeated mTBI (A). At 2 weeks, the EGFP immunofluorescence decreased significantly $p=0.0015$. Representative images of the spinal cords are shown at 10x magnification (B, C). Close-up confocal images of $EGFP^+$ cells (D), along with DAPI (E), and EGFP merged with DAPI (F) are shown. One way ANOVA followed by Dunnett's test was performed, significance was determined when *= $p\leq0.05$. Data is presented as the group mean $\pm$ SEM with 4-8 mice per group.

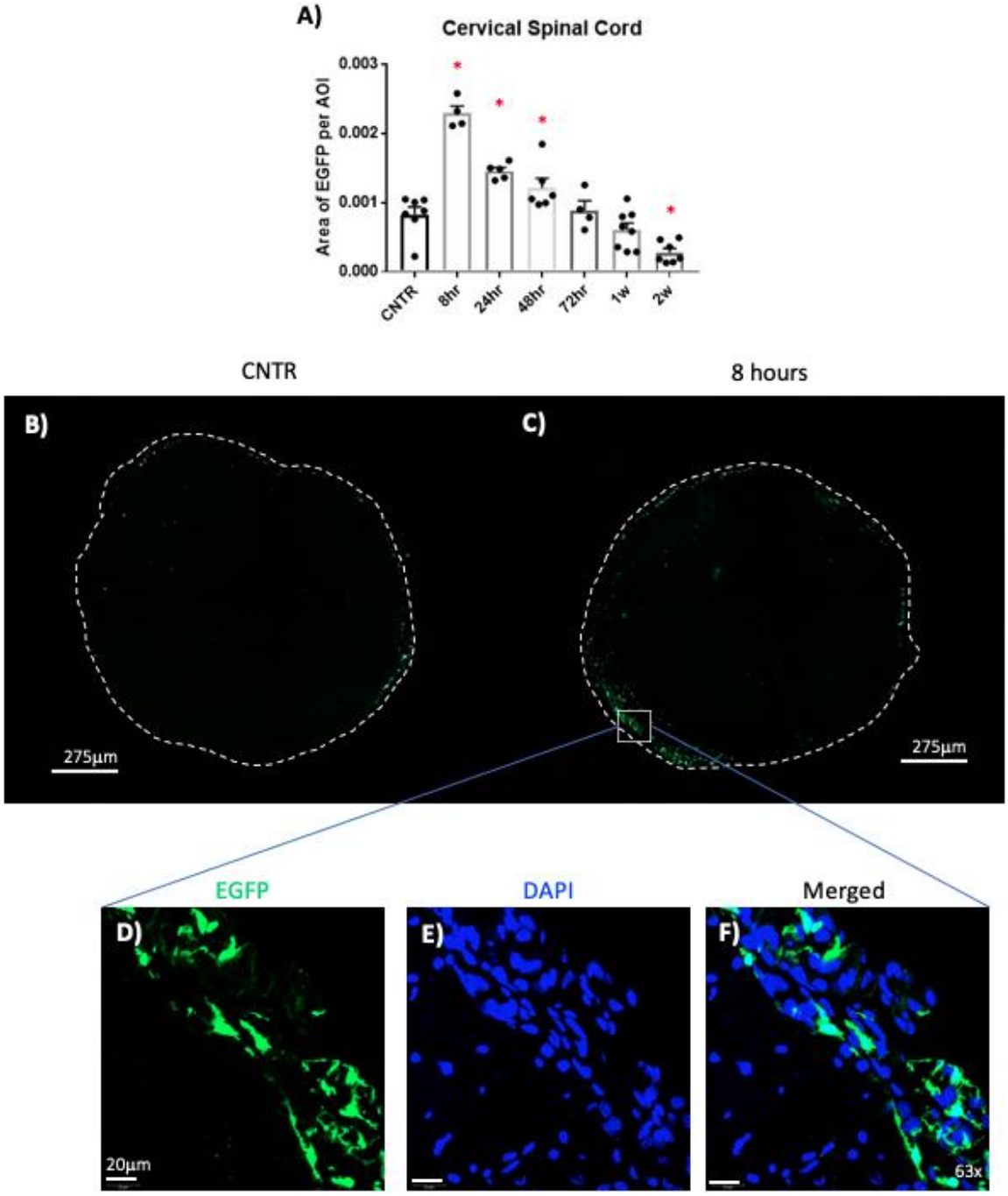
A)
Cervical Spinal Cord
Area of EGFP per AOI
0.003
0.002
0.001
0.000
CNTR
8hr
24hr
48hr
72hr
1w
2w
CNTR
8 hours
B)
C)
275µm
275µm
EGFP
DAPI
Merged
D)
E)
F)
20µm
63x

CHAPTER 4 – DISCUSSION

The overarching goal of this project was to investigate the temporal and spatial appearance of the local CNS and peripheral immune cells that contribute to the evolving inflammatory response following repetitive concussion. The closed-head mouse model of repetitive mTBI generated robust neuroinflammation and some evidence of systemic inflammation. By using the *lys*-EGFP-*ki* transgenic mice, I was able to track the most prominent inflammatory cells at acute time points following mTBI and distinguish the brain resident microglia from the hematogenous myeloid cells that extravasate into the brain parenchyma. Following three concussive impacts, the injured mice exhibited brain pathologies including significant accumulation of $EGFP^+$ cells in the brain, activated microglia and white matter abnormalities at sub-acute time points, in the absence of gross lesions. Furthermore, the injury caused significant increases in $EGFP^+$ cells surrounding the cervical spinal cord at 8 hours and in the lungs at 24 hours. Altogether, these results demonstrated that repetitive, mild closed-head injuries produced a robust inflammatory response in the brain as well as subtle but measurable inflammatory response in the periphery. This suggests that our model of repetitive concussion is useful for investigating human concussion and could be further explored to test anti-inflammatory therapies as a means of providing neuroprotection against secondary injury.

This project investigated the early changes in microglial activity following repeated concussive injury. The link between multiple concussions and chronic neurodegeneration has been established in the literature, but, the acute pathological changes following mild brain injuries need to be further elucidated. Human studies have shown increased microglial and astrocyte activity through position emission tomography imaging in young NFL players, which indicate the early onset of neuroinflammation (149). This emphasizes the importance of understanding the early changes seen in concussion which may help design future diagnostic approaches and therapeutics before neurodegeneration and neurocognitive decline. The results of my research showed that this model of concussive injury produced key pathological hallmarks of repetitive concussion in the absence of visible contusions and gross lesions. Just 8 hours following the last injury, there was significant microglial activity as shown by quantitative analysis, Iba-1 immunoreactivity was markedly higher in the mTBI brains compared to healthy controls. Whether this is due

to cell proliferation, increase in cell size or both is unclear and requires clarification with further experiments. It is known that TBI alters the activation state of microglia which is characterized by distinct morphological features, including extended processes, amoeboid and hypertrophied appearance of the cell body (150). Although this does not reflect the RNA expression profile phenotype, it is still considered as a marker for neuroinflammation as it indicates that the cells are responding to altered homeostasis. Supported by the Iba-1 staining, mTBI brains had microglia that appeared amoeboid, hypertrophied and bushy compared to controls which showed ramified morphology associated with normal surveillance activity. This finding is in accordance with other studies of repetitive concussion (75).

My data clearly demonstrated the infiltration of hematogenous myeloid cells into the brain following repetitive mTBI. Examining five different sections (500μm apart) of the brain underneath the site of impact showed that EGFP immunoreactivity remained consistent between these sections. However, when observing the various areas of the brain structure within one section, areas near the site of injury (regions encompassing the superior cerebral cortex) and areas the most ventral from the site of injury (base of the brain) had the highest levels of EGFP fluorescent signal. I speculate that this could be due to the "coup-contrecoup" effect. Since the force transmitted by the impactor drives the head and consequently the brain downward, the coup injury occurred directly underneath where the impactor made contact with the skull and the contrecoup injury occurred on the opposite side, which is the most ventral part of the brain. However, the brain is immersed in cerebral spinal fluid that absorbs the shock from an injury and restricts any significant movement caused by an external force (151). To further investigate the concept of "coup-contrecoup," the exact biomechanical measurements would be required.

The $EGFP^+$ myeloid cells were found in the brain parenchyma, along the choroid plexus of the lateral and third ventricles, in the pia mater, as well in the microvessels distributed throughout the parenchyma. Co-localization of $EGFP^+$ and $CD31^+$ cells in the parenchyma but not in the blood vessels associated with the ventricles or the pia mater suggests that the myeloid cells emerge from the brain microvasculature and relocate to other areas. The existence of perivascular, meningeal and choroid plexus macrophages was previously established in the literature (152). These are non-parenchymal macrophages that

mediate immune responses at brain boundaries. This explains the presence of $EGFP^+$ cells in the control brains. However, during neuroinflammatory conditions, the myeloid cells accumulated significantly more in the parenchyma as well in other areas of the brain. Additionally, recent research showed the existence of lymphatic vessels in the meninges that could allow peripheral immune cells to enter and exit the brain as well (153).

It is still controversial as to whether the presence and function of monocyte-derived macrophages are beneficial or detrimental to recovery following TBI. Traditionally, it was believed that the recruited peripheral immune cells were more damaging to the brain. Since the initial wave of infiltrating monocytes involved are likely pro-inflammatory innate immune cells (154), they are thought to be inherently pathogenic in the context of a sterile injury such as mTBI. Thus, numerous research efforts have focused on preventing the entry of monocytes and macrophages by suppressing CCR2 signaling pathway. Reports have shown that abrogating CCR2-mediated events, thus, impeding monocyte/macrophage recruitment reduced neuroinflammation and cognitive decline by altering the expression of pro and anti-inflammatory cytokines (155). Other studies have shown that impaired CCR2 signaling prevented monocyte accumulation and this reduced cavity volume and axonal pathology following FPI (156). In contrast, some researchers have suggested that peripheral macrophages enter the CNS to modulate microglial activity and ultimately reduce inflammation post-TBI (157). This latter *in vitro* study showed evidence of monocyte-derived macrophages engaging in cell-to-cell interactions with microglia where infiltrating macrophages provided ways to mitigate detrimental acute and long-term microglial mediated inflammation. This occurred through negatively regulating the NF-κB signaling pathway in microglia to reduce inflammatory mediators (157). Further studies are required to functionally phenotype the hematogenous macrophages in the mTBI brain and this may shine light on the role that these cells play in the course of TBI resolution or TBI induced neurodegenerative disease development.

My results showed that in mild concussion-like head injuries, neutrophils were not the most prominent myeloid cells to infiltrate the brain parenchyma. However, in the literature, experimental severe TBI lead to the upregulation and release of inflammatory signals that initiate neutrophil trafficking into the brain (158). Neutrophils are among the first peripheral immune cells to arrive to the site of lesion, usually within hours after the

initial impact. They have been shown to extravasate across inflamed vessels, or through the choroid plexus and circulate in the cerebral spinal fluid near the lesion (158, 159). Additionally, neutrophils predominately migrate from the brain vasculature to the ipsilateral leptomeninges and choroid plexus as early as 4 hours after the initial injury and enter the parenchyma from 24 to 48 hours (160). This is incongruent with my preliminary results, which showed no neutrophils in the mTBI brains at all examined time points. This difference could be explained by the much less severe injury in this model of concussion as opposed to a severe TBI from open-head injury employed in the studies described above. It is also possible that the neutrophils had already reached and underwent apoptosis after the first impact. Since the injury was delivered a total of three times and the earliest time the brains were examined was 8 hours following the last impact, the neutrophils could have potentially entered and left the brain within those hours. Thus, shorter time points should also be examined as well as the between the injury intervals.

An important pathological finding that is consistent across the spectrum of TBI severity (161), as well as in both animal and human studies (162-164) is the selective damage to axons, known as diffuse axonal injury. While the entire brain suffers from the mechanical force and the whole brain is susceptible to tissue deformation, white matter tracts are at the greatest risk of damage due to their direction specific, highly organized structure (165). The tensile and shear forces from rotational acceleration can damage the long axonal tracts. TBI causes breaks in the microtubule structures within the axons which serve as anatomical tracks for protein transport (166). This leads to proteins piling up at the microtubule disconnections and the evidence of this can be discerned by the appearance of varicose swelling (164, 166). Although this model of repetitive mTBI induced linear acceleration, axonal pathology was confirmed in the corpus callosum with silver staining that specifically reveals the presence of axonal varicosities. DAI is an important secondary injury marker of repeated concussions that could explain the accelerated path to neurodegeneration (167-169). Interestingly, $EGFP^+$ cells were also found within the corpus callosum where there was prominent silver staining axonal varicosities, suggesting a possible cell-to-cell interaction between the damaged neurons and peripheral myeloid cells.

Although concussion is a CNS injury, the extracranial effects of TBI cannot be underestimated. In humans, damage to the CNS through acquired TBI can lead to the

development of a systemic inflammatory response, that may evolve into multiple organ failure (170). Out of which, lungs are the most affected organ, manifested by ARDS (170). Pulmonary dysfunction is a critical condition that affects 20-25% of all brain injured patients and is an important independent factor determining mortality (171). While this is a more common occurrence in moderate to severe TBI, the effects of mTBI on peripheral organs is just being elucidated. In this model of repetitive mTBI, a significant accumulation of $EGFP^+$ myeloid cells 24 hours after injury was shown in the lungs. This is in agreement with other recent experiments showing significant interstitial neutrophils in a FPI model of mTBI (172). This latter study demonstrated that concussion primes the lungs for subsequent neutrophil-mediated injury in a mouse model of mTBI (172). It was shown that mTBI increased pulmonary susceptibility to secondary injury such as microaspiration of acid which was mediated by alveolar neutrophil influx that developed into pulmonary hemorrhage (172).

Additionally, focal brain injuries have shown to elicit a rapid hepatic response (173). This suggested that the production of chemokines by the liver in response to TBI acts as an amplifier of the initial inflammatory cascade. In a rat spinal contusion model of spinal cord injury (SCI), liver inflammation was detected through increased pro-inflammatory gene expression, increased $CD68^+$ macrophages as well as increased serum alanine transaminase, which is used to detect liver damage (174). These pathologies indicated that SCI could produce chronic liver damage with symptoms that resemble those of nonalcoholic fatty liver disease. Although SCI pathologies differ from that of TBI, SCI is still an injury inflicted on the CNS that elicits an inflammatory response in the periphery. No significant changes in $EGFP^+$ myeloid cells were seen in the liver in my experiments at acute time points, however, repetitive concussion may still induce liver inflammation. Thus, longer time points post-injury as well as other inflammatory markers should be investigated.

Interestingly, a significant increase in $EGFP^+$ myeloid cells surrounding the cervical region of the spinal cord was observed at 8 hours following repetitive concussion. Dr. Arthur Brown's lab from Western University, ON, coordinated with engineers also from Western University to capture a high-speed video of the closed-head injury of concussion in slow motion. Due to the high-speed impact of the TBI device, at the moment of injury,

the head of the mouse rapidly accelerates up and down. This could create a strain on the spinal cord, since the cervical part of the cord directly attaches to the brainstem. This could potentially explain the accumulation of $EGFP^+$ cells in this region of the spinal cord. However, conflictingly, DAI and $EGFP^+$ cells increased in the brain at 1 and 2 weeks following repetitive concussion and not at 8 hours. Additional silver staining of the cervical spinal cord would be required to determine whether axonal injury correlates with the accumulation of $EGFP^+$ cells in the spinal cord at 8 hours. This would determine whether concussion affects both the brain and spinal cord independently of each other regardless of their anatomical close proximity.

Lastly, an early loss of circulating classical monocytes and neutrophils was observed at 8 hours which was sustained for a week after the injury. This decrease may be associated with these cells shifting from the blood into other organs and or brain since there was an increase in the $EGFP^+$ cells in the lungs and cervical spinal cord. The sudden increase in the frequencies of these cells at 2 weeks could be explained by the animal attempting to replenish the initial loss of the $EGFP^+$ cells. Less obvious, yet, similar trends were seen in the spleen as well, where the classical monocytes and neutrophils slightly decreased at the earlier time points before increasing at 2 weeks. Importantly, it should be noted that the results of this study yielded a much lower frequency value of both spleen monocyte and neutrophil populations. While normal, murine spleen monocyte cell frequency is reported to be between 3.5-5% and neutrophil frequency is between 4-6% of total leukocytes (175), frequency values for both in these experiments are 10-fold lower. It is difficult to speculate the reason for these discrepancies as all cohorts showed the same lowered values and thus, this part of the project must be redone. Some researchers have suggested that in an ischemic injury, there exists a separate population of infiltrating monocytes that originate from the spleen and not from the circulation (176). Hence, it is believed that the splenic population of monocytes will behave differently from the monocytes in circulation when activated or recruited to tissues. This is relevant for this study in that raises the question of where the $EGFP^+$ cells that are found in the organs originate from and whether their functions differ depending on their origin.

In addition to the myeloid cell populations, 3-hit model of concussion induced some alterations in the adaptive immune cell populations. While the B cell frequency in

circulation decreased from 24 to 48 hours, the T cells remained at control levels until a striking increase at 1 week. In the literature however, a handful of studies have shown no changes in the frequency, absolute number, or proliferative capacity of B cells following severe TBI (177-180). In contrast, severe TBI caused significant decrease in the percentage and absolute number of T lymphocytes in circulation (178, 181) observed within 24 hours of injury as well as 4 days. The differences found between my data and what has been reported in the literature could be explained by the severity of the injury in the concussion models. Since the role of lymphocytes are not as extensively studied in the TBI literature, it is difficult to speculate on the changes seen in this model and remains as an area that needs to be the further explored. Lastly, although the sham-injured cohort was initially included in the experiments, due to the limited time of this study, the immunohistochemical results were not completed. A comparison to the sham-injured mice would be necessary to ensure that the effects of the injury were strictly due to the concussive impacts rather than from the effects of the anaesthesia and skin incisions.

Possible future directions for this project could be extended from looking beyond the time points that were examined in my studies. The follow up experiments could investigate whether the accumulation of $EGFP^+$ cells and axonal injury subside in the brain and identify the time-point associated with this attenuation. This could clarify the relationship between peripheral myeloid cells and axonal damage found in the white matter tracts and help delineate the complex role of myeloid immune cells in the chronic effects of repetitive mild brain injuries. Additionally, immunohistochemical staining should be performed to look for gross histological abnormalities. Furthermore, immunostaining brain sections for a marker of astrocytes with glial fibrillary acidic protein (GFAP) antibody would also contribute to the overall understanding of the different cell types that play a role in concussion. Equally as important as the pathological changes, concussion can result in negative cognitive changes in humans. Thus, behavioural tests should be conducted in mouse models to determine whether pathological changes correlate with behavioural changes. An example of such sophisticated behavioural test that could be used is the 5-choice serial reaction time test. This is an advanced cognitive testing procedure applicable to rodents using the touchscreen technology. These tests would model whether the animals experience decreased mental concentration, slower reaction time by measuring their

attentional control (182) and cognitive flexibility (183). It is critical to use cognitive testing that is reflective and relevant to clinical populations. Lastly, sex differences in TBI pathogenesis should be further explored as there is much evidence to support sexual dimorphism in the neuroinflammatory response to TBI. Studies have shown that the inflammatory response in male mice after moderate-CCI differed in comparison to age-matched females and exhibited greater myeloid cell infiltration and microglial activation (184). Along with TBI, Alzheimer's disease and ischemic stroke injury all lead to sexually dimorphic outcomes, suggesting sex-related and specific inflammatory signals (185) which must be accounted for when studying these diseases.

Collectively, my data demonstrated that repetitive, closed-head injury in mice produces several known pathologies attributed to human concussion including localized, brain-specific inflammation as well as some evidence of systemic inflammation. Using the *lys*-EGFP-*ki* transgenic mouse model, I characterized the temporal and spatial progression of the inflammatory process involving the brain resident microglia and monocyte-derived macrophages in the context of TBI pathology. In addition to neuroinflammation, this model of concussive injury produced diffuse axonal damage, which is another key hallmark of concussion. Finally, I concluded that repetitive concussion not only affects the brain, but also mobilizes the myeloid cells into other organs as well, potentially inducing a cascade of inflammatory events systemically. Overall, my project sets the stage for further investigation on the inflammatory response in the CNS and in the periphery. Understanding the time course of events that lead to these pathologies is critical for the development of targeted therapies that could impede the progression towards potential long-term impairments.

Citations

1. Cassidy, J. D., L. J. Carroll, P. M. Peloso, J. Borg, H. von Holst, L. Holm, J. Kraus, V. G. Coronado, and W. H. O. C. C. T. F. o. M. T. B. Injury. 2004. Incidence, risk factors and prevention of mild traumatic brain injury: results of the WHO Collaborating Centre Task Force on Mild Traumatic Brain Injury. *J Rehabil Med*: 28-60.
2. Numminen, H. J. 2011. The incidence of traumatic brain injury in an adult population--how to classify mild cases? *Eur J Neurol* 18: 460-464.
3. Bazarian, J. J., J. McClung, M. N. Shah, Y. T. Cheng, W. Flesher, and J. Kraus. 2005. Mild traumatic brain injury in the United States, 1998--2000. *Brain Inj* 19: 85-91.
4. Taylor, C. A., J. M. Bell, M. J. Breiding, and L. Xu. 2017. Traumatic Brain Injury-Related Emergency Department Visits, Hospitalizations, and Deaths - United States, 2007 and 2013. *MMWR Surveill Summ* 66: 1-16.
5. Marklund, N., and L. Hillered. 2011. Animal modelling of traumatic brain injury in preclinical drug development: where do we go from here? *Br J Pharmacol* 164: 1207-1229.
6. Margulies, S., R. Hicks, and L. Combination Therapies for Traumatic Brain Injury Workshop. 2009. Combination therapies for traumatic brain injury: prospective considerations. *J Neurotrauma* 26: 925-939.
7. Mayer, A. R., D. K. Quinn, and C. L. Master. 2017. The spectrum of mild traumatic brain injury: A review. *Neurology* 89: 623-632.
8. Petraglia, A. L., M. L. Dashnaw, R. C. Turner, and J. E. Bailes. 2014. Models of mild traumatic brain injury: translation of physiological and anatomic injury. *Neurosurgery* 75 Suppl 4: S34-49.
9. Petraglia, A. L., B. A. Plog, S. Dayawansa, M. L. Dashnaw, K. Czerniecka, C. T. Walker, M. Chen, O. Hyrien, J. J. Iliff, R. Deane, J. H. Huang, and M. Nedergaard. 2014. The pathophysiology underlying repetitive mild traumatic brain injury in a novel mouse model of chronic traumatic encephalopathy. *Surg Neurol Int* 5: 184.
10. Collins, M. W., M. R. Lovell, G. L. Iverson, R. C. Cantu, J. C. Maroon, and M. Field. 2002. Cumulative effects of concussion in high school athletes. *Neurosurgery* 51: 1175-1179; discussion 1180-1171.
11. Giza, C. C., and D. A. Hovda. 2001. The Neurometabolic Cascade of Concussion. *J Athl Train* 36: 228-235.
12. Guskiewicz, K. M., M. McCrea, S. W. Marshall, R. C. Cantu, C. Randolph, W. Barr, J. A. Onate, and J. P. Kelly. 2003. Cumulative effects associated with recurrent concussion in collegiate football players: the NCAA Concussion Study. *JAMA* 290: 2549-2555.
13. LaRoche, A. A., L. D. Nelson, P. K. Connelly, K. D. Walter, and M. A. McCrea. 2016. Sport-Related Concussion Reporting and State Legislative Effects. *Clin J Sport Med* 26: 33-39.
14. Kenzie, E. S., E. L. Parks, E. D. Bigler, M. M. Lim, J. C. Chesnutt, and W. Wakeland. 2017. Concussion As a Multi-Scale Complex System: An Interdisciplinary Synthesis of Current Knowledge. *Front Neurol* 8: 513.
15. Sharp, D. J., and P. O. Jenkins. 2015. Concussion is confusing us all. *Pract Neurol* 15: 172-186.

16. Menon, V. 2011. Large-scale brain networks and psychopathology: a unifying triple network model. *Trends Cogn Sci* 15: 483-506.
17. Halstead, M. E., K. D. Walter, M. Council on Sports, and Fitness. 2010. American Academy of Pediatrics. Clinical report--sport-related concussion in children and adolescents. *Pediatrics* 126: 597-615.
18. Giza, C. C., and D. A. Hovda. 2014. The new neurometabolic cascade of concussion. *Neurosurgery* 75 Suppl 4: S24-33.
19. Teasdale, G., and B. Jennett. 1974. Assessment of coma and impaired consciousness. A practical scale. *Lancet* 2: 81-84.
20. Gaddis, G. M., and M. L. Gaddis. 1994. Non-normality of distribution of Glasgow Coma Scores and Revised Trauma Scores. *Ann Emerg Med* 23: 75-80.
21. Mayeux, R., R. Ottman, G. Maestre, C. Ngai, M. X. Tang, H. Ginsberg, M. Chun, B. Tycko, and M. Shelanski. 1995. Synergistic effects of traumatic head injury and apolipoprotein-epsilon 4 in patients with Alzheimer's disease. *Neurology* 45: 555-557.
22. McKee, A. C., R. C. Cantu, C. J. Nowinski, E. T. Hedley-Whyte, B. E. Gavett, A. E. Budson, V. E. Santini, H. S. Lee, C. A. Kubilus, and R. A. Stern. 2009. Chronic traumatic encephalopathy in athletes: progressive tauopathy after repetitive head injury. *J Neuropathol Exp Neurol* 68: 709-735.
23. Hutson, C. B., C. R. Lazo, F. Mortazavi, C. C. Giza, D. Hovda, and M. F. Chesselet. 2011. Traumatic brain injury in adult rats causes progressive nigrostriatal dopaminergic cell loss and enhanced vulnerability to the pesticide paraquat. *J Neurotrauma* 28: 1783-1801.
24. Guskiewicz, K. M., S. W. Marshall, J. Bailes, M. McCrea, R. C. Cantu, C. Randolph, and B. D. Jordan. 2005. Association between recurrent concussion and late-life cognitive impairment in retired professional football players. *Neurosurgery* 57: 719-726; discussion 719-726.
25. Hart, J., Jr., M. A. Kraut, K. B. Womack, J. Strain, N. Didehbani, E. Bartz, H. Conover, S. Mansinghani, H. Lu, and C. M. Cullum. 2013. Neuroimaging of cognitive dysfunction and depression in aging retired National Football League players: a cross-sectional study. *JAMA Neurol* 70: 326-335.
26. Koerte, I. K., A. P. Lin, M. Muehlmann, S. Merugumala, H. Liao, T. Starr, D. Kaufmann, M. Mayinger, D. Steffinger, B. Fisch, S. Karch, F. Heinen, B. Ertl-Wagner, M. Reiser, R. A. Stern, R. Zafonte, and M. E. Shenton. 2015. Altered Neurochemistry in Former Professional Soccer Players without a History of Concussion. *J Neurotrauma* 32: 1287-1293.
27. Satarasinghe, P., D. K. Hamilton, R. J. Buchanan, and M. T. Koltz. 2019. Unifying Pathophysiological Explanations for Sports-Related Concussion and Concussion Protocol Management: Literature Review. *J Exp Neurosci* 13: 1179069518824125.
28. McIntosh, T. K., D. H. Smith, D. F. Meaney, M. J. Kotapka, T. A. Gennarelli, and D. I. Graham. 1996. Neuropathological sequelae of traumatic brain injury: relationship to neurochemical and biomechanical mechanisms. *Lab Invest* 74: 315-342.
29. Cernak, I. 2005. Animal models of head trauma. *NeuroRx* 2: 410-422.
30. DeKosky, S. T., P. M. Kochanek, R. S. Clark, J. R. Ciallella, and C. E. Dixon. 1998. Secondary Injury After Head Trauma: Subacute and Long-term Mechanisms. *Semin Clin Neuropsychiatry* 3: 176-185.

31. Takahashi, H., S. Manaka, and K. Sano. 1981. Changes in extracellular potassium concentration in cortex and brain stem during the acute phase of experimental closed head injury. *J Neurosurg* 55: 708-717.
32. Katayama, Y., D. P. Becker, T. Tamura, and D. A. Hovda. 1990. Massive increases in extracellular potassium and the indiscriminate release of glutamate following concussive brain injury. *J Neurosurg* 73: 889-900.
33. Prince, D. A., H. D. Lux, and E. Neher. 1973. Measurement of extracellular potassium activity in cat cortex. *Brain Res* 50: 489-495.
34. Bergsneider, M., D. A. Hovda, S. M. Lee, D. F. Kelly, D. L. McArthur, P. M. Vespa, J. H. Lee, S. C. Huang, N. A. Martin, M. E. Phelps, and D. P. Becker. 2000. Dissociation of cerebral glucose metabolism and level of consciousness during the period of metabolic depression following human traumatic brain injury. *J Neurotrauma* 17: 389-401.
35. Zetterberg, H., D. H. Smith, and K. Blennow. 2013. Biomarkers of mild traumatic brain injury in cerebrospinal fluid and blood. *Nat Rev Neurol* 9: 201-210.
36. Anderson, J. M., D. W. Hampton, R. Patani, G. Pryce, R. A. Crowther, R. Reynolds, R. J. Franklin, G. Giovannoni, D. A. Compston, D. Baker, M. G. Spillantini, and S. Chandran. 2008. Abnormally phosphorylated tau is associated with neuronal and axonal loss in experimental autoimmune encephalomyelitis and multiple sclerosis. *Brain* 131: 1736-1748.
37. Davis, G. A., R. J. Castellani, and P. McCrory. 2015. Neurodegeneration and sport. *Neurosurgery* 76: 643-655; discussion 655-646.
38. Joseph, J. R., J. S. Swallow, K. Willsey, A. P. Lapointe, S. Khalatbari, F. K. Korley, M. E. Oppenlander, P. Park, N. J. Szerlip, and S. P. Broglio. 2018. Elevated markers of brain injury as a result of clinically asymptomatic high-acceleration head impacts in high-school football athletes. *J Neurosurg*: 1-7.
39. Kornguth, S., N. Rutledge, G. Perlaza, J. Bray, and A. Hardin. 2017. A Proposed Mechanism for Development of CTE Following Concussive Events: Head Impact, Water Hammer Injury, Neurofilament Release, and Autoimmune Processes. *Brain Sci* 7.
40. Carman, A. J., R. Ferguson, R. Cantu, R. D. Comstock, P. A. Dacks, S. T. DeKosky, S. Gandy, J. Gilbert, C. Gilliland, G. Gioia, C. Giza, M. Greicius, B. Hainline, R. L. Hayes, J. Hendrix, B. Jordan, J. Kovach, R. F. Lane, R. Mannix, T. Murray, T. Seifert, D. W. Shineman, E. Warren, E. Wilde, H. Willard, and H. M. Fillit. 2015. Expert consensus document: Mind the gaps-advancing research into short-term and long-term neuropsychological outcomes of youth sports-related concussions. *Nat Rev Neurol* 11: 230-244.
41. Scopaz, K. A., and J. R. Hatzenbuehler. 2013. Risk modifiers for concussion and prolonged recovery. *Sports Health* 5: 537-541.
42. Osier, N., and C. E. Dixon. 2017. Mini Review of Controlled Cortical Impact: A Well-Suited Device for Concussion Research. *Brain Sci* 7.
43. McCrory, P., W. H. Meeuwisse, M. Aubry, B. Cantu, J. Dvorak, R. J. Echemendia, L. Engebretsen, K. Johnston, J. S. Kutcher, M. Raftery, A. Sills, B. W. Benson, G. A. Davis, R. G. Ellenbogen, K. Guskiewicz, S. A. Herring, G. L. Iverson, B. D. Jordan, J. Kissick, M. McCrea, A. S. McIntosh, D. Maddocks, M. Makdissi, L. Purcell, M. Putukian, K. Schneider, C. H. Tator, and M. Turner. 2013. Consensus

statement on concussion in sport: the 4th International Conference on Concussion in Sport held in Zurich, November 2012. *Br J Sports Med* 47: 250-258.

44. Weinstein, E., M. Turner, B. B. Kuzma, and H. Feuer. 2013. Second impact syndrome in football: new imaging and insights into a rare and devastating condition. *J Neurosurg Pediatr* 11: 331-334.
45. Webbe, F. M., and J. T. Barth. 2003. Short-term and long-term outcome of athletic closed head injuries. *Clin Sports Med* 22: 577-592.
46. Prins, M. L., D. Alexander, C. C. Giza, and D. A. Hovda. 2013. Repeated mild traumatic brain injury: mechanisms of cerebral vulnerability. *J Neurotrauma* 30: 30-38.
47. Weil, Z. M., K. R. Gaier, and K. Karelina. 2014. Injury timing alters metabolic, inflammatory and functional outcomes following repeated mild traumatic brain injury. *Neurobiol Dis* 70: 108-116.
48. Jassam, Y. N., S. Izzy, M. Whalen, D. B. McGavern, and J. El Khoury. 2017. Neuroimmunology of Traumatic Brain Injury: Time for a Paradigm Shift. *Neuron* 95: 1246-1265.
49. Simon, D. W., M. J. McGeachy, H. Bayir, R. S. B. Clark, D. J. Loane, and P. M. Kochanek. 2017. The far-reaching scope of neuroinflammation after traumatic brain injury. *Nat Rev Neurol* 13: 572.
50. Acosta, S. A., N. Tajiri, K. Shinozuka, H. Ishikawa, B. Grimmig, D. M. Diamond, P. R. Sanberg, P. C. Bickford, Y. Kaneko, and C. V. Borlongan. 2013. Long-term upregulation of inflammation and suppression of cell proliferation in the brain of adult rats exposed to traumatic brain injury using the controlled cortical impact model. *PLoS One* 8: e53376.
51. Hernandez-Ontiveros, D. G., N. Tajiri, S. Acosta, B. Giunta, J. Tan, and C. V. Borlongan. 2013. Microglia activation as a biomarker for traumatic brain injury. *Front Neurol* 4: 30.
52. Corps, K. N., T. L. Roth, and D. B. McGavern. 2015. Inflammation and neuroprotection in traumatic brain injury. *JAMA Neurol* 72: 355-362.
53. Bianchi, M. E. 2007. DAMPs, PAMPs and alarmins: all we need to know about danger. *J Leukoc Biol* 81: 1-5.
54. Loane, D. J., and A. Kumar. 2016. Microglia in the TBI brain: The good, the bad, and the dysregulated. *Exp Neurol* 275 Pt 3: 316-327.
55. Hickman, S. E., N. D. Kingery, T. K. Ohsumi, M. L. Borowsky, L. C. Wang, T. K. Means, and J. El Khoury. 2013. The microglial sensome revealed by direct RNA sequencing. *Nat Neurosci* 16: 1896-1905.
56. Hellewell, S., B. D. Semple, and M. C. Morganti-Kossmann. 2016. Therapies negating neuroinflammation after brain trauma. *Brain Res* 1640: 36-56.
57. Thal, S. C., and W. Neuhaus. 2014. The blood-brain barrier as a target in traumatic brain injury treatment. *Arch Med Res* 45: 698-710.
58. Das, M., S. Mohapatra, and S. S. Mohapatra. 2012. New perspectives on central and peripheral immune responses to acute traumatic brain injury. *J Neuroinflammation* 9: 236.
59. Muradashvili, N., and D. Lominadze. 2013. Role of fibrinogen in cerebrovascular dysfunction after traumatic brain injury. *Brain Inj* 27: 1508-1515.
60. Glushakova, O. Y., D. Johnson, and R. L. Hayes. 2014. Delayed increases in microvascular pathology after experimental traumatic brain injury are associated

with prolonged inflammation, blood-brain barrier disruption, and progressive white matter damage. *J Neurotrauma* 31: 1180-1193.

61. Erturk, A., S. Mentz, E. E. Stout, M. Hedehus, S. L. Dominguez, L. Neumaier, F. Krammer, G. Llovera, K. Srinivasan, D. V. Hansen, A. Liesz, K. A. Scearce-Levie, and M. Sheng. 2016. Interfering with the Chronic Immune Response Rescues Chronic Degeneration After Traumatic Brain Injury. *J Neurosci* 36: 9962-9975.
62. Xiong, Y., A. Mahmood, and M. Chopp. 2018. Current understanding of neuroinflammation after traumatic brain injury and cell-based therapeutic opportunities. *Chin J Traumatol* 21: 137-151.
63. Bergold, P. J. 2016. Treatment of traumatic brain injury with anti-inflammatory drugs. *Exp Neurol* 275 Pt 3: 367-380.
64. Perez-Cerda, F., M. V. Sanchez-Gomez, and C. Matute. 2015. Pio del Rio Hortega and the discovery of the oligodendrocytes. *Front Neuroanat* 9: 92.
65. Ginhoux, F., and M. Guilliams. 2016. Tissue-Resident Macrophage Ontogeny and Homeostasis. *Immunity* 44: 439-449.
66. Hoeffel, G., and F. Ginhoux. 2015. Ontogeny of Tissue-Resident Macrophages. *Front Immunol* 6: 486.
67. Ginhoux, F., M. Greter, M. Leboeuf, S. Nandi, P. See, S. Gokhan, M. F. Mehler, S. J. Conway, L. G. Ng, E. R. Stanley, I. M. Samokhvalov, and M. Merad. 2010. Fate mapping analysis reveals that adult microglia derive from primitive macrophages. *Science* 330: 841-845.
68. Li, Q., and B. A. Barres. 2018. Microglia and macrophages in brain homeostasis and disease. *Nat Rev Immunol* 18: 225-242.
69. Frost, J. L., and D. P. Schafer. 2016. Microglia: Architects of the Developing Nervous System. *Trends Cell Biol* 26: 587-597.
70. Schafer, D. P., and B. Stevens. 2015. Microglia Function in Central Nervous System Development and Plasticity. *Cold Spring Harb Perspect Biol* 7: a020545.
71. Cunningham, C. L., V. Martinez-Cerdeno, and S. C. Noctor. 2013. Microglia regulate the number of neural precursor cells in the developing cerebral cortex. *J Neurosci* 33: 4216-4233.
72. Prinz, M., and J. Priller. 2014. Microglia and brain macrophages in the molecular age: from origin to neuropsychiatric disease. *Nat Rev Neurosci* 15: 300-312.
73. Crotti, A., and R. M. Ransohoff. 2016. Microglial Physiology and Pathophysiology: Insights from Genome-wide Transcriptional Profiling. *Immunity* 44: 505-515.
74. Soltys, Z., M. Ziaja, R. Pawlinski, Z. Setkowicz, and K. Janeczko. 2001. Morphology of reactive microglia in the injured cerebral cortex. Fractal analysis and complementary quantitative methods. *J Neurosci Res* 63: 90-97.
75. Madathil, S. K., B. S. Wilfred, S. E. Urankar, W. Yang, L. Y. Leung, J. S. Gilsdorf, and D. A. Shear. 2018. Early Microglial Activation Following Closed-Head Concussive Injury Is Dominated by Pro-Inflammatory M-1 Type. *Front Neurol* 9: 964.
76. Donat, C. K., G. Scott, S. M. Gentleman, and M. Sastre. 2017. Microglial Activation in Traumatic Brain Injury. *Front Aging Neurosci* 9: 208.
77. Kreutzberg, G. W. 1996. Microglia: a sensor for pathological events in the CNS. *Trends Neurosci* 19: 312-318.
78. Takaki, J., K. Fujimori, M. Miura, T. Suzuki, Y. Sekino, and K. Sato. 2012. L-glutamate released from activated microglia downregulates astrocytic L-glutamate

transporter expression in neuroinflammation: the 'collusion' hypothesis for increased extracellular L-glutamate concentration in neuroinflammation. *J Neuroinflammation* 9: 275.

79. Ohsawa, K., Y. Imai, Y. Sasaki, and S. Kohsaka. 2004. Microglia/macrophage-specific protein Iba1 binds to fimbrin and enhances its actin-bundling activity. *J Neurochem* 88: 844-856.
80. Kohler, C. 2007. Allograft inflammatory factor-1/Ionized calcium-binding adapter molecule 1 is specifically expressed by most subpopulations of macrophages and spermatids in testis. *Cell Tissue Res* 330: 291-302.
81. Hazeldine, J., J. M. Lord, and A. Belli. 2015. Traumatic Brain Injury and Peripheral Immune Suppression: Primer and Prospectus. *Front Neurol* 6: 235.
82. Junger, W. G., S. G. Rhind, S. B. Rizoli, J. Cuschieri, A. J. Baker, P. N. Shek, D. B. Hoyt, and E. M. Bulger. 2013. Prehospital hypertonic saline resuscitation attenuates the activation and promotes apoptosis of neutrophils in patients with severe traumatic brain injury. *Shock* 40: 366-374.
83. Liao, Y., P. Liu, F. Guo, Z. Y. Zhang, and Z. Zhang. 2013. Oxidative burst of circulating neutrophils following traumatic brain injury in human. *PLoS One* 8: e68963.
84. Rhind, S. G., N. T. Crnko, A. J. Baker, L. J. Morrison, P. N. Shek, S. Scarpelini, and S. B. Rizoli. 2010. Prehospital resuscitation with hypertonic saline-dextran modulates inflammatory, coagulation and endothelial activation marker profiles in severe traumatic brain injured patients. *J Neuroinflammation* 7: 5.
85. Akashi, K., D. Traver, T. Miyamoto, and I. L. Weissman. 2000. A clonogenic common myeloid progenitor that gives rise to all myeloid lineages. *Nature* 404: 193-197.
86. Mantovani, A., M. A. Cassatella, C. Costantini, and S. Jaillon. 2011. Neutrophils in the activation and regulation of innate and adaptive immunity. *Nat Rev Immunol* 11: 519-531.
87. Khajah, M., B. Millen, D. C. Cara, C. Waterhouse, and D. M. McCafferty. 2011. Granulocyte-macrophage colony-stimulating factor (GM-CSF): a chemoattractive agent for murine leukocytes in vivo. *J Leukoc Biol* 89: 945-953.
88. Beyrau, M., J. V. Bodkin, and S. Nourshargh. 2012. Neutrophil heterogeneity in health and disease: a revitalized avenue in inflammation and immunity. *Open Biol* 2: 120134.
89. Liu, Y. W., S. Li, and S. S. Dai. 2018. Neutrophils in traumatic brain injury (TBI): friend or foe? *J Neuroinflammation* 15: 146.
90. Hazeldine, J., P. Hampson, and J. M. Lord. 2014. The impact of trauma on neutrophil function. *Injury* 45: 1824-1833.
91. Keeling, K. L., R. R. Hicks, J. Mahesh, B. B. Billings, and G. J. Kotwal. 2000. Local neutrophil influx following lateral fluid-percussion brain injury in rats is associated with accumulation of complement activation fragments of the third component (C3) of the complement system. *J Neuroimmunol* 105: 20-30.
92. Bennett, G., S. al-Rashed, J. R. Hoult, and S. D. Brain. 1998. Nerve growth factor induced hyperalgesia in the rat hind paw is dependent on circulating neutrophils. *Pain* 77: 315-322.
93. Royo, N. C., V. Conte, K. E. Saatman, S. Shimizu, C. M. Belfield, K. M. Soltesz, J. E. Davis, S. T. Fujimoto, and T. K. McIntosh. 2006. Hippocampal vulnerability

following traumatic brain injury: a potential role for neurotrophin-4/5 in pyramidal cell neuroprotection. *Eur J Neurosci* 23: 1089-1102.

94. Fenn, A. M., J. C. Hall, J. C. Gensel, P. G. Popovich, and J. P. Godbout. 2014. IL-4 signaling drives a unique arginase+/IL-1beta+ microglia phenotype and recruits macrophages to the inflammatory CNS: consequences of age-related deficits in IL-4Ralpha after traumatic spinal cord injury. *J Neurosci* 34: 8904-8917.
95. Csuka, E., M. C. Morganti-Kossmann, P. M. Lenzlinger, H. Joller, O. Trentz, and T. Kossmann. 1999. IL-10 levels in cerebrospinal fluid and serum of patients with severe traumatic brain injury: relationship to IL-6, TNF-alpha, TGF-beta1 and blood-brain barrier function. *J Neuroimmunol* 101: 211-221.
96. Johnson, E. A., T. L. Dao, M. A. Guignet, C. E. Geddes, A. I. Koemeter-Cox, and R. K. Kan. 2011. Increased expression of the chemokines CXCL1 and MIP-1alpha by resident brain cells precedes neutrophil infiltration in the brain following prolonged soman-induced status epilepticus in rats. *J Neuroinflammation* 8: 41.
97. Aloisi, F., A. Care, G. Borsellino, P. Gallo, S. Rosa, A. Bassani, A. Cabibbo, U. Testa, G. Levi, and C. Peschle. 1992. Production of hemolymphopoietic cytokines (IL-6, IL-8, colony-stimulating factors) by normal human astrocytes in response to IL-1 beta and tumor necrosis factor-alpha. *J Immunol* 149: 2358-2366.
98. Worthen, G. S., B. Schwab, 3rd, E. L. Elson, and G. P. Downey. 1989. Mechanics of stimulated neutrophils: cell stiffening induces retention in capillaries. *Science* 245: 183-186.
99. Yang, L., R. M. Froio, T. E. Sciuto, A. M. Dvorak, R. Alon, and F. W. Luscinskas. 2005. ICAM-1 regulates neutrophil adhesion and transcellular migration of TNF-alpha-activated vascular endothelium under flow. *Blood* 106: 584-592.
100. Allport, J. R., H. Ding, T. Collins, M. E. Gerritsen, and F. W. Luscinskas. 1997. Endothelial-dependent mechanisms regulate leukocyte transmigration: a process involving the proteasome and disruption of the vascular endothelial-cadherin complex at endothelial cell-to-cell junctions. *J Exp Med* 186: 517-527.
101. Bolton, S. J., D. C. Anthony, and V. H. Perry. 1998. Loss of the tight junction proteins occludin and zonula occludens-1 from cerebral vascular endothelium during neutrophil-induced blood-brain barrier breakdown in vivo. *Neuroscience* 86: 1245-1257.
102. Grossetete, M., J. Phelps, L. Arko, H. Yonas, and G. A. Rosenberg. 2009. Elevation of matrix metalloproteinases 3 and 9 in cerebrospinal fluid and blood in patients with severe traumatic brain injury. *Neurosurgery* 65: 702-708.
103. Hayashi, T., Y. Kaneko, S. Yu, E. Bae, C. E. Stahl, T. Kawase, H. van Loveren, P. R. Sanberg, and C. V. Borlongan. 2009. Quantitative analyses of matrix metalloproteinase activity after traumatic brain injury in adult rats. *Brain Res* 1280: 172-177.
104. Liu, X., B. Sui, and J. Sun. 2017. Blood-brain barrier dysfunction induced by silica NPs in vitro and in vivo: Involvement of oxidative stress and Rho-kinase/JNK signaling pathways. *Biomaterials* 121: 64-82.
105. Spahn, J. H., and D. Kreisel. 2014. Monocytes in sterile inflammation: recruitment and functional consequences. *Arch Immunol Ther Exp (Warsz)* 62: 187-194.
106. Wong, K. L., W. H. Yeap, J. J. Tai, S. M. Ong, T. M. Dang, and S. C. Wong. 2012. The three human monocyte subsets: implications for health and disease. *Immunol Res* 53: 41-57.

107. Schwulst, S. J., D. M. Trahanas, R. Saber, and H. Perlman. 2013. Traumatic brain injury-induced alterations in peripheral immunity. *J Trauma Acute Care Surg* 75: 780-788.
108. Serbina, N. V., and E. G. Pamer. 2006. Monocyte emigration from bone marrow during bacterial infection requires signals mediated by chemokine receptor CCR2. *Nat Immunol* 7: 311-317.
109. Gerszten, R. E., E. A. Garcia-Zepeda, Y. C. Lim, M. Yoshida, H. A. Ding, M. A. Gimbrone, Jr., A. D. Luster, F. W. Luscinskas, and A. Rosenzweig. 1999. MCP-1 and IL-8 trigger firm adhesion of monocytes to vascular endothelium under flow conditions. *Nature* 398: 718-723.
110. Szmydynger-Chodobska, J., N. Strazielle, J. R. Gandy, T. H. Keefe, B. J. Zink, J. F. Ghersi-Egea, and A. Chodobski. 2012. Posttraumatic invasion of monocytes across the blood-cerebrospinal fluid barrier. *J Cereb Blood Flow Metab* 32: 93-104.
111. Geissmann, F., S. Jung, and D. R. Littman. 2003. Blood monocytes consist of two principal subsets with distinct migratory properties. *Immunity* 19: 71-82.
112. Auffray, C., D. Fogg, M. Garfa, G. Elain, O. Join-Lambert, S. Kayal, S. Sarnacki, A. Cumano, G. Lauvau, and F. Geissmann. 2007. Monitoring of blood vessels and tissues by a population of monocytes with patrolling behavior. *Science* 317: 666-670.
113. Shimonkevitz, R., D. Bar-Or, L. Harris, K. Dole, L. McLaughlin, and R. Yukl. 1999. Transient monocyte release of interleukin-10 in response to traumatic brain injury. *Shock* 12: 10-16.
114. Chan, M. W. Y., and S. Viswanathan. 2019. Recent progress on developing exogenous monocyte/macrophage-based therapies for inflammatory and degenerative diseases. *Cytotherapy* 21: 393-415.
115. Lord, J. M., M. J. Midwinter, Y. F. Chen, A. Belli, K. Brohi, E. J. Kovacs, L. Koenderman, P. Kubes, and R. J. Lilford. 2014. The systemic immune response to trauma: an overview of pathophysiology and treatment. *Lancet* 384: 1455-1465.
116. Manson, J., C. Thiemermann, and K. Brohi. 2012. Trauma alarmins as activators of damage-induced inflammation. *Br J Surg* 99 Suppl 1: 12-20.
117. Burk, A. M., M. Martin, M. A. Flierl, D. Rittirsch, M. Helm, L. Lampl, U. Bruckner, G. L. Stahl, A. M. Blom, M. Perl, F. Gebhard, and M. Huber-Lang. 2012. Early complementopathy after multiple injuries in humans. *Shock* 37: 348-354.
118. Huber-Lang, M., A. Kovtun, and A. Ignatius. 2013. The role of complement in trauma and fracture healing. *Semin Immunol* 25: 73-78.
119. Reino, D. C., D. Palange, E. Feketeova, R. P. Bonitz, D. Z. Xu, Q. Lu, S. U. Sheth, G. Pena, L. Ulloa, A. De Maio, R. Feinman, and E. A. Deitch. 2012. Activation of toll-like receptor 4 is necessary for trauma hemorrhagic shock-induced gut injury and polymorphonuclear neutrophil priming. *Shock* 38: 107-114.
120. Zemans, R. L., S. P. Colgan, and G. P. Downey. 2009. Transepithelial migration of neutrophils: mechanisms and implications for acute lung injury. *Am J Respir Cell Mol Biol* 40: 519-535.
121. Matthay, M. A., L. B. Ware, and G. A. Zimmerman. 2012. The acute respiratory distress syndrome. *J Clin Invest* 122: 2731-2740.
122. Smedly, L. A., M. G. Tonnesen, R. A. Sandhaus, C. Haslett, L. A. Guthrie, R. B. Johnston, Jr., P. M. Henson, and G. S. Worthen. 1986. Neutrophil-mediated injury

to endothelial cells. Enhancement by endotoxin and essential role of neutrophil elastase. *J Clin Invest* 77: 1233-1243.

123. Hietbrink, F., L. Koenderman, M. Althuizen, and L. P. Leenen. 2009. Modulation of the innate immune response after trauma visualised by a change in functional PMN phenotype. *Injury* 40: 851-855.
124. Pavlov, V. A., H. Wang, C. J. Czura, S. G. Friedman, and K. J. Tracey. 2003. The cholinergic anti-inflammatory pathway: a missing link in neuroimmunomodulation. *Mol Med* 9: 125-134.
125. Borovikova, L. V., S. Ivanova, M. Zhang, H. Yang, G. I. Botchkina, L. R. Watkins, H. Wang, N. Abumrad, J. W. Eaton, and K. J. Tracey. 2000. Vagus nerve stimulation attenuates the systemic inflammatory response to endotoxin. *Nature* 405: 458-462.
126. Tracey, K. J. 2002. The inflammatory reflex. *Nature* 420: 853-859.
127. Wang, H., M. Yu, M. Ochani, C. A. Amella, M. Tanovic, S. Susarla, J. H. Li, H. Wang, H. Yang, L. Ulloa, Y. Al-Abed, C. J. Czura, and K. J. Tracey. 2003. Nicotinic acetylcholine receptor alpha7 subunit is an essential regulator of inflammation. *Nature* 421: 384-388.
128. Wang, H., H. Liao, M. Ochani, M. Justiniani, X. Lin, L. Yang, Y. Al-Abed, H. Wang, C. Metz, E. J. Miller, K. J. Tracey, and L. Ulloa. 2004. Cholinergic agonists inhibit HMGB1 release and improve survival in experimental sepsis. *Nat Med* 10: 1216-1221.
129. Wojnarowicz, M. W., A. M. Fisher, O. Minaeva, and L. E. Goldstein. 2017. Considerations for Experimental Animal Models of Concussion, Traumatic Brain Injury, and Chronic Traumatic Encephalopathy-These Matters Matter. *Front Neurol* 8: 240.
130. Brodhun, M., H. Fritz, B. Walter, I. Antonow-Schlorke, K. Reinhart, U. Zwiener, R. Bauer, and S. Patt. 2001. Immunomorphological sequelae of severe brain injury induced by fluid-percussion in juvenile pigs--effects of mild hypothermia. *Acta Neuropathol* 101: 424-434.
131. Shultz, S. R., D. F. MacFabe, K. A. Foley, R. Taylor, and D. P. Cain. 2011. A single mild fluid percussion injury induces short-term behavioral and neuropathological changes in the Long-Evans rat: support for an animal model of concussion. *Behav Brain Res* 224: 326-335.
132. Povlishock, J. T., and H. A. Kontos. 1985. Continuing axonal and vascular change following experimental brain trauma. *Cent Nerv Syst Trauma* 2: 285-298.
133. Ziebell, J. M., S. E. Taylor, T. Cao, J. L. Harrison, and J. Lifshitz. 2012. Rod microglia: elongation, alignment, and coupling to form trains across the somatosensory cortex after experimental diffuse brain injury. *J Neuroinflammation* 9: 247.
134. Cortez, S. C., T. K. McIntosh, and L. J. Noble. 1989. Experimental fluid percussion brain injury: vascular disruption and neuronal and glial alterations. *Brain Res* 482: 271-282.
135. Atkinson, J. L., R. E. Anderson, and M. J. Murray. 1998. The early critical phase of severe head injury: importance of apnea and dysfunctional respiration. *J Trauma* 45: 941-945.

136. Dixon, C. E., B. G. Lyeth, J. T. Povlishock, R. L. Findling, R. J. Hamm, A. Marmarou, H. F. Young, and R. L. Hayes. 1987. A fluid percussion model of experimental brain injury in the rat. *J Neurosurg* 67: 110-119.
137. Schmidt, R. H., K. J. Scholten, and P. H. Maughan. 2000. Cognitive impairment and synaptosomal choline uptake in rats following impact acceleration injury. *J Neurotrauma* 17: 1129-1139.
138. Foda, M. A., and A. Marmarou. 1994. A new model of diffuse brain injury in rats. Part II: Morphological characterization. *J Neurosurg* 80: 301-313.
139. Marmarou, A., M. A. Foda, W. van den Brink, J. Campbell, H. Kita, and K. Demetriadou. 1994. A new model of diffuse brain injury in rats. Part I: Pathophysiology and biomechanics. *J Neurosurg* 80: 291-300.
140. Namjoshi, D. R., W. H. Cheng, K. A. McInnes, K. M. Martens, M. Carr, A. Wilkinson, J. Fan, J. Robert, A. Hayat, P. A. Cripton, and C. L. Wellington. 2014. Merging pathology with biomechanics using CHIMERA (Closed-Head Impact Model of Engineered Rotational Acceleration): a novel, surgery-free model of traumatic brain injury. *Mol Neurodegener* 9: 55.
141. Dixon, C. E., G. L. Clifton, J. W. Lighthall, A. A. Yaghmai, and R. L. Hayes. 1991. A controlled cortical impact model of traumatic brain injury in the rat. *J Neurosci Methods* 39: 253-262.
142. Lighthall, J. W., H. G. Goshgarian, and C. R. Pinderski. 1990. Characterization of axonal injury produced by controlled cortical impact. *J Neurotrauma* 7: 65-76.
143. Smith, D. H., H. D. Soares, J. S. Pierce, K. G. Perlman, K. E. Saatman, D. F. Meaney, C. E. Dixon, and T. K. McIntosh. 1995. A model of parasagittal controlled cortical impact in the mouse: cognitive and histopathologic effects. *J Neurotrauma* 12: 169-178.
144. Lighthall, J. W. 1988. Controlled cortical impact: a new experimental brain injury model. *J Neurotrauma* 5: 1-15.
145. Shaw, N. A. 2002. The neurophysiology of concussion. *Prog Neurobiol* 67: 281-344.
146. Xiong, Y., A. Mahmood, and M. Chopp. 2013. Animal models of traumatic brain injury. *Nat Rev Neurosci* 14: 128-142.
147. Faust, N., F. Varas, L. M. Kelly, S. Heck, and T. Graf. 2000. Insertion of enhanced green fluorescent protein into the lysozyme gene creates mice with green fluorescent granulocytes and macrophages. *Blood* 96: 719-726.
148. Wilson, E. H., W. Weninger, and C. A. Hunter. 2010. Trafficking of immune cells in the central nervous system. *J Clin Invest* 120: 1368-1379.
149. Coughlin, J. M., Y. Wang, I. Minn, N. Bienko, E. B. Ambinder, X. Xu, M. E. Peters, J. W. Dougherty, M. Vranesic, S. M. Koo, H. H. Ahn, M. Lee, C. Cottrell, H. I. Sair, A. Sawa, C. A. Munro, C. J. Nowinski, R. F. Dannals, C. G. Lyketsos, M. Kassiou, G. Smith, B. Caffo, S. Mori, T. R. Guilarte, and M. G. Pomper. 2017. Imaging of Glial Cell Activation and White Matter Integrity in Brains of Active and Recently Retired National Football League Players. *JAMA Neurol* 74: 67-74.
150. McPherson, C. A., B. A. Merrick, and G. J. Harry. 2014. In vivo molecular markers for pro-inflammatory cytokine M1 stage and resident microglia in trimethyltin-induced hippocampal injury. *Neurotox Res* 25: 45-56.
151. Huff, T., P. Tadi, and M. Varacallo. 2019. Neuroanatomy, Cerebrospinal Fluid. In *StatPearls*, Treasure Island (FL).

152. Ransohoff, R. M., and A. E. Cardona. 2010. The myeloid cells of the central nervous system parenchyma. *Nature* 468: 253-262.
153. Louveau, A., I. Smirnov, T. J. Keyes, J. D. Eccles, S. J. Rouhani, J. D. Peske, N. C. Derecki, D. Castle, J. W. Mandell, K. S. Lee, T. H. Harris, and J. Kipnis. 2015. Structural and functional features of central nervous system lymphatic vessels. *Nature* 523: 337-341.
154. Nahrendorf, M., F. K. Swirski, E. Aikawa, L. Stangenberg, T. Wurdinger, J. L. Figueiredo, P. Libby, R. Weissleder, and M. J. Pittet. 2007. The healing myocardium sequentially mobilizes two monocyte subsets with divergent and complementary functions. *J Exp Med* 204: 3037-3047.
155. Morganti, J. M., T. D. Jopson, S. Liu, L. K. Riparip, C. K. Guandique, N. Gupta, A. R. Ferguson, and S. Rosi. 2015. CCR2 antagonism alters brain macrophage polarization and ameliorates cognitive dysfunction induced by traumatic brain injury. *J Neurosci* 35: 748-760.
156. Gyoneva, S., D. Kim, A. Katsumoto, O. N. Kokiko-Cochran, B. T. Lamb, and R. M. Ransohoff. 2015. Ccr2 deletion dissociates cavity size and tau pathology after mild traumatic brain injury. *J Neuroinflammation* 12: 228.
157. Greenhalgh, A. D., J. G. Zarruk, L. M. Healy, S. J. Baskar Jesudasan, P. Jhelum, C. K. Salmon, A. Formanek, M. V. Russo, J. P. Antel, D. B. McGavern, B. W. McColl, and S. David. 2018. Peripherally derived macrophages modulate microglial function to reduce inflammation after CNS injury. *PLoS Biol* 16: e2005264.
158. Baruch, K., A. Kertser, Z. Porat, and M. Schwartz. 2015. Cerebral nitric oxide represses choroid plexus NFkappaB-dependent gateway activity for leukocyte trafficking. *EMBO J* 34: 1816-1828.
159. Szmydynger-Chodobska, J., N. Strazielle, B. J. Zink, J. F. Ghersi-Egea, and A. Chodobski. 2009. The role of the choroid plexus in neutrophil invasion after traumatic brain injury. *J Cereb Blood Flow Metab* 29: 1503-1516.
160. Carlos, T. M., R. S. Clark, D. Franicola-Higgins, J. K. Schiding, and P. M. Kochanek. 1997. Expression of endothelial adhesion molecules and recruitment of neutrophils after traumatic brain injury in rats. *J Leukoc Biol* 61: 279-285.
161. Johnson, V. E., J. E. Stewart, F. D. Begbie, J. Q. Trojanowski, D. H. Smith, and W. Stewart. 2013. Inflammation and white matter degeneration persist for years after a single traumatic brain injury. *Brain* 136: 28-42.
162. Smith, D. H., R. Hicks, and J. T. Povlishock. 2013. Therapy development for diffuse axonal injury. *J Neurotrauma* 30: 307-323.
163. Meaney, D. F., and D. H. Smith. 2011. Biomechanics of concussion. *Clin Sports Med* 30: 19-31, vii.
164. Johnson, V. E., W. Stewart, and D. H. Smith. 2013. Axonal pathology in traumatic brain injury. *Exp Neurol* 246: 35-43.
165. Smith, D. H. 2016. Neuromechanics and Pathophysiology of Diffuse Axonal Injury in Concussion. *Bridge (Wash D C)* 46: 79-84.
166. Tang-Schomer, M. D., V. E. Johnson, P. W. Baas, W. Stewart, and D. H. Smith. 2012. Partial interruption of axonal transport due to microtubule breakage accounts for the formation of periodic varicosities after traumatic axonal injury. *Exp Neurol* 233: 364-372.
167. Smith, D. H., V. E. Johnson, and W. Stewart. 2013. Chronic neuropathologies of single and repetitive TBI: substrates of dementia? *Nat Rev Neurol* 9: 211-221.

168. Johnson, V. E., W. Stewart, and D. H. Smith. 2010. Traumatic brain injury and amyloid-beta pathology: a link to Alzheimer's disease? *Nat Rev Neurosci* 11: 361-370.
169. Hay, J., V. E. Johnson, D. H. Smith, and W. Stewart. 2016. Chronic Traumatic Encephalopathy: The Neuropathological Legacy of Traumatic Brain Injury. *Annu Rev Pathol* 11: 21-45.
170. Zygun, D. A., J. B. Kortbeek, G. H. Fick, K. B. Laupland, and C. J. Doig. 2005. Non-neurologic organ dysfunction in severe traumatic brain injury. *Crit Care Med* 33: 654-660.
171. Holland, M. C., R. C. Mackersie, D. Morabito, A. R. Campbell, V. A. Kivett, R. Patel, V. R. Erickson, and J. F. Pittet. 2003. The development of acute lung injury is associated with worse neurologic outcome in patients with severe traumatic brain injury. *J Trauma* 55: 106-111.
172. Humphries, D. C., S. O'Neill, E. Scholefield, D. A. Dorward, A. C. Mackinnon, A. G. Rossi, C. Haslett, P. J. D. Andrews, J. Rhodes, and K. Dhaliwal. 2018. Cerebral Concussion Primes the Lungs for Subsequent Neutrophil-Mediated Injury. *Crit Care Med* 46: e937-e944.
173. Anthony, D. C., Y. Couch, P. Losey, and M. C. Evans. 2012. The systemic response to brain injury and disease. *Brain Behav Immun* 26: 534-540.
174. Sauerbeck, A. D., J. L. Laws, V. V. Bandaru, P. G. Popovich, N. J. Haughey, and D. M. McTigue. 2015. Spinal cord injury causes chronic liver pathology in rats. *J Neurotrauma* 32: 159-169.
175. BIO-RAD. Cell frequencies in common samples.
176. Kim, E., J. Yang, C. D. Beltran, and S. Cho. 2014. Role of spleen-derived monocytes/macrophages in acute ischemic brain injury. *J Cereb Blood Flow Metab* 34: 1411-1419.
177. Meert, K. L., M. Long, J. Kaplan, and A. P. Sarnaik. 1995. Alterations in immune function following head injury in children. *Crit Care Med* 23: 822-828.
178. Mrakovcic-Sutic, I., V. S. Tokmadzic, G. Laskarin, H. Mahmutefendic, P. Lucin, Z. Zupan, and A. Sustic. 2010. Early changes in frequency of peripheral blood lymphocyte subpopulations in severe traumatic brain-injured patients. *Scand J Immunol* 72: 57-65.
179. Quattrocchi, K. B., E. H. Frank, C. H. Miller, S. T. Dull, R. R. Howard, and F. C. Wagner, Jr. 1991. Severe head injury: effect upon cellular immune function. *Neurol Res* 13: 13-20.
180. Hoyt, D. B., A. N. Ozkan, J. F. Hansbrough, L. Marshall, and M. vanBerkum-Clark. 1990. Head injury: an immunologic deficit in T-cell activation. *J Trauma* 30: 759-766; discussion 766-757.
181. Smrcka, M., A. Mrlian, and M. Klabusay. 2005. Immune system status in the patients after severe brain injury. *Bratisl Lek Listy* 106: 144-146.
182. Beraldo, F. H., A. Thomas, B. Kolisnyk, P. H. Hirata, X. De Jaeger, A. C. Martyn, J. Fan, D. F. Goncalves, M. F. Cowan, T. Masood, V. R. Martins, R. Gros, V. F. Prado, and M. A. Prado. 2015. Hyperactivity and attention deficits in mice with decreased levels of stress-inducible phosphoprotein 1 (STIP1). *Dis Model Mech* 8: 1457-1466.
183. Bussey, T. J., A. Holmes, L. Lyon, A. C. Mar, K. A. McAllister, J. Nithianantharajah, C. A. Oomen, and L. M. Saksida. 2012. New translational assays

for preclinical modelling of cognition in schizophrenia: the touchscreen testing method for mice and rats. *Neuropharmacology* 62: 1191-1203.

184. Doran, S. J., R. M. Ritzel, E. P. Glaser, R. J. Henry, A. I. Faden, and D. J. Loane. 2019. Sex Differences in Acute Neuroinflammation after Experimental Traumatic Brain Injury Are Mediated by Infiltrating Myeloid Cells. *J Neurotrauma* 36: 1040-1053.
185. Spychala, M. S., P. Honarpisheh, and L. D. McCullough. 2017. Sex differences in neuroinflammation and neuroprotection in ischemic stroke. *J Neurosci Res* 95: 462-471.

Appendix

Appendix 1. Animal ethics approval.

Western

2016-019:3:

AUP Number: 2016-019
AUP Title: Experimental CNS Injury

Yearly Renewal Date: 10/01/2019

The YEARLY RENEWAL to Animal Use Protocol (AUP) 2016-019 has been approved by the Animal Care Committee (ACC), and will be approved through to the above review date.

Please at this time review your AUP with your research team to ensure full understanding by everyone listed within this AUP.

As per your declaration within this approved AUP, you are obligated to ensure that:

1) Animals used in this research project will be cared for in alignment with:
   a) Western's Senate MAPPs 7.12, 7.10, and 7.15
   http://www.uwo.ca/univsec/policies_procedures/research.html
   b) University Council on Animal Care Policies and related Animal Care Committee procedures
   http://uwo.ca/research/services/animalethics/animal_care_and_use_policies.html
2) As per UCAC's Animal Use Protocols Policy,
   a) this AUP accurately represents intended animal use;
   b) external approvals associated with this AUP, including permits and scientific/departmental peer approvals, are complete and accurate;
   c) any divergence from this AUP will not be undertaken until the related Protocol Modification is approved by the ACC; and
   d) AUP form submissions - Annual Protocol Renewals and Full AUP Renewals - will be submitted and attended to within timeframes outlined by the ACC. http://uwo.ca/research/services/animalethics/animal_use_protocols.html
3) As per MAPP 7.10 all individuals listed within this AUP as having any hands-on animal contact will
   a) be made familiar with and have direct access to this AUP;
   b) complete all required CCAC mandatory training (_training@uwo.ca); and
   c) be overseen by me to ensure appropriate care and use of animals.
4) As per MAPP 7.15,
   a) Practice will align with approved AUP elements;
   b) Unrestricted access to all animal areas will be given to ACVS Veterinarians and ACC Leaders;
   c) UCAC policies and related ACC procedures will be followed, including but not limited to:
      i) Research Animal Procurement
      ii) Animal Care and Use Records
      iii) Sick Animal Response
      iv) Continuing Care Visits
5) As per institutional OH&S policies, all individuals listed within this AUP who will be using or potentially exposed to hazardous materials will have completed in advance the appropriate institutional OH&S training, facility-level training, and reviewed related (M)SDS Sheets, http://www.uwo.ca/hr/learning/required/index.html

Submitted by: Copeman, Laura
on behalf of the Animal Care Committee
University Council on Animal Care

Appendix 2. The Iba-1 antibody specificity. Panel A and B show different areas of the brain that are not Iba-1^+ due to the lack of primary Iba-1 antibody. Panel C and D show Iba-1^+ staining in different brain regions when the primary Iba-1 antibody is added. This confirms the specificity of the Iba-1 antibody.

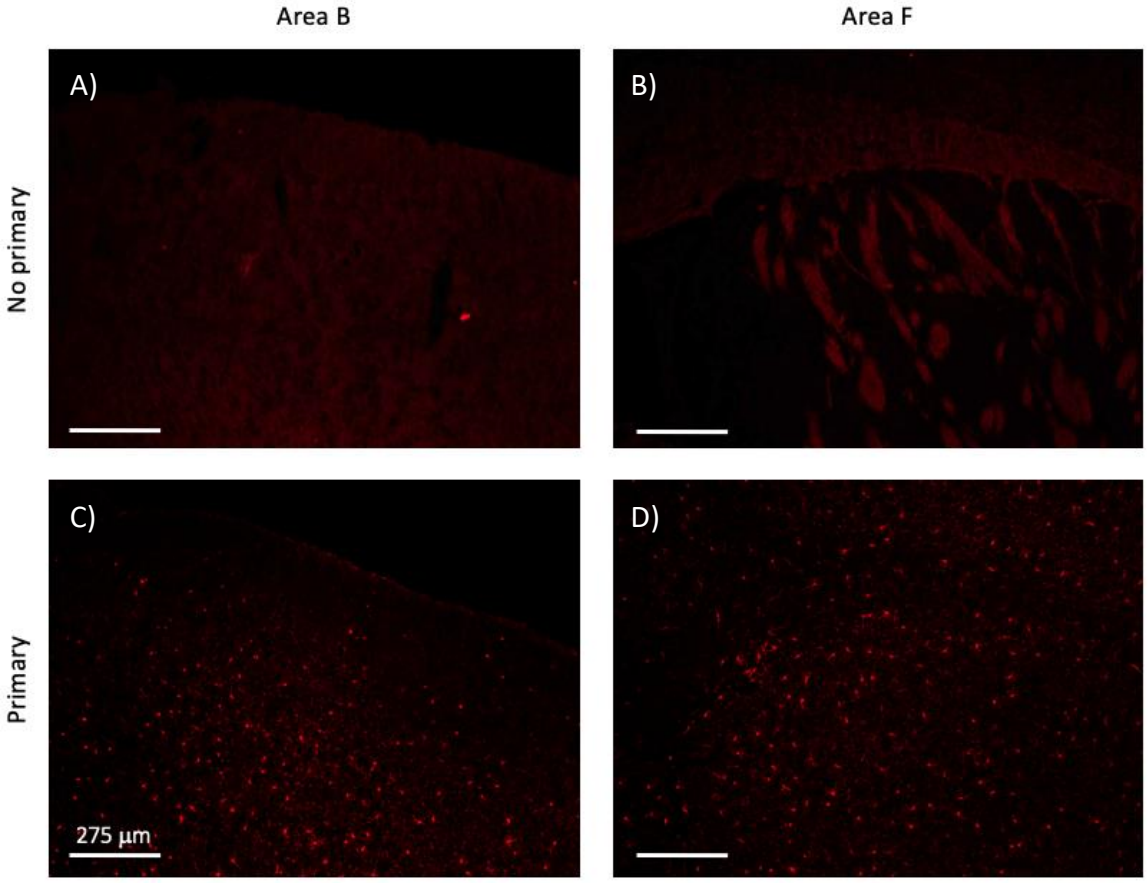

Appendix 3. Optimized gating strategy for identifying myeloid lineage cell populations in both blood and spleen via flow cytometry. First, the counting beads were separated from the cell scatter, then viable and single cells were selected. Myeloid cells were gated for $CD45^{+}CD11b^{+}$ and discriminated against $CD19^{+}$, $CD3\varepsilon^{+}$ and $NKp46^{+}$ cells. Classical monocytes were identified as $F4/80^{+}CD115^{+}Ly6C^{+}GFP^{+}$, non-classical monocytes as $F4/80^{+}CD115^{+}Ly6C^{-}GFP^{+}$ and neutrophils are $Ly6G^{+}GFP^{+}$.

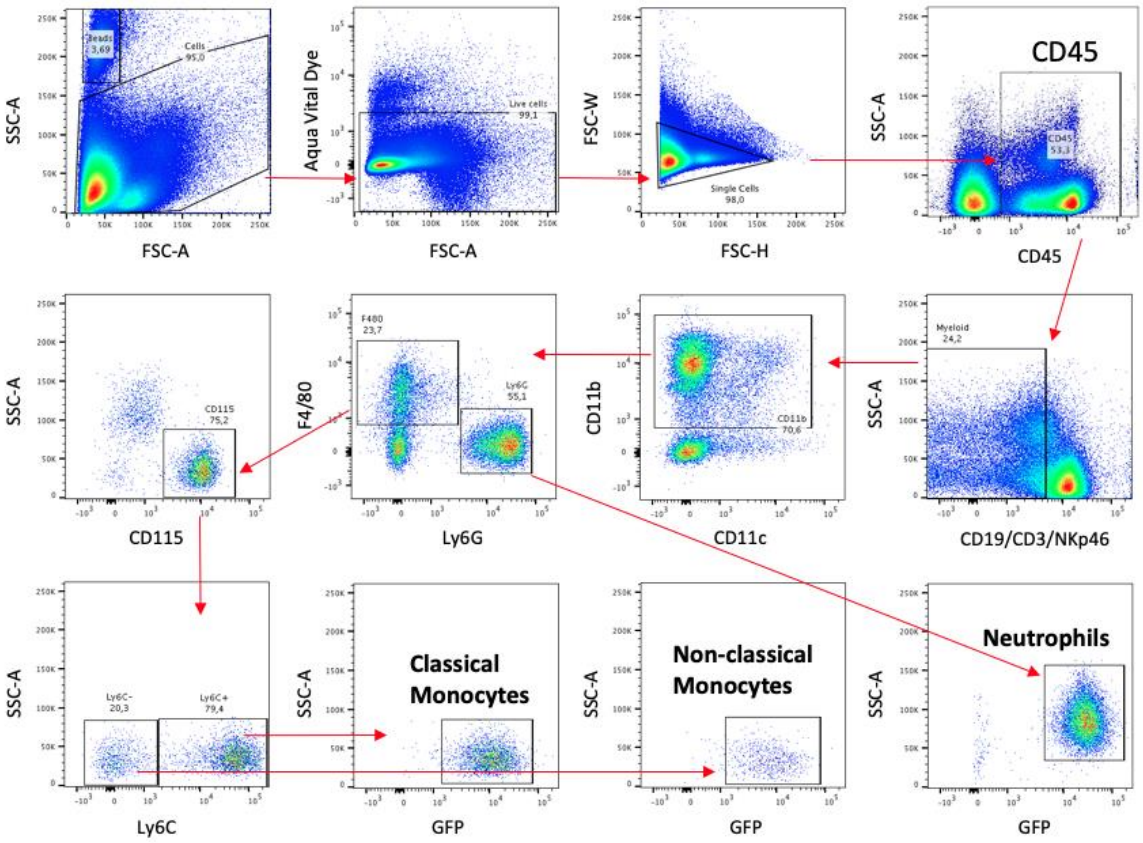

Appendix 4. Optimized gating strategy for identifying lymphoid lineage cell populations in both blood and spleen via flow cytometry. First, the counting beads were separated from the cell scatter, then $EGFP^+$ myeloid cell populations were gated out to select for lymphoid cells. After viable cells, singlets and $CD45^+$ cell population were selected, T cells were identified by $EGPF^-CD45^+CD3\varepsilon^+$, B cells as $EGFP^-CD45^+CD19^+$, NK cells as $EGFP^-CD45^+NKp46^+$.

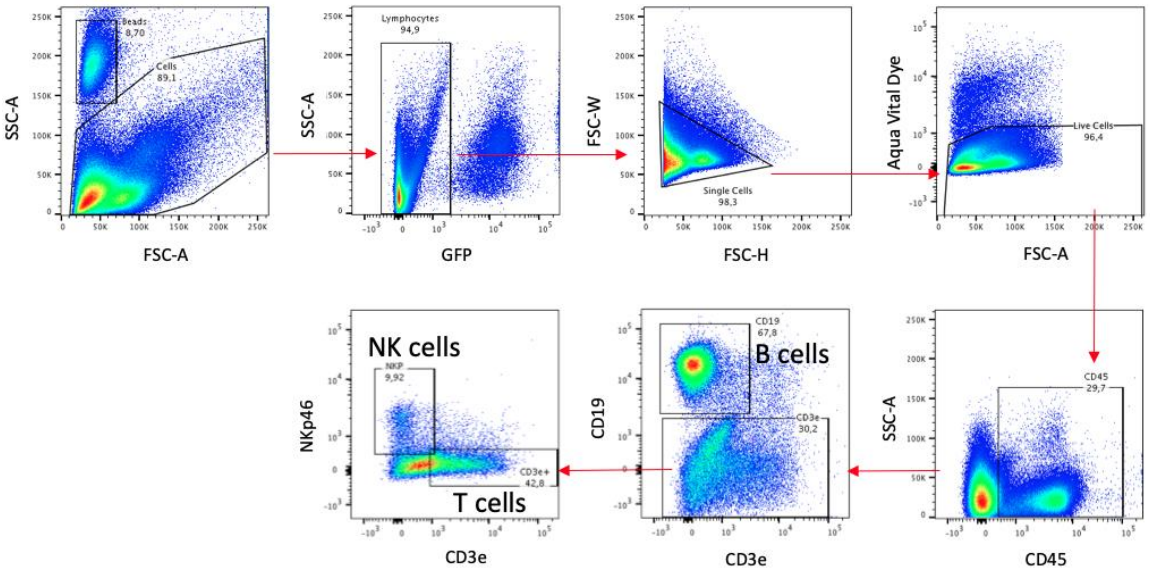

Curriculum Vitae

So Young Eo

Education

2017 – 2019	Master of Science (M.Sc.) Department of Microbiology and Immunology Schulich School of Medicine and Dentistry Western University, London, Ontario
2013 – 2017	Bachelor of Science Honours, specialization in Life Sciences Department of Biomedical and Molecular Sciences Queen's University, Kingston, Ontario

Awards

2017 – 2019	Western Graduate Research Scholarship, Western University, London, Ontario
2017	FW Luney Entrance Scholarship of Microbiology and Immunology Western University, London, Ontario
2013 – 2017	Dean's Honour list, Queen's University, Kingston, Ontario
2013	Principal Entrance Scholarship, Queen's University, Kingston, Ontario

Presentations and publications

Eo, S., Xu, K., Brown, A., Dekaban, G. 2019. "*Brain-specific and systemic inflammatory response following repetitive concussive impact in a mouse model*." Poster presentation at Robarts Research Retreat at Western University, London, Ontario.

Eo, S., Xu, K., Brown, A., Dekaban, G. 2019. "*Brain-specific and systemic inflammatory response following repetitive concussive impact in a mouse model*." Robarts data club oral presentation at Robarts Research Institute, London, Ontario.

Eo, S., Xu, K., Brown, A., Dekaban, G. 2019. "*Brain-specific and systemic inflammatory response following repetitive concussive impact in a mouse model.*" Poster presentation at the Neuroscience research day, London, Ontario.

Kourko O., R. Smyth, D. Cino, K. Seaver, C. Petes, **S. Eo**, S. Basta, and K. Gee. 2019. "*Poly(I:C)-mediated death of human prostate cancer cell lines is induced by IL-27 treatment.*" Journal of Interferon and Cytokine Research.

Eo, S., Xu, K., Brown, A., Dekaban, G. 2018. "*Brain-specific and systemic inflammatory response following repetitive concussive impact in a mouse model*." Robarts data club oral presentation at Robarts Research Institute, London, Ontario.

Eo, S., Xu, K., Brown, A., Dekaban, G. 2018. "*Brain-specific and systemic inflammatory response following repetitive concussive impact in a mouse model*." Poster presentation at Robarts Research Retreat, London, Ontario.

Eo, S., Xu, K., Brown, A., Dekaban, G. 2018. "*Brain-specific and systemic inflammatory response following repetitive concussive impact in a mouse model."* Poster presentation at the annual Canadian Society of Immunology general meeting, London, Ontario

Eo, **S.**, Xu, K., Brown, A., Dekaban, G. 2018. "*Brain-specific and systemic inflammatory response following repetitive concussive impact in a mouse model*." Poster presentation at the Infection and Immunity Research Forum, Stratford, Ontario.

Eo, S., Xu, K., Brown, A., Dekaban, G. 2017. "*Brain-specific and systemic inflammatory response following repetitive concussive impact in a mouse model*." Poster presentation at the Infection and Immunity Research Forum, London, Ontario.

Eo, S., Petes, C., Basta, S., Gee, K. 2017. "Regulation of interleukin-27 expression and function in human cancer cell lines." Poster presentation at Queen's Research Day, Kingston, Ontario.

Eo, S., Petes, C., Basta, S., Gee, K. 2017. "Regulation of interleukin-27 expression and function in human cancer cell lines." Oral presentation at 499 Presentation Day, Kingston, Ontario.

Related Work experiences

2017	Summer research student, immunology laboratory supervisor: Dr. Gregory Dekaban Robarts research institute, London, Ontario, Canada
2016	Summer research student, microbiology & immunology laboratory Supervisor: Dr. Katrina Gee Queen's University, Kingston, Ontario, Canada
2014 – 2016	Volunteer, microbiology & immunology laboratory Supervisor: Dr. Katrina Gee Queen's University, Kingston, Ontario, Canada